**UNIVERSITY OF SASSARI**

*PhD School in*
**Biomolecular and Biotechnological Sciences**
*Curriculum:* Biochemistry and Molecular Biology
*Director*: Prof. Claudia Crosio
"XXVI Ciclo"

# *Physiopathology of ALS: from oxidative stress to RNA metabolism.*

*PhD Student*: **Sonia Esposito**

*Supervisor*: **Prof. Claudia Crosio**

Academic Year 2012-2013

# *INDEX*

***CHAPTER 1: INTRODUCTION.***

# *CHAPTER 1:*

# *INTRODUCTION.*

## *1.1 Amyotrophic Lateral Sclerosis (ALS).*

Amyotrophic lateral sclerosis (ALS; also known as Lou Gehring's disease) is the most common adult-onset motor neuron disease, described for the first time by Jean-Martin Charcot in 1874 [1]. The pathology incidence and prevalence is around 2.5 and 4-6 cases per 100,000 people each year, respectively, with a slightly higher incidence of disease in men. The hallmark of this disease is the selective degeneration of cortical, bulbar and spinal motor neurons, except for those that control the bladder and the eye movement (Fig. 1). This leads to generalised muscle weakness leading to progressive paralysis of voluntary muscles until death caused by respiratory failure. The average age of onset is 50-55 years with a typical survival time of 3-4 years after diagnosis, but this parameter is influenced by age at symptom, clinical presentation, age at respiratory dysfunction and nutrition state of the patient [2,3]. ALS may present as a predominantly lower motor neuron (LMN) form designates progressive muscular atrophy (PMA), a predominantly upper lower motor neuron (UMN) form called primary lateral sclerosis (PLS), or more commonly with mixed UMN and LMN deficits [4].

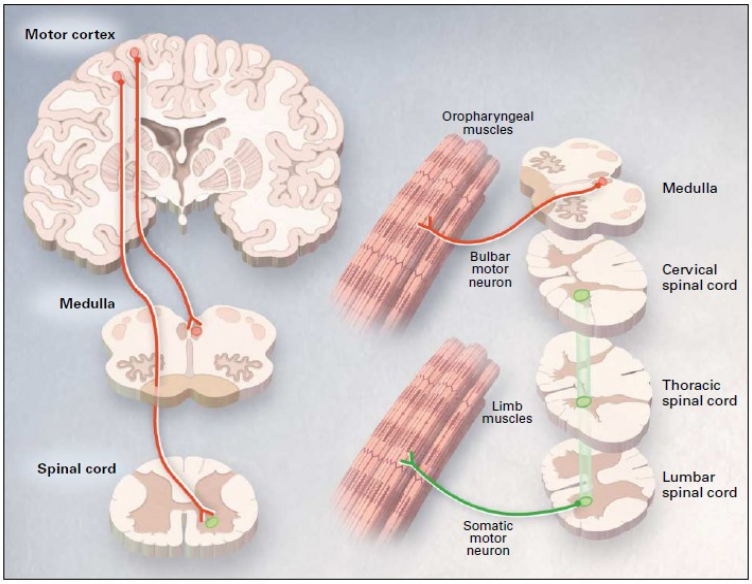


Figure 1: Motor neurons selectively affected in ALS. Degeneration of motor neurons in the motor cortex leads to clinically apparent signs of upper motor neuron abnormalities. Degeneration of motor neurons in the brain stem and spinal cord causes muscle atrophy, weakness and fasciculation [1].

Although the majority of cases are classed as sporadic ALS (sALS), approximately 10% of ALS cases are inherited (familial ALS, fALS), with multiple autosomal dominant and recessive forms. Sporadic and familial ALS share common clinical and neuropathological manifestations, and ALS patients show some degree of heterogeneity as far as symptoms, age of onset and disease duration are concerned, furthermore all genes found mutated in fALS cases have also been found mutated in sALS [5,6].

The causes of the majority of ALS cases are still obscure. Although numerous pathological mechanisms have been elucidated, ALS remains an invariably fatal disease in the absence of any effective therapy. The heterogeneity of the disease and the failure to develop satisfactory therapeutic protocols reinforce the view that ALS is a multi-factorial and multi-systemic disease. Up to now, Riluzole is the only approved medication as ALS treatment, it has the effect to slow the disease in humans but only slightly, prolonging survival by 3 months and not clearly improving the quality of life of patients [7]. Numerous other treatments are currently in different phases of clinical trials and include anti-inflammatories, neurotrophic, anti-oxidants and anti-apoptotic molecules [8].

## *1.2 Aetiology of ALS.*

ALS, like many other neurodegenerative diseases, presents an extremely complex aetiology determined by environmental and genetic factors. In fact, in most cases to disease development contribute both genetic and environmental factors, and only a small percentage of cases can be attributed simply one of the two factors.

The pathogenic mechanisms that underlie ALS remain mostly unclear, even if different alterations of cellular function in ALS motor neurons, including protein misfolding, RNA metabolism dysfunction, mitochondrial defects, oxidative stress, altered axonal transport, excitotoxicity, insufficient growth factor signaling and inflammation have been identified [9,10]. Several factors are proposed to instigate these phenomena, including various environmental risk factors (for example, insecticides, pesticides and cigarette smoking)[11,12] latent infections by viral and non-viral agents [13], toxins and autoimmune reactions [14].

Lately there has been rising interest the role played by non-neuronal neighbouring cells in the pathogenesis of motor neuron damage. In fact ALS is considered also a glial pathology and disruption of glial cells/motoneurons communication contribute to neurodegeneration and the propagation of motor neuron injury [15].

### *1.2.1 ALS environmental factors.*

Given that sALS represents approximately 90% of all ALS cases, it has been hypothesized that exposure to different environmental factors may interact with individual genetic susceptibility playing a remarkable role in the pathogenesis of the disease.

Firstly it was hypothesized that cigarette smoking and many chemicals contains, could contribute to ALS development through lipid peroxidation via formaldehyde exposure [11,16]. Second it appears that life style as well as particular occupation could be associated to ALS for their continued exposure to toxic agents. In particular, consumption of food with high concentrations of the

neurotoxic aminoacid (β-methyl-amino-L-alanine)[17], use of cholesterol-lowering drugs [18], and environmental toxicants such as heavy metals [19], pesticides or herbicides [12,20] may be potential risk factors. Evidences in several case-control studies as well as in experimental studies showed that exposure to these toxicants could induce progressive brain damage by increase of ratio between reactive oxygen species (ROS) and reactive nitrogen species (RNS)[21], decrease activation of astrocytes with neuroprotective effects [22] and inhibition of acetylcholinesterase, resulting in excessive stimulation of cholinergic receptors and excitotoxicity [23]. Also intensive and strenuous physical exercise of professional and amateur football players (Italian and English soccer players)[24,25] as well as military service (Gulf War veterans in the US Army)[26] could represent a risk factor for ALS linked to the intermittent occupational hypoxia resulting in the production of ROS[27] or to the repeated head injuries [28].

In short, as just described over the years a growing list of potential environmental risk factors for ALS has been proposed, but at present there is no ascertained causal link between any of them and ALS pathogenesis [29].

Recently, it has been evidenced the involvement of epigenetic factors on the progression of many human pathologies, including neurodegenerative diseases such as ALS. The epigenetic modifications could provide a possible link between the environmental risk factors and the gene expression alterations responsible for the ALS onset [30]. In fact, it has been proposed that epigenetic silencing of genes important to motor neurons functions could underlie ALS development. In support to this hypothesis, it has been shown that treatment with histone deacetylase enzymes (HDAC) inhibitors significantly prolong survival, improves motor performance and reduce the loss of motor neurons in mouse models of ALS [31,32].

### *1.2.2 ALS genetic factors.*

In the last years, there has been a rapid progress in our knowledge of genetic causes for ALS. Familial ALS can be inherited as an autosomal dominant or autosomal recessive trait. Up to date, more than 20 loci have been identified by genetic analysis, and several have been assigned to specific genes (Table 1).

| Genetic subtype | Chromosomal locus | Gene | Protein | Onset | Inheritance | Clinical feature |
|---|---|---|---|---|---|---|
| ALS1 | 21q22.1 | SOD1 | Cu/Zn SOD-1 | Adult | AD/AR | Typical ALS |
| ALS2 | 2q33-2q35 | Alsin | Alsin | Juv | AR | Slowly progressive, predominantly UMN signs like limb& facial spasticity |
| ALS3 | 18q21 | Unknown | Unknown | Adu | AD | Typical ALS with limb onset especially lower limb |
| ALS4 | 9q34 | SETX | Senataxin | Juv | AD | Slowly progressive, distal hereditary motor neuropathy with pyramidal signs |
| ALS5 | 15q15-21 | SPG 11 | Spatacsin | Juv | AR | Slowly progressive |
| ALS6 | 16p11.2 | FUS | Fused in Sarcoma | Juv/ Adu | AD/AR | Typical ALS |
| ALS8 | 20q13.3 | VAPB | VAPB | Adu | AD | Typical and atypical ALS |
| ALS9 | 14q11.2 | ANG | Angiogenin | Adu | AD | Typical ALS, FTD and Parkinsonism |
| ALS10 | 1p36.2 | TARDBP | DNA-binding protein | Adu | AD | Typical ALS |
| ALS11 | 6q21 | FIG 4 | Phosphoinositide-5phosphatease | Adu | AD | Rapid progressive with prominent corticospinal tract signs |
| ALS12 | 10p13 | OPTN | Optineurin | Adu | AD/AR | Slowly progressive with limb onset and predominant UMN signs |
| ALS14 | 9p13.3 | VCP | VCP | Adu | AD | Adult onset, with or without FTD |
| ALS15/ALSX | Xp11 | UBQLN2 | Ubiquilin 2 | Adu/ Juv | XD | UMN signs proceeding LMN signs |
| ALS16 | 9p13.2-21.3 | SIGMAR1 | SIGMAR1 | Juv | AR | Juvenile onset typical ALS |
| ALS-FTD1 | 9q21-22 | unknown | unknown | Adu | AD | ALS with FTD |
| ALS-FTD2 | 9p21 | C9ORF72 | C9ORF72 | Adu | AD | ALS with FTD |
| NA | 2p13 | DCTN1 | Dynactin | Adu | AD | Distal hereditary motor neuropathy with vocal paresis |
| **Other rare-occurring ALS genes** | | | | | | |
| ALS3 | 18q21 | Unknown | Unknown | Adu | AD | Typical ALS with limb onset especially lower limb |
| ALS7 | 20ptel-p13 | Unknown | Unknown | Adu | AD/AR | Typical ALS |
| NA | 12q22-23 | DAO | DAO | Adu | AD | Typical ALS |

Table 1: The genetics of fALS. More than 20-ALS genes have been identified in fALS. These genetic mutations represent different molecular pathways of motor neuron degeneration. Abbreviations: AD: Autosomal dominant; AR: Autosomal recessive; VAPB: Vesicle associated membrane protein associated protein B; VCP: Valosin Containing Protein; SIGMAR1:Sigma Non Opioid Intracellular Receptor; C9ORF72: Chromosome 9 open reading frame 72; DAO:D-Amino Acid Oxidase; FTD: Frontal-temporal dementia; UMN: upper motor neuron; LMN: lower motor neuron [33].

Linkage studies indicated that both types of inheritance are represented by more than one genetic entity. The relationship between the genetic subtypes and the pathological subtypes as well as clinical phenotype has become more and more clear. Although in many cases the function of mutant protein is not yet clearly identified or many different functions have been proposed, the available data shows that fALS proteins are involved in several cellular processes, from RNA processing to antioxidant response, axonal and vesicular transport and angiogenesis [3,33].

## *1.3 ALS1/Superoxide Dismutase 1 (SOD1).*

### *1.3.1 Structure and functions.*

Eukaryotic copper, zinc superoxide dismutase (SOD1) is a 32-kDa homodimeric metalloenzyme, encoded on chromosome 21 (21q22.1) and found predominantly in the cytosol, but also in the mitochondrial intermembrane space, nucleus and peroxisomes. SOD1 is an abundant protein in the CNS, accounting for about 1% of brain protein, but it is also ubiquitously expressed in all other tissues [34,35]. Each subunit of SOD1 forms an eight-stranded β-barrel and contains an active site that binds a catalytic copper ion (binding residues: His46, His48, His63 and His120), a structural zinc ion (binding residues: His63, His71, His80 and Asp83) and a disulphide bond. Through cyclical reduction and oxidation (dismutation) of copper, SOD1 converts the superoxide anion to dioxygen and hydrogen peroxide preventing the further generation of reactive oxygen species (ROS)[36,37,38] (Fig. 2).

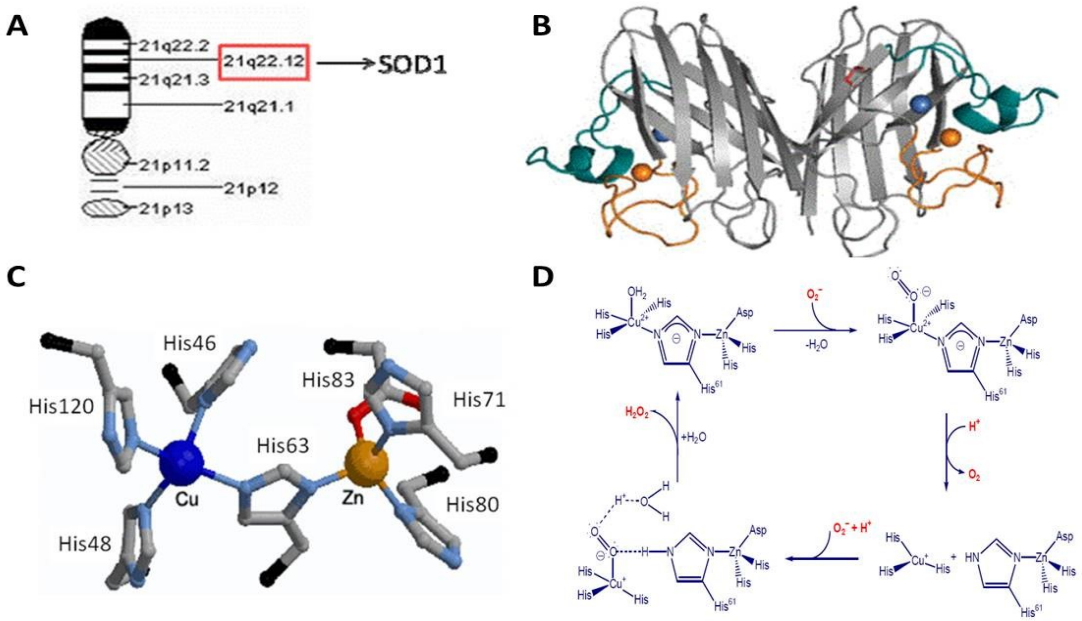


Figure 2: Structure and function of SOD1. A) SOD1 gene position on chromosome 21. B) Tridimensional structure of human SOD1. C) Active site of Cu/Zn SOD1. D) Mechanism cyclic oxidation-reduction catalysed by SOD1.

### *1.3.2 SOD1 mutations.*

About 20% of all fALS and 1-4% of sALS cases carry mutations in the locus ALS1 on chromosome 21 that codes for SOD1 (Cu, Zn superoxide dismutase 1, OMIM #105400). After the first report in 1993, more than 150 different mutations have been identified in all five exons of SOD1 predominantly in missense mutations, but also a small percentage of nonsense mutations, insertions and deletions. Most mutations act dominantly except two, N86S and D90A, that are

linked to recessive inheritance [39,40] although the former mutation was described in rare juvenile onset ALS (Fig.3).

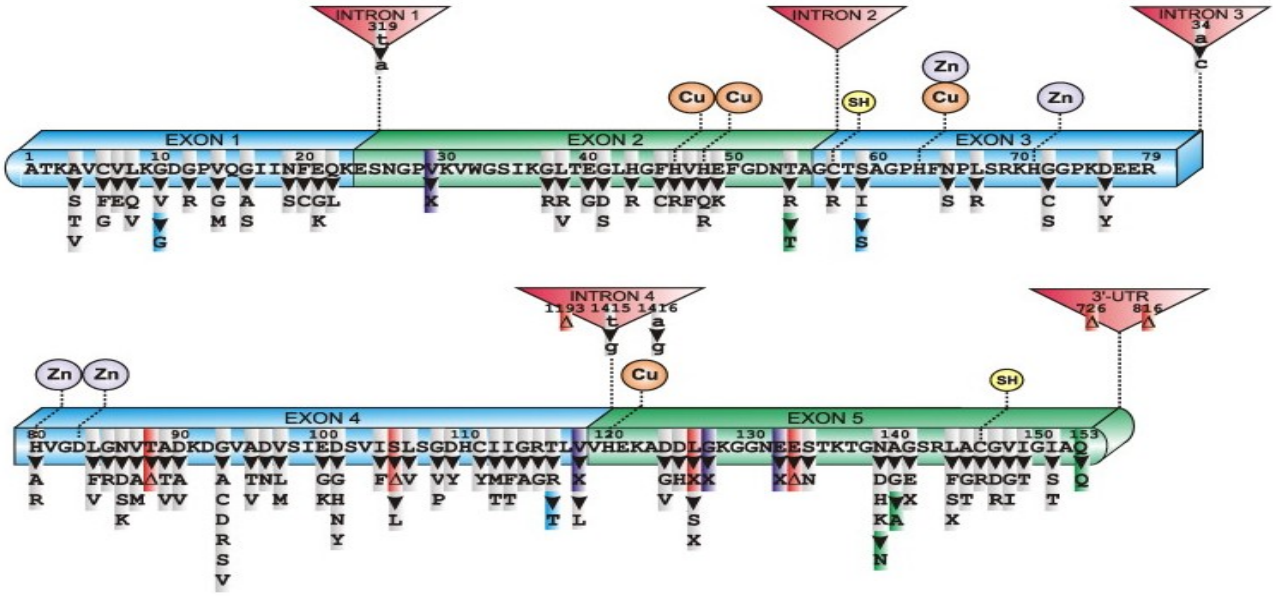


Figure 3: Schematic diagram of human SOD1 primary sequence with exons, introns, metal binding domains (Cu, Zn), intramolecular disulphide bond (SH) and mutations linked to sporadic and familial ALS. Mutations are distributed throughout all exons with high prevalence in exons 4 and 5. No clear structure–function relationship to fALS appears evident. Mutation legend: grey, missense; purple, insertion; red, deletion; blue/green, silent; (D) in frame deletion; X, truncation [41].

Since some mutations concern the metal binding residues at the active site, while others may concern correct folding or stability of the homodimer, the biochemical and biophysical properties of ALS-associated mutant SOD1 proteins are rather heterogeneous [42]. In fact, studies on recombinant mutant SOD1 proteins have been proved that ALS-associated SOD1 mutations can be attributed at two mutant classes, the "wild type like" (WTL) SOD1 mutants which retain the ability to bind copper and zinc and exhibit normal specific activity, indicate a native-like structure with only subtle changes to the backbone fold, in contrast the "metal-binding region" (MBR) SOD1 mutants that are deficient in copper and zinc and exhibit severe thermal destabilization and structural disorder of conserved loops near the metal-binding sites [43]. G93A and H80R SOD1 mutants belong respectively to the two classes of mutants described above.

There is no clear correlation between enzyme activity, clinical progression and disease phenotype [44]. ALS cases linked to SOD1 mutants show ample variation in the phenotype in the age of onset, severity, rate of disease progression and duration. However, patients carrying the A4V missense mutation (the most common SOD1 mutation in North America) have shorter survival with death occurring in less than one year after the diagnosis and limited upper motor neuron involvement [45], while D90A mutation (the most common SOD1 mutation worldwide and in the sporadic

population) correlates with non-penetrant or slowly progressive disease. Remarkably, 2‑3% of the population, in northern Scandinavia, is heterozygous for the D90A mutation, which is a benign polymorphism [46]. However, homozygous individuals for D90A in that region develop slowly progressive motor neuron disease with prominent corticospinal signs and prolonged survival of more than a decade. By contrast, patients who are D90A heterozygotes outside this genetic pool develop classic ALS with survival times of 3‑5 years [47].

It is important to note that some SOD1 mutations can remain asymptomatic throughout life, suggesting that not all SOD1 mutations cause ALS onset and some are rather polymorphisms. The clinical phenotype associated with a certain mutation in the SOD1 gene is obviously not only dependent on the mutation itself, but may also be influenced by the genetic background of the patient as well as by environmental factors [48].

Up to date, there is no conclusive explanation about how the SOD1 mutations cause ALS onset. At first, it was hypothesized that mutations would impair the enzymatic activity of the SOD1, thus resulting in increased cellular levels of reactive oxygen species (ROS), oxidative stress and then neuronal death [49]. However, results obtained through both *in vitro* and *in vivo* experimental models has provided numerous evidences that led to abandon this initial hypothesis in favour of a new hypothesis that result into the acquisition of a novel toxic function to motor neurons (gain-of function hypothesis). In fact, it has been demonstrated that the overexpression of SOD1 WTL-mutants in cell models induces apoptosis in neurons [50] and that SOD1 knockout mice do not develop motor neuron disease [51].

To date, different hypothesis have been made to explain the SOD1 toxicity. The aggregation hypothesis is particularly attractive because protein aggregates are frequently associated with neurodegenerative diseases as ALS [5]. Numerous studies revealed that SOD1 mutant is incline to misfolding and to form cytoplasmic aggregates. In turn, these aggregates could lead to cell death by sequestering other cytoplasmic proteins essential for neuronal survival, by clogging the ubiquitin/proteasome system, by chaperones depletion, or by disrupting mitochondria, cytoskeleton and/or axonal transport [52]. Another hypothesis was that the misfolding of SOD1 induced by mutations would allow the access of abnormal substrates such as peroxynitrite to the catalytic site leading to the nitration of tyrosine residues [53].

## *1.4 ALS6/Fused in sarcoma/Translocated in liposarcoma (FUS/TLS).*

### *1.4.1 Structure and functions.*

FUS/TLS (Fused in sarcoma/Translocated in liposarcoma, also called FUS) was originally discovered as a result of characteristic chromosomal translocations in myxoid liposarcoma [54]. The gene is located in chromosome 16 (16p11.2) and consists of 15 exons that encode for a 526 amino acid protein, member of the TET family, a family of proteins implicated in various roles of gene expression [55,56]. It is characterized by an N-terminal transactivating domain enriched for glutamine, glycine, serine, and tyrosine (QGSY region), a glycine-rich region (GRR) followed by a RNA recognition motif region (RRM) which contains a nuclear export signal (NES) near its 5' end, a multiple arginine/glycine/glycine (RGG rich) repeats containing a zinc finger (ZnF) domain, and finally a nuclear localization signal (NLS)[57,58] (Fig. 4).

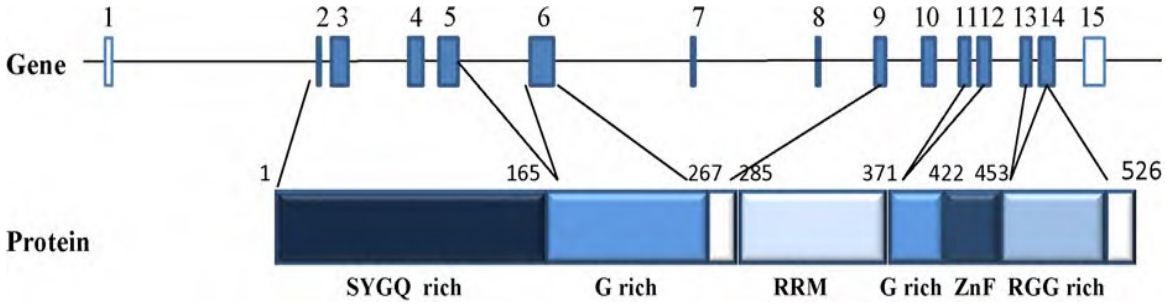


Figure 4: Genomic and structural organization of human FUS/TLS gene and protein. FUS/TLS gene is encoded by 15 exons that cover an 11.6 kb region on chromosome 16p11.2. Protein coding exons (filled boxes) and non-coding exons (open boxes) are drawn to scale. SYGQ rich: serine–tyrosine–glycine–glutamine rich domain; G rich: glycine rich domain; RRM: RNA recognition motif; ZnF: cysteine2/cysteine2 zinc finger motif; RGG rich: arginine–glycine–glycine rich domain [59].

FUS is an ubiquitously expressed and highly conserved multifunctional protein, mostly localized into the nucleus and with low levels in the cytoplasm. The precise role of FUS is not fully elucidated but it is now known that it is involved in multiple levels of RNA processing including transcription, splicing, transport and translation [60]. FUS acts also as a transcription regulator. It interacts with several gene-specific transcription factors such as NF-κB and it is also associated with the general transcriptional machinery and may influence transcription initiation and promoter selection by interacting with RNA polymerase II and the TFIID complex [61,62]. Less is known about the role of FUS in splicing regulation. Proteomic analysis identified this protein as part of the spliceosome machinery [63]. It has been shown that FUS associates in vitro with large transcription–splicing complexes that bind the 5' splice sites of pre-mRNA [64] and has been also proposed to directly bind pre-mRNA 3' splice site [65]. FUS seems to play roles in micro-RNA processing. It has been found (by mass spectrometry) associated with Drosha, the nuclear RNase

III-type protein that mediates the first step in miRNA maturation [66]. FUS plays also a cytosolic role in regulation of RNA subcellular localization, translation and decay. In particular, FUS was shown to relocalize to the cytoplasm upon inhibition of RNA polymerase II transcription [67] and increasing evidences suggest that it is integral component of RNA stress granules (SGs), cytoplasmic microscopically visible foci consisting of mRNA and RNP complexes that stall translation under stress conditions [68]. Furthermore, several lines of evidence suggest that FUS is required for the maintenance of genomic integrity and may have a role in DNA double-strand break repair. Indeed, FUS promotes the annealing of homologous DNA and the formation of DNA D-loops, an essential step in DNA repair by homologous recombination [69].

### *1.4.2 FUS mutations.*

About 5% of all fALS and 1-2% of sALS cases are due to mutations in the locus ALS6 on chromosome 16 that codes for FUS (Fused in Sarcoma, OMIM #608030). After the first report in 2009 by two independent groups [70,71], a total of 47 mutations have been described in ALS patients, among these the majority are missense mutations, but they also include deletions (only R495X), truncations and in-frame insertions[72]. Almost all of the pathological mutations show an autosomal dominant inheritance pattern except for one recessive mutation (H517Q) found in a family of Cape Verdean origin [70]. Most of FUS ALS-linked mutations are clustered at the C-terminal domain of the protein and in particular in the Nuclear Localization Signal (all 5 the arginines in this region have been identified to be mutated in ALS). The majority of the other ALS associated FUS mutations occur in the GRR (Fig.5). The redistribution of the protein from the nucleus to the cytoplasm is related to the onset and progression of the disease and mutations that affect amino acid residues responsible for the binding to Transportin receptors (thus affecting the nuclear import of the protein) result in a more severe disease progression [73].

The site and age of disease onset are variable within families, and incomplete penetrance has been documented for several FUS/TLS mutations, which may account, at least in part, for the absence of family history in sporadic patients. Interestingly, several patients harbouring the same R521C mutation developed an unusual presentation including an early-onset drop-head syndrome [74,75].

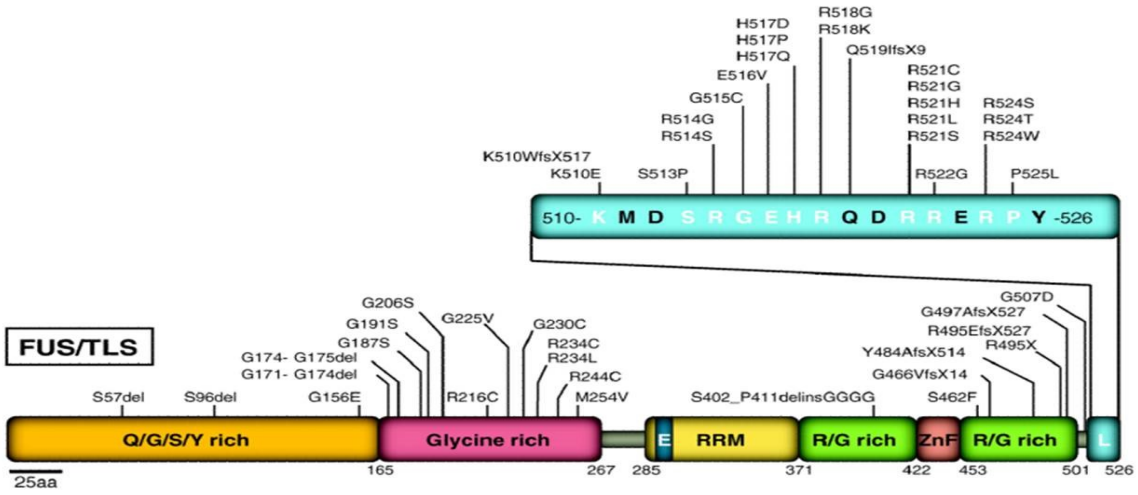


Figure 5: FUS mutations in ALS. Forty-seven mutations have been identified in FUS/TLS in sporadic and familial ALS patients. Most mutations are clustered in the last 17 amino acids and in the glycine-rich region and the putative prion domain comprises amino acids 1–239 [76].

This is an atypical phenotype, as only 1% of ALS patients present with severe weakness of neck extensor muscles in the early stage of the disease course [77]. Most patients with FUS develop a classical ALS phenotype without cognitive defect. The truncating mutation R495X and the missense mutation K510R, discovered in four German ALS families, were associated with an aggressive disease course and with a mild phenotype with disease duration ranging from 6 to 8 years, respectively [78]. Analysis of brain and spinal cords from patients with FUS mutations revealed normal nuclear levels in the nuclei of many neurons and glial cells, but with FUS cytoplasmic aggregations in neurons [71,70]. It has not been reported if FUS inclusions are also present in glial cells. Cytoplasmic inclusions of FUS protein are absent in controls, in patients with SOD1 mutation and in sporadic ALS cases that are presumably positive for TDP-43 aggregations. Importantly, TDP43 positive inclusions are absent in FUS mutant patients, implying that neurodegenerative processes driven by FUS mutations are independent of TDP-43 aggregation [71].

## *1.5 ALS10/Transactive response DNA-binding protein-43 (TARDBP-43/TDP43).*

### *1.5.1 Structure and functions.*

TAR-DNA binding protein (TARDBP or TDP43) was identified in 1995 as a 43-kDa cellular factor binding TAR regulatory sequence of LTR in HIV-1 virus genome. The gene is located on chromosome 1 (1p36.22) and consists of 6 exons that encode for a 414 amino acid protein, member of the family hnRNPs, RNA binding proteins family [60] containing a nuclear export signal (NES) and a nuclear localization signal (NLS), that enable it to shuttle between the nucleus and the cytoplasm, potentially to transport bound mRNAs [79], two RNA recognition motifs (RRM1 and 2),

able to interacts with RNA and DNA, and a C-terminal glycine-rich region which is able to mediate protein–protein interactions [80,81] (Fig. 6).

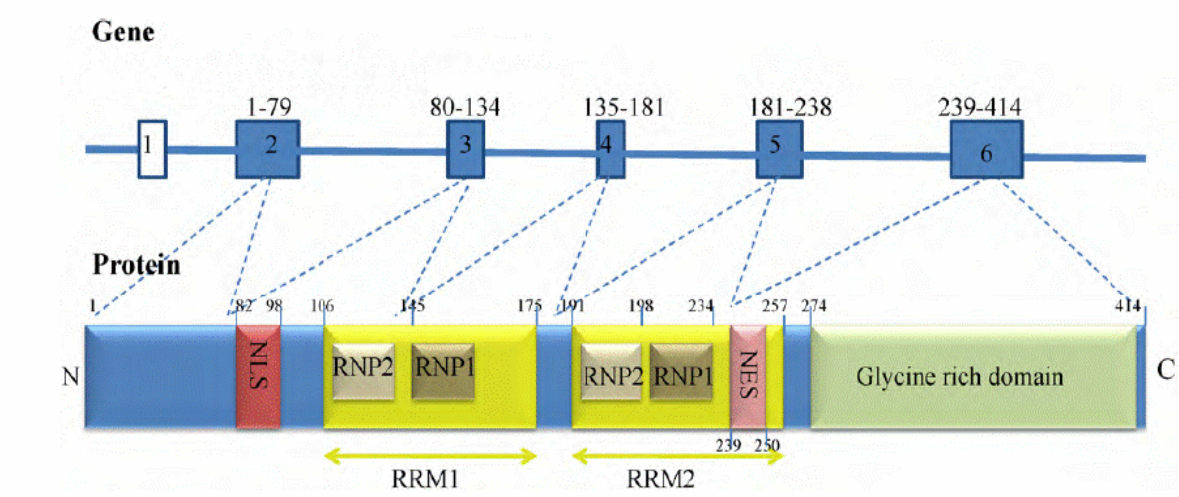


Figure 6: Schematic diagram of the TARDBP gene and TDP-43 protein. Exon 1 of TARDBP is non-coding and exons 2–6 are protein coding. TDP-43 contains five known functional domains: nuclear localisation signal (NLS), nuclear export signal (NES), two RNA recognition motifs (RRM1 and RRM2) and a glycine-rich C-terminal region. Each RRM has two highly conserved regions, ribonucleoprotein 1 (RNP1) and ribonucleoprotein 2 (RNP2) [82].

TDP-43 is predominantly localized into the nucleus with low levels in the cytoplasm. TDP-43 is a multifunctional protein involved in various steps of RNA processing including transcription, pre-mRNA splicing, mRNA transport and translation, although the exact cellular functions remain elusive [82]. TDP43 acts as a transcription factor and has been shown to bind to chromosomally integrated TAR DNA to repress transcription of HIV-1 [80]. It has also been shown to bind to the promoter of the mouse SP-10 gene, which is required for spermatogenesis. The C-terminal domain of TDP43 is involved with exon skipping and splicing inhibitory activity through the interaction with other hnRNP family proteins [60]. TDP43 also plays a role in RNA post-transcriptional regulation. TDP43 is recruited to stress granules (mRNA and RNP complexes where protein synthesis is temporarily arrested), indicating that TDP43 may play a protective role against cellular insult [83]. TDP43 may play a role in microRNA biogenesis and processing as it has been found to associate with Drosha, the RNase III enzyme responsible for initiating the processing of miRNA [60]. Independent studies using knockout mouse models have shown that TDP43 protein is essential for normal prenatal development and viability [84]. Knockdown of TDP43 in human cells resulted in cell cycle disruption and increased apoptosis, thereby demonstrating a critical role for TDP43 in cell survival possibly through maintaining genomic stability [85]. TDP43 silencing in human embryonic kidney (HEK293) and neuronal (SH-SY5Y) cells has resulted in downregulation of HDAC6, a protein necessary for protein aggregate formation and degradation [64].

### *1.5.2 TDP43 mutations.*

In early 2008, the successful identification of dominant mutations as a primary cause of ALS provided evidence that aberrant TDP43 can directly trigger neurodegeneration. Up to date, more than 40 mutations have been found in the locus ALS10 (OMIM #612069) of ALS patients, accounting for about 5 % fALS cases and 2% of sALS [86]. Most of the mutations identified are localized in the glycine-rich region encoded by exon 6 (Fig. 7). All mutations are dominant missense changes with the exception of a truncating mutation at the extreme C-terminal of the protein (Y374X) [87]. Several variants lying in the non-coding regions of the TARDBP gene have been identified in patients but further studies are necessary to prove their pathogenic effect [88,89].

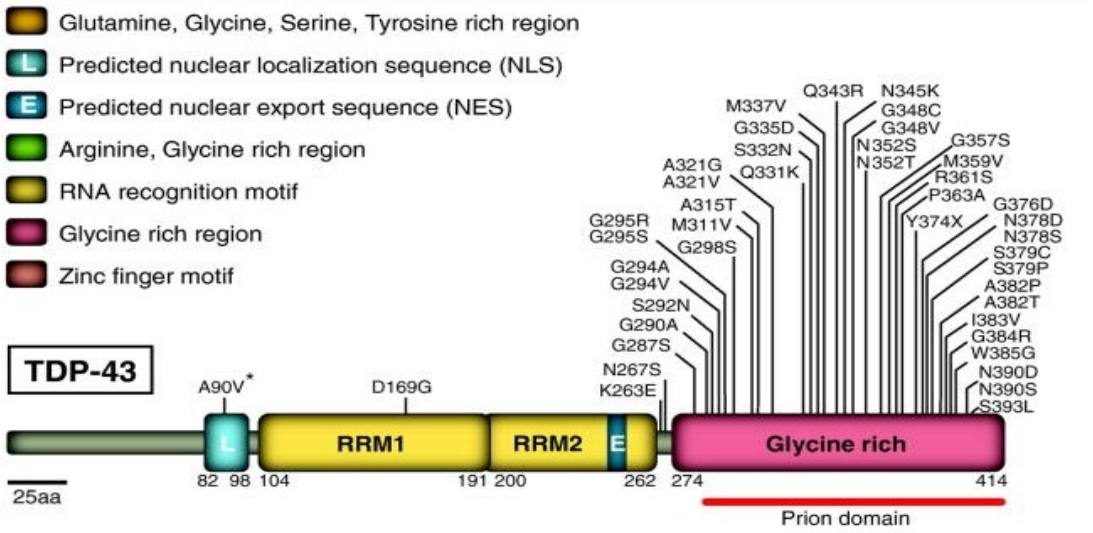


Figure 7: TDP43 mutations in ALS. Forty-four mutations have been identified in TDP43 in sporadic and familial ALS patients, with most lying in the C-terminal glycine-rich region. All are missense mutations, except for the truncating mutation TDP43$^{Y374X}$. Abbreviations: NLS, nuclear localization signal; NES, nuclear export signal [76].

Most patients with TDP43 mutation develop a classical ALS phenotype without cognitive deficit, with some variability within families in the site and age of onset [90,91]. The A382T mutation, first identified in two fALS cases from France [92], has the highest prevalence since it was then described in 48 fALS families and 47 sALS. Interestingly, the A382T mutation was identified as a founder mutation in ALS patients from Sardinia, where 40 fALS and 30 sALS cases shared this mutation. The mutational frequency for A382T is about 30% in Sardinia (50%–80% fALS, 9%–23% sALS) [93,94]. Geographically, most of the mutations identified were in ALS patients from Europe. However, a considerable number of ALS patients with TDP43 mutations have been identified in patient cohorts from Japan, Australia, North America, and China, suggesting that TDP43 mutations are a global cause of ALS [95].

Postmortem analysis of patients with TDP43 mutations found a pattern similar to the TDP43 pathology described in sporadic ALS and FTLD patients. TDP43 inclusions are not restricted to

motor neurons but can be widespread in brain in ALS patients with or without dementia [96,97]. A very curious, and mechanistically unexplained, aspect of TDP43 pathology is a significant TDP-3 nuclear clearance in a proportion of neurons containing cytoplasmic aggregates, suggesting that pathogenesis may be driven, at least in part, by loss of one or more nuclear TDP43 functions [98,99]. Although a plethora of early reports did not establish how prominent this nuclear clearing was and whether it escalates in frequency during disease progression, further efforts, especially the work of Giordana et al. [97], have established that the cytoplasmic redistribution of TDP43 appears to be an early event in ALS. The pre-inclusions and the larger TDP43 inclusions are only partially labelled with anti-ubiquitin antibodies [97], whereas intranuclear and cytoplasmic inclusions are strongly recognized by phosphorylation-specific antibodies to TDP43 [100,101]. Interestingly, the composition of TDP43 inclusions seems to differ between cortical brain and spinal cord in ALS patients, as inclusions from cortical regions are preferentially labelled by C-terminal antibodies, whereas spinal cord inclusions display equivalent immunoreactivity between N- and C-terminal-specific antibodies [99]. In accordance with this, spinal cord extracts showed an absence or only weak accumulation of 25 kDa CTFs compared with brain extracts [101].

## *1.6 ALS experimental models.*

In order to better understand the pathophysiological processes of the ALS onset, have been created over the years several model systems such as cell lines and transgenic animals, expressing different ALS-causative genes (SOD1, FUS and TDP43) in the wild type form or with the several pathological mutations.

### *1.6.1 Cellular and animal models for SOD1.*

Over time, several cellular models stably or transiently espressing the SOD1 gene linked to ALS have been generated. These have helped to elucidate the molecular cascade of events able to induce cellular toxicity and the cellular mechanisms of disease [35].

The first model of motor neuron degeneration SOD1-related was created inhibiting chronically SOD1 expression through the use of antisense oligodeoxynucleotides or diethyldithiocarbamate in organotypic cultures of spinal cord. This study showed that chronic inhibition of SOD1 was able to induce the apoptotic degeneration of spinal neurons, including motor neurons, and that the degeneration increased when it was also inhibited glutamate transport [102]. The same results were obtained in a study conducted on PC12 cells (rat pheochromocytoma cells), where it has been observed apoptotic cell death after downregulation of the SOD1 expression [103]. Recently it was shown that the expression of SOD1-G93A, in co-cultures of human glioblastoma and

neuroblastoma cells, induces caspase-1 activation, release of cytokines and activation of apoptotic pathways, as also confirmed for other pathological mutants related to fALS (G37R, G85R and I113T) [15].

A limit of transient or stable transfection experiments both in human and mouse cells is the low endogenous gene expression level due at the low efficiency of conventional transfection methods. In recent studies it was tried to solve this problem by infecting different cellular models with replication-deficient recombinant adenoviruses, encoding for wild type SOD1 or with pathological mutations, to obtain similar expression levels both exogenous and endogenous SOD1 proteins. In an *in vitro* cell culture system, it has been revealed that infection of mouse NSC-34 motor neuron-like cells with adenovirus encoding for mutant SOD1-G93A gene increased cellular oxidative stress, mitochondrial dysfunction, cytochrome c release and motor neuron cell death [104].

The animal models if compared to cellular models allow to more closely mimic the human disease and to follow the trend of disease in order to develop effective therapies. Up to date, several transgenic mouse and rat strains were created by the introduction of the sequence coding for human SOD1 under the control of a promoter that enables ubiquitous expression of the transgene. Unlike SOD1 knockouts, transgenic mice and rats with human fALS–SOD1 added to their own enzyme exhibit the ALS-like clinical features: hind limb weakness and muscle tremor followed by more severe manifestations such as progressive motor paralysis, inability to walk, drink and eat, and death within some week. Differences in the age of disease onset among these strains seem to depend primarily on the transgene copy number, mice with high transgene copy numbers are affected by early onset, while mice carrying small transgene copy numbers are affected by late-onset, slowly progressive disease [105,106]. Moreover, several biochemical alterations observed in patients are, in most cases, preserved in these models such as the appearance of oxidative-stress markers, alterations of mitochondria in motor neurons and muscle and the activation of phosphorylation cascades [107]. Several transgenic lines have been developed, carrying mutations at different positions in SOD1. There are, however, some differences between the various mutant SOD1 mouse strains depending especially on the mutation and copy number of the transgene [37]. For example, the progression of the disease is much more rapid in transgenic mice for the G86R mutation of the mouse SOD1 (three days) or for the human G85R mutation (7–14 days) than in mice that are transgenic for human SOD1-G93A (60-110 days) [106].

Transgenic mice carrying 20 copies of SOD1 with the G93A mutation are the most extensively studied. The progression of symptoms in these mice is preceded and paralleled by a sequence of structural and functional alterations of motor neurons. As for other diseases, the great advantage

of animal models that mimics human pathology is the possibility to follow the stepwise progression of the disease for the design of potential therapeutic strategies. However, the expression levels of mutant SOD1, in heterozygous ALS patients, needed to exert its toxic effects is much lower than for transgenic rodents. In fact, in these models is necessary an increase about 10-30 fold of mutant protein level to induce the pathological phenotype. This is due to differences between mice and man and it should not be overlooked when using mice models [5].

### *1.6.2 Cellular and animal models for FUS.*

To date, the role of FUS in ALS pathogenesis has not been established. It has been suggested that the toxicity of FUS could be the result of a gain-of-function for this protein, instead if mutated is possible a loss of function probably through its sequestration in stress granules. The generation of cellular and animal models of FUS could be provide several key insights into understanding the molecular mechanisms that might contribute to ALS pathogenesis.

Due to ALS-linked mutations, FUS becomes redistributed to the cytoplasm, a consistent observation well documented in human FUS-related ALS patients [70,71]. These observations suggest that the cytoplasmic localization of mutant FUS might be a pre-requisite for causing toxicity. In several cell culture experiments have been analyzed the effects on subcellular localization of FUS carrying different C-terminal NLS mutations. Strong cytoplasmic localization was seen in transfected murine N2a cells when a consensus nucleotide of the NLS was mutated (the strongest effect corresponded to human FUS amino acids K510, R522 and P525). Mutations in the NLS that are not part of the consensus sequence gave weaker cytoplasmic localization [108]. Studies on stable HEK-293 cell lines that express GFP-tagged FUS constructs, including wild type FUS or mutants, revealed a mutant-specific response to cellular stress that leads to the incorporation of cytoplasmic fALS-linked FUS protein into stress granules. The same results have been confirmed injecting mRNAs encoding GFP-FUS (WT or mutants) in zebrafish eggs at the 1–2 cell stage [109]. Several groups have generated a yeast model of FUS-related neurodegeneration by expressing WT and disease associated FUS. Yeast cells expressing the C-terminal fragment with the zinc finger and GRR domain of FUS with ALS-associated mutations causes cytotoxicity under certain conditions [110]. Another study has demonstrated that FUS localized to the cytoplasm and nucleus when expressed starting from a weak promoter, suggesting that the FUS expression level is an important determinant of localization and aggregation of FUS in yeast cells. It is possible that the non-canonical NLS of FUS might not be functional in yeast cells or that predominant nuclear localization of FUS requires additional factors such as post translational modifications [110,111].

Drosophila models of FUS related neurodegeneration were recently generated that recapitulate several features of the human disease [112,113]. In one study, ectopic expression of FUS with ALS linked mutations in the fly eyes caused moderate to severe external eye degeneration when compared to ectopic expression of FUS WT. Interestingly, targeted expression of FUS in the fly brain and motor neurons led to the pupal lethality and larval locomotor defects. Conditional expression of mutant FUS in neurons drastically reduced the life span and adult climbing abilities as compared to FUS WT expressing animals [114]. Recently, it has been demonstrated that knocking down endogenous FUS in zebrafish leads to defects such as motor neuron degeneration, hyperbranched axons from motor neurons and behavioural phenotypes such as a defect in touch-evoked escape response, suggesting that loss of FUS function can lead to neurodegeneration [115]. These observations are further supported by another study where knocking out endogenous cabeza (the fly homologue of human FUS) can cause motoneurons degeneration in Drosophila [113]. Interestingly, the motor phenotypes caused by zebrafish FUS knockdown can be rescued by expressing human FUS WT, suggesting that human and zebrafish FUS are functionally related proteins. Furthermore, the expression of the ALS-linked mutation R521H also leads to motor neuron phenotypes, indicating that FUS with disease-causing mutations acquires a toxic gain of function. Two independent groups have generated FUS knock out (KO) mouse models long before the identification of ALS-linked mutations in FUS. The FUS KO mice were smaller in size as compared to non-transgenic animals, they have shown a chromosomal abnormalities indicating that FUS plays an important role in the stability of the genome and a complete male sterility and reduced fertility in females indicating that FUS is required for normal development and fertility. Many of them died within 16 h of birth, suggesting that normal levels of FUS are required for viability of neonatal animals [116,117]. Studies on rat models have demonstrated that overexpression of FUS WT was enough to cause neurodegeneration at an advanced age with a moderate but significant loss of neurons in the brain. However, expression of mutant FUS led to severe neurodegeneration at an early age as compared to FUS WT expressing rats [118]. Moreover, only rats espressing mutant FUS have shown paralysis and accumulation of ubiquitinated proteins in the cortex and spinal cord. Interestingly, the ubiquitinated inclusions were only present in the FUS expressing cells, but there was no colocalization between FUS and ubiquitinated inclusions. The ubiquitinated inclusions have showed reactivity with a mitochondrial marker protein in this rat models of mutant FUS, suggesting that damaged mitochondria might be ubiquitinated and subsequently degraded [118].

### *1.6.3 Cellular and animal models for TDP43.*

More and more groups are engaging in research that examines the role of TDP43 in the pathogenesis of ALS. An increasing number of disease cellular or animal models have been set up to provide insights into the molecular mechanism of ALS with TDP43 proteinopathy. Nonetheless, the exact role of TDP43 in the pathogenesis of FLTD/ALS still has not been fully unravelled and probably both a gain of toxic properties and a loss of function via its sequestration in aggregates could be possible.

In several cell culture experiments, the expression of TDP43 proteins carrying mutations that disrupt its NLS led to localization primarily within the cytoplasm [119]. A study on rat primary cortical neurons, through an automated microscopy system for long-term visualization, has shown that overexpression of wild-type TDP43 led to increased cytoplasmic localization of TD-43 and cell death independently of mutation, pathogenic TDP43 mutations increased the proportion of cytoplasmic TDP43 [120]. As reported in different studies the overexpression of WT or mutant hTDP43 in transgenic mice induced motor dysfunction, such as gait disorders. In particular, it has been shown that moderate expression of hTDP43 (about 2.5 fold) can promote cytoplasmic TDP43 expression, TDP43 truncation, TDP43 phosphorylation and TDP43 aggregation, which mimics the TDP43 proteinopathy in CNS of ALS. Besides TDP43 proteinopathy, abnormal mitochondrial aggregation is observed in hTDP-43-overexpressing transgenic mice, indicating the involvement of TDP43 in mitochondrial trafficking [121,122]. The overexpression of WT-hTDP43 or mutant hTDP43 in rat models increases cytoplasmic TDP43 expression. However, only rats expressing mutant hTDP43 (M337V-hTDP43) exhibited significant motor dysfunction, which is different from other mouse models. M337V-hTDP43 expression in rat also reproduces the biochemical features of ALS including hyper phosphorylation of TDP43, formation of TDP43 inclusion and expression of truncated TDP43. Most importantly, the ubiquitous expression of M337V-hTDP43 in rat is seen to cause more severe neurodegeneration in the motor system than in the CNS [123]. Similar results were also obtained non-human primate models [124] and on non-mammalian transgenic animal models as *C. elegans* [125], Zebrafish [126] and Drosophila [127].

Fragments (20–25 kDa) containing the carboxy-proximal portion of TDP43 accumulate in detergent (sarkosyl)-insoluble fractions derived from patient CNS tissues. The truncated TDP43 (~25 KDa) has been involved in disease progression by gain of toxic function [98]. When expressed in cells, the 25 kDa CTFs recapitulate some of the pathological features such as increased cytoplasmic accumulation, insolubility, hyperphosphorylation, polyubiquitination and cytotoxicity [99,128]. Transgenic mice expressing the 25 kDa C-terminal fragment of TDP43 develop cognitive deficits

without cytoplasmic TDP43 inclusions and trigger the processing of endogenous TDP43, which suggest that TDP43 inclusions are independent of cognitive dysfunction [129,130]. Caspase-3, which is activated during apoptosis, has been proposed to be the main protease generating the 25 kDa CTF in cells [128,131]. The role of TDP43 ubiquitination in disease pathogenesis remains unknown, although it is likely to be a late event, since in patients the pre-inclusions and most TDP43 inclusions are either weakly or not at all ubiquitinated [97,100]. Nevertheless, extensive ubiquitination of the pathologic CTFs in cells [132] suggests that cellular degradation machineries such as the ubiquitin-proteasome system (UPS) and/or autophagy [133] may be involved in removing TDP43 aggregates.

To investigate the linkage between the loss-of-function of TDP43 and pathological features ALS, TDP43 knockout models have been created. TDP43 is important for early embryonic development, in fact TDP43 knockout in mice would result in peri-implantation lethality [84]. Targeted depletion of TDP43 in motor neurons could trigger mice with age-dependent progressive motor neuron degeneration, muscle atrophy and motor dysfunction, which are reminiscent of human ALS patients. These findings indicated that TDP43 might be important for the long-term maintenance of motor neuron [134 135]. Therefore, the mouse model with depletion of TDP43 expression in motor neuron not only has a longer lifespan compared to the whole body knockout, but also could be a valuable model for studying the role of TDP43 in motor neurons [136].

Further studies on the molecular mechanism of ALS with TDP43 proteinopathy are needed.

## *1.7 Physiopathological mechanisms of ALS.*

Current hypotheses on biology underlying both sporadic and familiar ALS forms in humans outline a complex model in which non-competing mechanisms including not only gene mutations and environmental factors but also oxidative stress, protein aggregation, excitotoxicity, changes in the ubiquitin-proteasome system and autophagy pathways, defects in RNA metabolism, abnormal axonal transport, as well as neuroinflammatory processes involving astrocytes and microglia, are likely to converge in various unfortunate patterns to mediate selective motor neuron degeneration (Fig. 8).

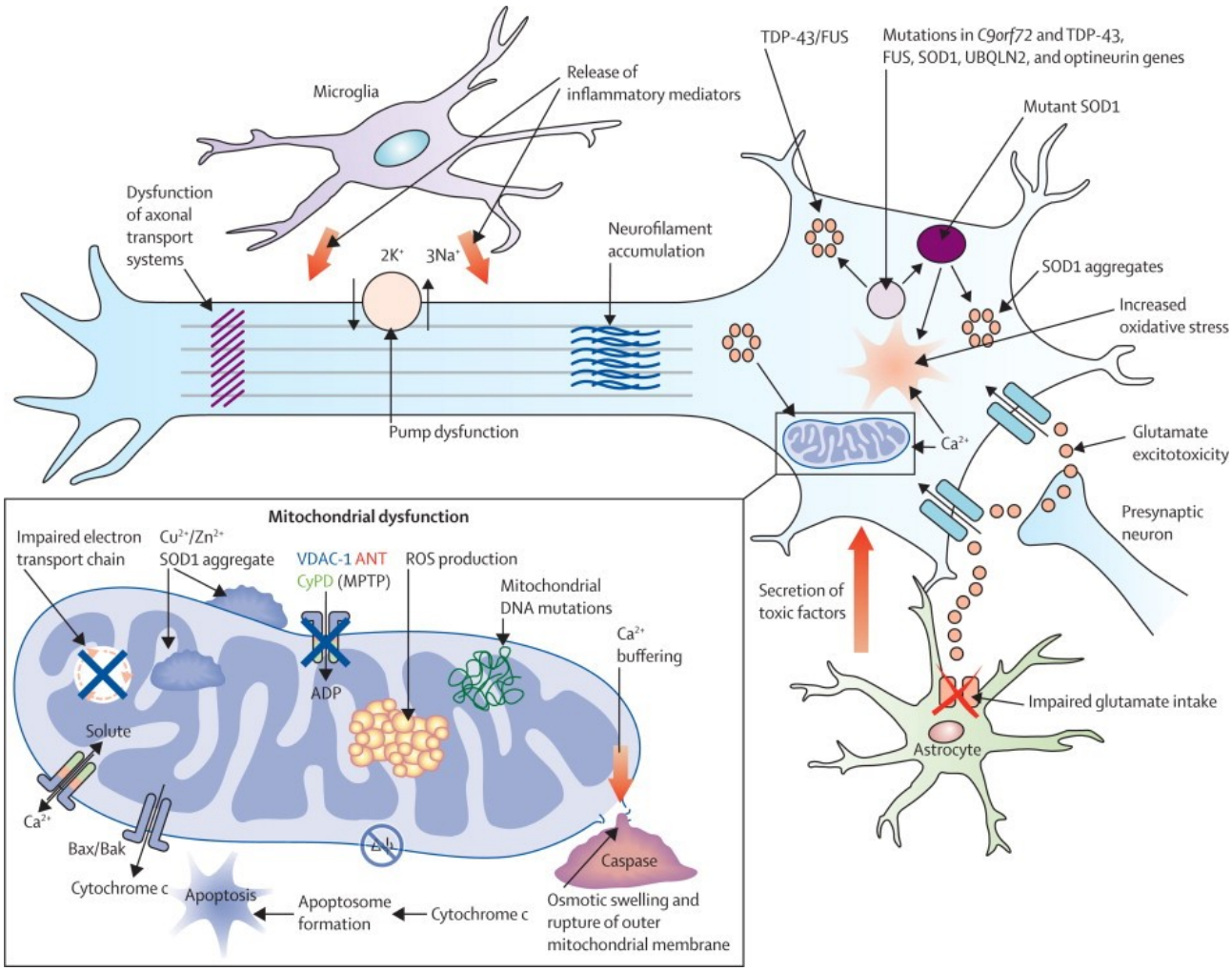


Figure 8: Proposed mechanisms underlying neurodegeneration in ALS. Many of these pathways are mechanisms of cell death common to a range of neurological disorders, although in the case of amyotrophic lateral sclerosis (ALS), have been derived from studies undertaken predominantly using the SOD1 mouse model. Pathophysiological mechanisms involving more recent genetic discoveries, particularly the *C9orf72* hexanucleotide repeat expansion, have yet to be elucidated. Neurodegeneration in ALS might reflect combinations of glutamate excitoxicity, generation of free radicals, mutant SOD1 enzymes, along with mitochondrial dysfunction and disruption of axonal transport processes through accumulation of neurofilament intracellular aggregates. Mutations in several ALS-related genes are associated with the formation of intracellular aggregates, which appear harmful to neurons. Activation of microglia results in secretion of proinflammatory cytokines resulting in further toxicity. Failure of cytoplasmic mitochondria induces increased susceptibility to glutamate-mediated excitotoxicity, perturbations in motor neuronal energy production, and apoptosis. Mitochondrial dysfunction is associated with increased production of reactive oxygen species (ROS). Cytoplasmic aggregates of SOD1 might directly inhibit conductance of VDAC1, thereby reducing the supply of ADP to mitochondria for ATP generation. $\Delta\ \psi$ =mitochondrial membrane potential [39].

### *1.7.1 Oxidative Stress.*

Oxidative stress arises when the levels of ROS/RNS exceed the quantities required for normal redox signalling. There has been particular interest in the role of oxidative stress in ALS but the exact role of ROS/RNS in disease processes is uncertain [137]. ROS are able to cause permanent oxidative damage to several cellular components such as proteins, DNA, lipids, and cell membranes [138]. They has been detected in the spinal cord and cerebrospinal fluid (CSF) of sALS

patients [139]. SOD1 and its antioxidant properties have been studied extensively from the perspective of redox regulation in ALS [140]. The first hypothesis proposes that mutations in SOD1 alter its ability to act as an antioxidant but further evidences showed that disease onset is not associated with its enzymatic activity [141]. However, mutant SOD1 could accept peroxynitrite or hydrogen peroxide as a substrate, and thereby catalyse the nitration of tyrosine residues of SOD1 and hydroxyradicals [53,142], in fact high levels of nitrotyrosine and nitrated proteins have been found in the CSF of both sALS and fALS patients [139].The second hypothesis suggests that mutant SOD1 fails to bind zinc correctly, allowing the rapid reduction of the SOD1-bound copper which catalyses the formation of superoxide anion rather than dismutation [143].

Mutant TDP-43 may be itself an inducer of oxidative stress, as suggested by studies in neuronal cells *in vitro* in which this protein was shown to down regulate heme oxygenase-1 [144] and in yeast, in which TDP-43 expression increased markers of oxidative stress and induced cell death [145].

### *1.7.2 Glutamate Excitotoxicity.*

Another component of neuronal degeneration in many neurodegenerative disorders is excessive glutamate-induced stimulation of postsynaptic glutamate receptors resulting in increased calcium intake and neuronal injury [146]. Glutamate uptake from most synapses in the CNS is controlled by excitatory amino acid transporter 2 (EAAC2; also known as SLC1A2 or GLT1) [147]. Increased levels of intracellular glutamate and decreased uptake of glutamate from the synapse have been observed in ALS patients [148]. Indeed, in most cases of sALS, and in transgenic rodent ALS models, there is a profound reduction in the expression and activity of EAAT2 in the cortex and spinal cord [149].

Excitotoxicity has provided one of the few examples of a mechanistic link between mutant SOD1 mediated the sporadic form of the disease. The presence of mutant SOD1 increases the sensitivity of motor neurons to glutamate toxicity [150], causes alteration in AMPA receptor subunit expression [151], and causes reduced expression of the major glutamate reuptake transporter EAAT2 [107]. Whether as a primary or a propagating process, it appears that glutamate toxicity plays a contributory role to the injury of motor neurons in ALS.

### *1.7.3 Mitochondrial Dysfunction.*

Numerous studies have focused on the role of the mitochondrion in the pathogenesis of neurodegenerative diseases like ALS. Indeed, mitochondrial alterations are observed in the spinal cord cells of SALS patients and role of mitochondria has been well studied in relation to ALS pathogenesis [152]. It has been demonstrated presence of abnormal and degenerate mitochondria

either in ALS patients [153] as well as in cellular and animal models of disease [154,155], although how is unclear relationship between non-functioning mitochondria and ALS onset.

In particular, expression of mutant SOD1 in motor neuron cell line (NSC34) results in the development of swollen mitochondria, impaired activity of complexes II and IV of the mitochondrial respiratory chain, impaired cellular bioenergetic status, and alteration in the mitochondrial proteome [156]. Similarly, G93A-SOD1 mice show reduced respiratory chain activity and reduced ATP synthesis [157]. Furthermore, recent studies have shown that overexpression of TDP-43 causes mitochondrial dysfunction and induces mitophagy in cell culture [158].The presence of ROS and impairment of the mitochondrial respiratory chain have also been observed in TDP-43 models [144].

Significantly, any pathological variations in regulation of the electron transport chain would result in more oxidative stress [159] causing further cellular redox dysregulation, leading to a potential vicious cycle of damage and degeneration.

### *1.7.4 Impaired Axonal Transport.*

Axonal transport is a key mechanism required for cellular viability in neuronal cells. The transport of molecules and organelles is a fundamental cellular process that is particularly important for the development, function and survival of neurons. Several findings indicate that dysfunction of axonal transport might contribute to the demise of motor neurons in ALS [155]. Firstly, neurofilaments (NF) accumulation in motor neurons is another histopathological hallmark of ALS [160] and transgenic mice that overexpress NF subunits in motor neurons develop a motor neuron disease with impaired axonal flow, as axonal defects cause delay in transportation of components required for the maintenance of axon [155]. Second, both slow and fast anterograde transport are slowed in transgenic G93A-SOD1 and G37R ALS mice prior to disease onset and these deficits are exacerbated. as the disease progresses [161]. Tird, retrograde transport is also disrupted in ALS mice [162]. A recent study demonstrated that oxidised wild-type SOD1 immunopurified from sALS patient tissues inhibited kinesin-based axonal transport in a manner similar to mutant SOD1 in fALS providing evidence for common pathogenic mechanisms in both sALS and fALS [163]. It has been showed that NF aggregations are associated with SOD1 and nitric oxide synthase activities leading to nitrotyrosine formation on NF [164]. Nitrotyrosine can inhibit phosphorylation of NF subunits and may alter axonal transport and initiate motor neuron death [164]. Taken together, these findings suggest a relation between redox regulation and axonal transport dysfunctions in ALS.

### *1.7.5 Inflammatory cascades and the role of non-neuronal cells.*

Recently there has been increasing interest in the possibility that non-neuronal cells, including activated microglia and astrocytes, may contribute to the pathogenesis or propagation of the disease process in ALS. Several studies on mouse models have indicated that expression of mutant SOD1 in neurons alone is insufficient to cause motor neuron degeneration and that participation of non-neuronal cells may be required [15].

Astrocytes have many functions relevant to motor neuron physiology. First, they express the most important glutamate transporter EAAT2/GLT-1, thus contributing to the clearance of this neurotransmitter; deficiency of astroglial EAAT2/GLT-1 causes severe motor neuron loss [165] and alteration of this transporter has been repeatedly invoked as a cause contributing to ALS [9]. Second, astrocytes are the major source of both trophic [166] and toxic factors [15] for motor neurons. Several cytokines have been proposed to play a role in ALS as reinforcing signals from glia cells, including interleukin-6 (IL6), tumour necrosis factor α (TNFα) and transforming growth factor β1 (TGFβ1) that were found increased in cerebrospinal fluid, plasma and epidermis from ALS patients, although with sometimes conflicting results [167]. In addition, the production of nitric oxide and the activation of cyclooxygenase type 2 (COX2) aggravate the toxic effects of mutant SOD1 in several experimental models for ALS. The production of all those proinflammatory mediators may be secondary to the induction of the transcription factor NF-κB, which is activated in the presence of reactive oxygen species (ROS) and by many other different signalling molecules associated with ALS onset and progression [168]. NF-κB activation has been observed in astrocytes from ALS patients and in human cells expressing mutant SOD1 [169]. NF-κB also regulates the expression of COX2 that may cause an increase in the synthesis of prostaglandins, which trigger astrocytic glutamate release and induce free radical formation, thus contributing to both excitotoxicity and oxidative damage. Indeed, treatment with COX2 inhibitors markedly protects motor neurones and significantly prolongs survival of ALS mice [170]. Surprising NF-κB downregulation in astrocytes, via expression of the dominant negative IκB-alpha-AA, fails to influence onset, severity, or progression of disease in a mutant SOD1-based ALS mice model [171].

Recently it has been shown that also microglia play a critical role as resident immunocompetent and phagocytic cells within the CNS. Activation is associated with transformation to phagocytic cells capable of releasing potentially cytotoxic molecules including reactive oxygen species, nitric oxide, proteases, and proinflammatory cytokines such as interleukin-1B, tumour necrosis factor a (TNFα), and interleukin 6 (IL-6) [172]. Given this, there is little doubt that activated microglia can inflict significant damage on neurons, but their role is complex and they are capable of stimulating

neuroprotective as well as neurotoxic effects. Proliferation of activated microglia is a prominent histological feature in the spinal ventral horn both in mutant SOD1 transgenic mice and in human ALS [173]. In the mice, microglial activation is present before the onset of significant motor neuron loss or motor weakness. Various inflammatory cytokines or enzymes are upregulated in the spinal cord of ALS patients (IL-6, IL-1β, cyclo-oxygenase 2 (COX2), and prostaglandin E2 (PGE2)) or, in the spinal cord of mutant SOD1 mice (IL-1β, TNFα, COX2, PGE2) [174]. Microglia appear to mediate the toxicity to neurons in patients with ALS by releasing factors that enhance glutamate toxicity [175]. In a recent study D'Ambrosi and colleagues have investigated about how mutant SOD1 affects P2 receptor-mediated proinflammatory microglial activation, considering that extracellular ATP is one of the most widespread microglia alarm signal endogenous to the CNS, and that ATP signaling evokes many proinflammatory functions of microglia. They observed up-regulation of P2X(4), P2X(7), and P2Y(6) receptors and down-regulation of ATP-hydrolysing activities in mutant SOD1 microglia. This potentiation of the purinergic machinery reflected into enhanced sensitivity mainly to 2'-3'-O-(benzoyl-benzoyl) ATP, a P2X(7) receptor preferential agonist, and translated into deeper morphological changes, enhancement of TNF-α and cyclooxygenase-2 content, and finally into toxic effects exerted on neuronal cell lines by microglia expressing mutant SOD1 [176]. The purinergic activation of microglia may thus constitute a new route involved in the progression of ALS to be exploited to potentially halt the disease.

### *1.7.6 Protein aggregation.*

Protein aggregates are often found in spinal motor neurons of all types of ALS patients. These inclusions contain many different proteins, some of which may have an intrinsic tendency to aggregate following mutation (such as SOD1, TDP-43 and FUS) while others may be simply entrapped in aggregates [177]. Now, there is hardly a general consensus on the assumption that the toxic function gained by SOD1 mutants is related by their tendency to aggregate and to mislocalize, as other ALS mutant proteins. This hypothesis is supported by the presence of intracellular cytoplasmic (but also mitochondrial) inclusions enriched in SOD1 protein in cellular models and in spinal cord motor neurons in animals as well as in motoneurons of ALS patients [177,178]. Over the years, several experimental evidences have been proposed to explain how aggregation of mutant SOD1 could be a major contributor to induce cellular toxicity in ALS patients, from the ability to sequester proteins required for normal motor neuron function [179], to the capacity to reduce proteasome activity needed for normal protein turnover and to inhibit

specific organelles function (as the mitochondria) by aggregation out or within the same organelles [156,180].

The fact that protein aggregation is a common theme in ALS and that the cellular degeneration in ALS depends upon the sensitiveness of motor neurons to protein aggregation is suggested also by the observation that, likewise to SOD1, also TDP43, FUS aggregate in tissues from ALS patients and models [181]. Anatomo-pathological observations of ALS-affected tissues showed that these two proteins abnormally aggregate as cytoplasmic inclusions (positive for ubiquitin, but negative for SOD1) and that ALS-related mutations seem to enhance the rate of aggregation [111,182]. Recently, it has been identified that aggregation of FUS and TDP43 relies on prion-like domains and that aggregated FUS or TDP43 can sequester native protein [183].

The formation of such intracellular aggregates may depend on the accumulation of misfolded proteins generated either as a direct consequence of mutation, or as a consequence of oxidative stress. In both instances, impairment of the ubiquitin-proteasome response (UPR) seems to play a major role. Not only ubiquitin-immunoreactive inclusions are the most frequently reported inclusions in all forms of ALS, but aggregates may be also reactive to p62, a protein which has a part in the formation of the sequestosome and in autophagy [184].

### *1.7.7 Misregulation in RNA processing.*

Two of the lately identified genetic factors in ALS, TDP43 and FUS, encode for proteins with an established role in RNA metabolism. Thus, RNA dismetabolism seems to be an important potential physiopathological mechanism in motoneurons degeneration. Since RNA metabolism involves several processes, such as pre-mRNA splicing, mRNA transport, translational regulation, or mRNA decay, the precise RNA pathway that is affected in ALS disease is still unclear, and it is not completely clear whether defects in RNA processing have a causative, direct role in the pathogenesis [3].

Under stress, a cell's top priority is to conserve energy and divert cellular resources toward survival and eventual recovery. In eukaryotic cells, a powerful way to conserve resources is rapidly assembly of non-translating mRNAs and their associated RNA-binding proteins into aggregate-like structures called RNP granules, including stress granules (SGs) [185]. In normal cells, TDP43 and FUS are nuclear proteins that can quickly be shuttled to the cytoplasm upon stress induction where they can rapidly associated with SGs [73,186]. Once the instigating stress resolves, SGs dissolve and TDP43 and FUS return to the nucleus. Thus, the nuclear-cytoplasmic shuttling of TDP43 and FUS, as well as their association with cytoplasmic SGs, are physiological and reversible processes.

However, in pathological conditions, the nuclear-cytoplasmic shuttling of TDP43 and FUS becomes dysregulated, possibly However, in pathological conditions, the nuclear-cytoplasmic shuttling of TDP43 and FUS becomes dysregulated, possibly owing to diverse genetic and environmental factors, or perhaps even aging itself [187]. Several models have been proposed to explain the role of FUS, TDP43, and SG biology in ALS pathogenesis: i) The gain-of-function (GOF) toxicity model asserts that pathological TDP43 or FUS aggregate in SGs, impeding normal SG-mediated RNA homeostasis. In this model, the excessive SG localization of FUS and TDP43 [109,188] might drive dysregulated assembly of inappropriate fibrillar aggregates [111], which perturb the localization of messenger RNPs (mRNPs) required for RNA processing and decay, thereby interfering with RNA sorting. If this process continues unabated, ultimately the assembly of translation initiation complexes could be affected by preventing the increase in local concentration of mRNAs and translation factors [189]. Finally, insoluble FUS and TDP43 aggregates alter SG dynamics even after stress resolution [190], resulting in SG persistence as has been observed in cells expressing ALS-associated TDP43 or FUS mutants [109,188]; ii) The cytoplasmic loss of function (LOF) model suggests that FUS and TDP43 are critical mediators of nuclear-cytoplasmic RNA transport and shuttling, which affect the physiology of SG formation during stressful conditions. TDP43 has been repeatedly demonstrated to have pronounced effects on SG dynamics, as delayed formation, reduced size, altered morphology, and limited stability of SGs are observed in HeLa cells and neuroblastoma cell lines depleted of TDP43 [191]. In addition, WT FUS appears to be recruited to dendrites by mGluR5 activation in neurons, where it mediates a rise in local RNA content, and FUS-null neurons demonstrate abnormal spine morphology and density [192], underscoring that loss of normal FUS function can contribute to pathogenesis; iii) Although the cytoplasmic LOF model is consistent with many aspects of TDP43 and FUS pathological interactions, both proteins have well established important nuclear roles as well, including premRNA splicing, RNA stability, and transcriptional regulation [60]. Thus, depletion of nuclear pools of TDP43 and FUS is likely to impact these essential functions. Moreover, ALS-linked mutations might even subtly impair nuclear TDP43 or FUS function in a manner that is selectively toxic for motor neurons upon aging and may not even require depletion of nuclear pools [193,194].

### *1.7.8 Autophagy dysfunction.*

It is known that autophagy is essential to neuronal homeostasis, and may in some settings be neuroprotective [133]. Mice with conditional knockout of Atg genes die prematurely with extensive neurodegeneration and ubiquitin-positive pathology, which illustrate the importance of autophagy

in neurodegeneration [195]. However, when autophagy is excessively induced or defective, it can result in autophagic cell death (type II cell death), which is defined by the massive accumulation of autophagosomes without nuclear condensation [196]. Growing evidence supports a role of autophagic dysfunction as a contributing factor in various neurodegenerative diseases associated with abnormal aggregation of disease-related mutant proteins [197]. Several important proteins including SOD1 and TDP43 have been identified within inclusions in both sporadic and familial ALS [47,98]. Studies report the altered autophagy in G93A mice that starts from the pre-symptomatic stage of the disease [198]. The number of LC3-labeled autophagic vacuoles is significant increased in the motor neurons of the spinal cords of G93A mice compared with the age-matched controls [198].However, it is not known whether the increased autophagic vacuoles in motor neurons are the result of autophagy induction or autophagy flux impairment. Furthermore, while autophagosomes are frequently observed in dying neurons, it is unclear whether autophagy actively participates in the process of motor neuron death in ALS. Accumulating evidence suggests that defects in autophagic flux or in specific autophagy-regulatory processes, rather than simply induction, may contribute to the motor neuron degeneration [199]. A recent report indicates that treatment of G93A mice with rapamycin significantly inactivates the mTOR signaling pathway, causes further accumulation of autophagic vacuoles, but fails to reduce the level of mutant SOD1 aggregates in the spinal cord of transgenic G93A mice [200]. This study indicates the possibility of abnormal autophagic flux in ALS. Recent studies show that inhibition of either the UPS or autophagy dramatically increases TDP43 aggregation, suggesting that TDP43 can be degraded by both degradative systems [201]. Autophagy induction by rapamycin is associated with reduced cytoplasmic TDP43 accumulation in neuronal cell lines [202]. In addition, an autophagy enhancer, trehalose, can reduce TDP43 aggregates by an mTOR-independent pathway way [203]. TDP43 aggregates co-localize with the marker of autophagy LC3 and the adaptor protein p62 [201,204]. Over-expression of p62 reduces TDP43 aggregation in an autophagy and proteasome-dependent manner [204]. A recent report demonstrates that mice overexpressing mutant TDP43 develop a progressive and fatal neurodegenerative disease reminiscent of ALS [205]. In this mice model, aggregates of ubiquitinated proteins selectively accumulated in spinal motor neurons and frontal cortex neurons [205](66). Because the ubiquitinated proteins are the substrates for both UPS and autophagy pathways, it is likely that mutant TDP43 may impair protein clearance pathways in motor neurons.

### *1.7.9 Apoptotic pathways.*

The apoptotic pathways play an essential part in several biologic events, including morphogenesis, cell turnover, removal of harmful cells, and balanced apoptosis is crucial to ensuring good health. There are two pathways of activation: i) intrinsic or death receptor pathway, cell death are initiated by the binding of a specific protein ligand to a cell surface transmembrane receptor; ii) extrinsic pathway or mitochondrial pathway, cell death are activated by perturbance of the mitochondria [206]. Both pathways induce activation of a series of proteases called caspases. Caspase 3 is the effector to both pathways and it is activated by caspase-8 in receptor pathway and by caspase-9 in mitochondrial pathway.

In mitochondrial pathway, caspase activation is mediated by an ATP-dependent multiprotein complex called *apoptosome*, which requires following release of cytochrome-c from mitochondria. In fact, Bcl-2 proteins family, located in the outer mitochondrial membrane, are important actors to prevent or permit apoptosis and to control release of cytochrome c [207]. The relative concentration of family members acts as a gauge for cell death. In fact, this family comprises antiapoptotic members (Bcl-2, Bcl-xL, Bcl-w, Bfl-1, and Mcl-1) that promote cell survival, and proapoptotic members (Bax and Bak) that act as death effectors [206]. The balance between pro- and antiapoptotic proteins (Bcl-2 family members) expressed in the outer mitochondrial membrane probably determines whether programmed cell death is initiated or whether the cell will survive [208].

Involvement of mitochondrial apoptotic pathway in ALS is reinforced by an extensive literature that has documented a plethora of apoptotic phenotypes in tissues from patients and transgenic mice, as well as in cultured cells overexpressing mutant SOD1s [177].

Alteration in the expression of the pro- and anti-apoptotic genes, activation of caspases and release of cytochrome-c have been found in the spinal cord of transgenic mice expressing SOD1 with the G93A mutation and in human ALS patients without SOD1 mutations [209,210]. It has demonstrated that overexpression of SOD1G93A requires the expression of Apaf1 to induce cell death [211] and that both WT and mutant SOD1 can bind Bcl2, providing evidence of a direct link between SOD1 and an apoptotic pathway [179]. Recent papers have investigated expression of the Bcl2 family members in spinal cords of transgenic SOD1G93A, SOD1WT and non-transgenic mice and it is resulted that Bcl2-A1 is the only member of this family to be upregulated in both asymptomatic and symptomatic G93A mice, through NF-kB-independent pathway, with a tendency to decrease in the final stages of disease. Interestingly, this upregulation is tissue specific, as Bcl2-A1 mRNA is increased neither in the brain nor in the muscle of G93A transgenic

mice. Moreover, induction of Bcl2-A1 in SOD1G93A transgenic mice occurs via NF-kB-independent pathway [212]. Moreover, it has been demonstrated in different cell cultures (NSC-34, undifferentiated and differentiated ETNA cells and primary cultures from spinal cords) that overexpression of Bcl2-A1 and SOD1G93A increases the level of cell death after exposure to TNF-α, a situation which mimics the condition of neuroinflammation occurring in ALS [212]. Furthermore, it has been reported in immortalized motor neurons (NSC-34) and transgenic mice expressing mutant SOD1, that up-regulation of Bcl2-A1 by mutant SOD1 is mediated by activation of the redox sensitive transcription factor AP1 and that Bcl2-A1 interacts with pro-caspase-3 via its C-terminal helix α9. Moreover, Bcl2-A1 inhibits pro-caspase-3 activation in immortalized motor neurons expressing mutant SOD1 and thus induction of Bcl2-A1 in ALS mice represents a pro-survival strategy aimed at counteracting the toxic effects of mutant SOD1 [213].

These observations, together with recent evidence on TDP43 models that has linked its overexpression with an increase cell death through up-regulation of Bim expression and down-regulation of Bcl-xL expression TDP43 models [214], argue for a primary role of mitochondrial apoptosis in ALS and suggest that other relevant pathways regulating mitochondrial apoptosis needs to be investigated to fully clarify this topic.

### *1.8 ALS therapeutic approaches.*

Up to date, the development of effective therapeutic approaches for ALS has been disappointing. Riluzole is the only approved treatment, it is a neuroprotective drug that blocks glutamatergic neurotransmission in the CNS but it showed limited therapeutic benefits with minimal effects on survival and no effect on muscle strength, quality of life or functional capacity, it prolongs life by only 2 to 3 months [215,216]. In recent years, several studies have enabled to better understand the molecular mechanisms underlying the neurodegenerative process and thus to identify new therapeutic targets and new therapeutic areas [217], among these we can mention:

- Stem-cell technologies represent a promising approach for treating ALS. Their developmental plasticity, i.e. the ability of stem cells to change their fate in response to extracellular signals, stimulated the performance of stem-cell trials in patients. It has been reported that transplantation of autologous mesenchymal stem cells into the spinal cord of ALS patients is safe and well tolerated [218]. However, preliminary stem-cell transplantation trials performed in ALS patients produced conflicting results, including with regard to efficacy of treatment [219]. The demonstration that a new pluripotent stem-cell type, namely induced pluripotent stem cells, may be generated from somatic cells, such as fibroblasts, by introducing the

transcription factors Oct3/4, Sox2, Klf4 and c-Myc, attracted a great deal of attention [220]. Moreover, the observation that induced pluripotent stem cells may be induced to differentiate into motor neurons brought new hope for ALS [221]. Nevertheless, whether these converted motor neurons can successfully rescue ALS awaits further validation [217].

- RNAi is a process by which noncoding micro RNA (miRNA) inhibits and regulates gene expression by binding mRNA [222]. Several hereditary neurodegenerative diseases are being targeted with RNAi therapy, including ALS [223]. Gene suppression can be achieved with oligonucleotide approaches, such as RNAi and AONs. These methods have been tested only with two genes, SOD1 and Fas, and important results have been reported in animal models [224]. The only trial in patients with FALS resulting from a SOD1 mutation was started in 2010 by Isis Pharmaceuticals, involving injection of SOD1 inhibitor directly into cerebrospinal fluid. The main problem with these new drug strategies is delivery of gene regulators to the target cells because of the necessity of crossing the blood–brain barrier and of obtaining compounds with long-lasting effects [225].
- Gene therapy with Vectors based on AAV and lentiviruses are proving to be particularly effective for the treatment of neurological disorders [226]. These vectors are attractive for their simplicity and their high transduction efficiency for neurons [227]. These vectors have been employed to deliver factors identified as crucial for neuronal survival such as IGF-1, G-CSF, ANG, or NT-3. These methods have not only been tested in small animal models, particularly in mice, but also in bigger animals such as cats and monkeys [228].

All of these new approaches have yielded quite promising results, although much experimental work remains to be done to achieve effective therapy for ALS patients [225].

## *1.9 High–throughput screening (HTS) approach based on multiple fluorescent probes to identify new drugs for treatment of Amyotrophic Lateral Sclerosis.*

The significant progresses in understanding the pathological mechanisms in ALS have not been matched with an effective disease-modifying pharmacotherapy. A critical step in designing more effective therapies for the treatment of neurodegenerative disorders, such as ALS, is the identification of drugs able to interfere with the first cellular alterations, prior to the onset of motoneuronal death. High–throughput experimental strategies (HTS) aimed at the finding of pharmacological compounds that might slow, stop or reverse disease progression may provide a unique and powerful tool for the indentification of new active drugs for treating ALS.

The main goal of HTS is to accelerate the discovery of new potential drugs using a fully automated robotic system able to screen a large libraries of compounds (genomic, protein and chemical libraries), in the range of 10.000-20.000 per day (100.000 data points generated per day for ultra-highthroughput screening) [229].

Crucial steps in performing successfully HTS approach are the choice of the appropriate technological platform but also of an adequate cellular model as basis for the biological assay chosen for the screening. To this purpose, the use of a cell-based assay, based on stable expression of sensitive fluorescent reporter able to monitor cellular toxicity induced upon expression of ALS causative genes by adenoviral delivery, could offer main advantages: i) the adenoviral delivery will allow an efficient ALS-causative gene expression; ii) fluorescence-based assays are widely used in HTS screening due to their high sensitivity, easy of both operation and readout; c) the screening of a large number of compounds would greatly increase the possibility of finding bioactive molecules, thus improving and accelerating drug design for ALS treatment.

### *1.9.1 Redox sensitive Green Fluorescent Protein (roGFP).*

Reactive oxygen species, oxidative stress, and antioxidant levels are widely believed to play key roles in health and disease. The recent development of fluorescent proteins (FP) engineered to be biosensor of redox unbalance offered a unique opportunity of monitoring redox changes in both physiological and pathological context of living animals and plants.

The first redox-sensitive FP (roFP), based on the yellow FP, was developed in 2001 by introducing two redox-active cysteins in position 149 and 202 (rxYFP149/202). The redox potential of the cysteine couple was found to be within the physiological range for redox-active cysteines, but the roYFP probe gives only an intensity change, not a ratiometric response [230]. In 2004, James Remington [231] and Roger Tsien [232] describe the independent development of several GFP-based indicators of redox status that are ratiometric by excitation. They evaluate roGFP1 (GFP with mutations C48S, S147C, and Q204C) and roGFP2 (the same plus S65T, that enhance GFP chromophore) with physiologically or toxicologically relevant oxidants in mammalian cells, including HeLa and macrophages cells. *In vitro* and *in vivo*, roGFP1 and roGFP2 show two-state changes in fluorescence emission in response to the ambient thiol/disulfide ratio. roGFP indicators are ratiometric by excitation, that is, they exhibit two excitation peaks (at about 390 and 475 nm), corresponding to the neutral and anionic chromophore forms, respectively (Fig. 9). Excitation of either peak gives rise to green fluorescence at about 510 nm. Upon oxidation of the redox-sensitive disulfide, the population of the neutral chromophore is favored at the expense of the anionic chromophore. Importantly, the redox-dependent fluorescence ratio exhibited by roGFP2 is

insensitive to pH changes in the physiological range [233]. These indicators have been shown to be suitable for use in relative reducing subcellular environments such as mitochondria or the cytoplasm in both animal and plant cells [231,232]. Different peptide signals have been used to drive the expression of roGFP sensors in mitochondria matrix and inner membrane space, with similar results.

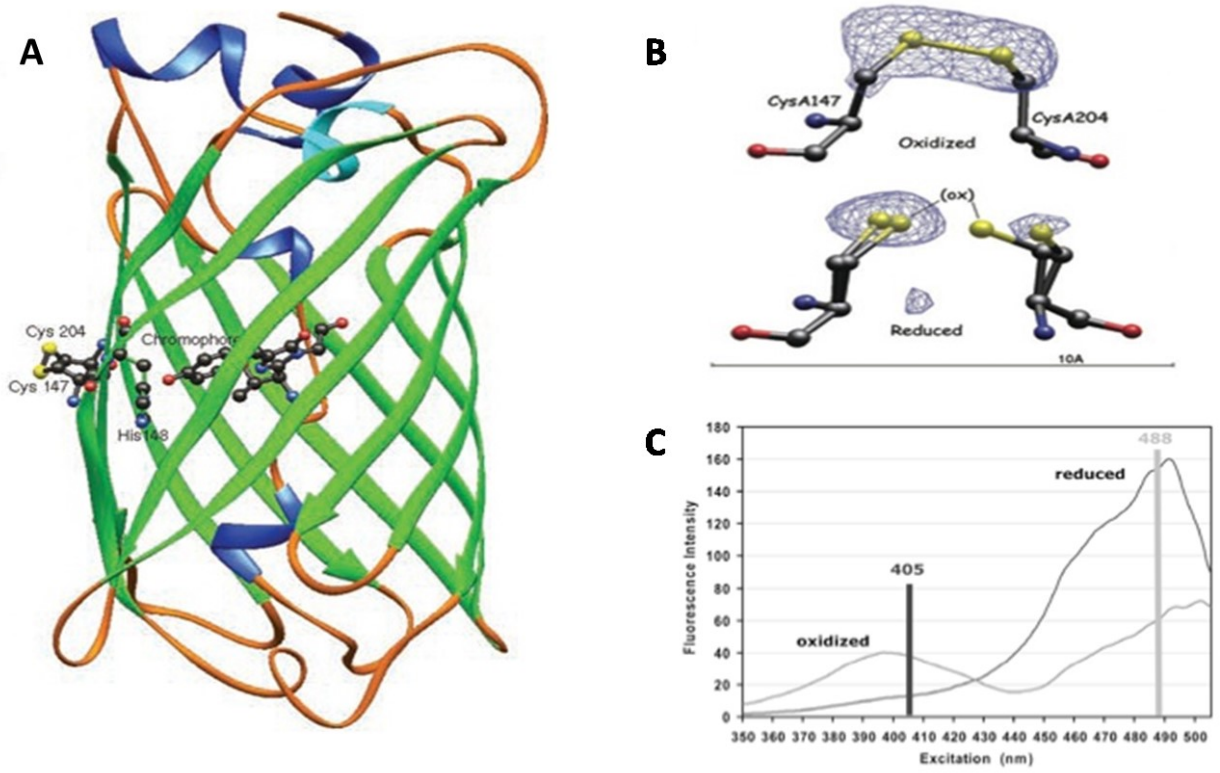


Figure 9: Key structural features of roGFP. A) Tridimensional structure of roGFP that highlights the amino acid modifications around the chromophore. B) Simulation through ball-and-stick model of disulfide bond between engineered residues Cys147 and Cys204. C) Fluorescence excitation spectra of roGFP.

### *1.9.2 Yellow Fluorescent Protein$^{u}$ (YFP$^{u}$).*

Protein aggregates and ubiquitin/proteasome system (UPS) impairment are believed to play key roles in several disease such as neurodegenerative diseases, included ALS.

The yellow fluorescent protein$^{u}$ (YFP$^{u}$) is a FP engineered to be biosensor to investigate the specific relation between protein aggregation and the function of the UPS. This reporter consisting of a short degron (ACKNWFSSLSHFVIHL), CL1 [234], fused to the COOH-terminus of yellow fluorescent protein [235]. In particular, the yellow fluorescent proteins (YFPs) were created by mutating Thr203 of the *Aequorea victoria* green fluorescent protein (GFP) [236,237] to aromatic amino acids, typically Tyr. The resulting π-π stacking and increased local polarizability immediately adjacent to the chromophore are believed to be responsible for the 20-nm shift to longer excitation and emission wavelengths [238]. The presence of short degron CL1 in fusion with the YFP makes this reporter a

good marker to UPS activity. In fact, in basal conditions this fusion-protein is rapidly degraded through the UPS system, while if the proteasome was altered (i.e. inhibitors, saturation due to misfolded proteins) occurs the accumulation of the protein, and then the fluorescence in the living cells [239](Fig. 10).

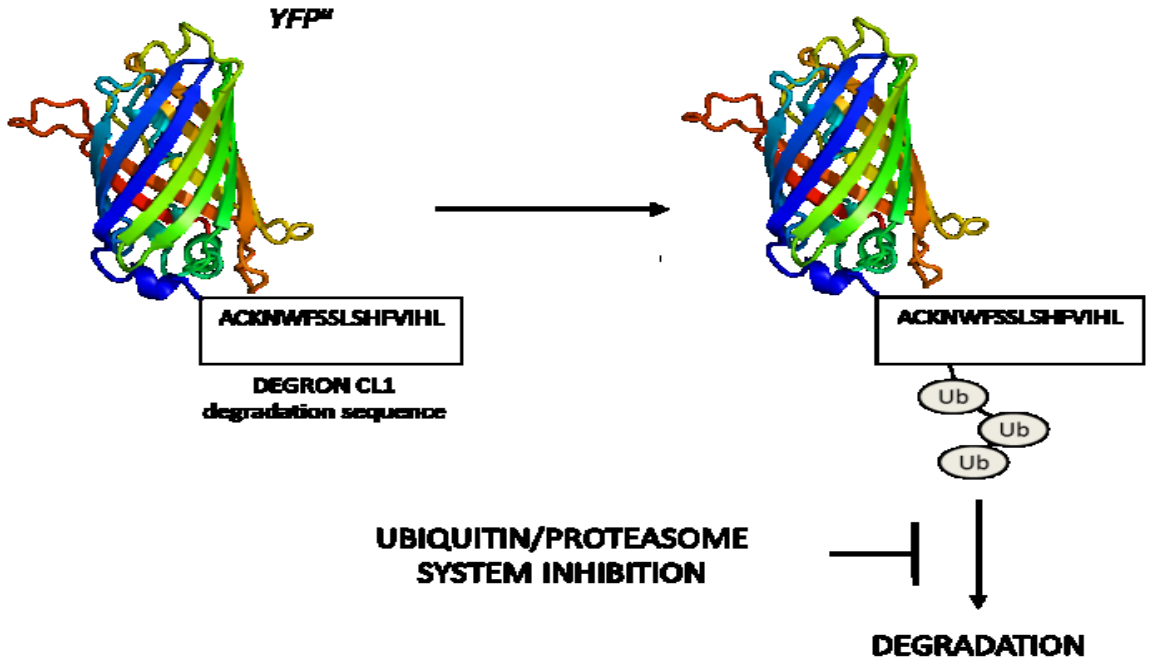


Figure 10: Structure and function of $YFP^{u}$. In basal cellular conditions, the $YFP^{u}$ is degraded by the proteasome. The presence of proteasome inhibitors causes protein accumulation as well as fluorescence accumulation.

### *1.9.3 DsRed-LC3-GFP reporter.*

Autophagy is an intracellular lysosomal degradation process, which plays an important role in cell growth and development, and keeping cellular homeostasis in all eukaryotes. Autophagy has multiple physiological functions, including protein degradation, organelle turnover and response to stress. Growing evidence supports a role of autophagic dysfunction as a contributing factor in various neurodegenerative diseases associated with abnormal aggregation of disease-related mutant proteins [197,240].

The DsRed-LC3-GFP sensor is a dual colour reporter between two spectrally distinct fluorescent protein: the DsRed fluorescent protein, responsible for the red coloration around the oral disk of a coral of the *Discosoma* genus, the fluorescent protein with the longest excitation/emission spectrum yet reported for a wild-type spontaneously fluorescent protein (excitation and emission maxima at 558 and 583 nm, respectively) [241], in fusion with the classical GFP-tagged LC3 reporter [242]. This reporter provides two readouts for autophagy activity: the number of DsRed-LC3 puncta and a flow cytometric measurement (called autophagy index). Like previous results obtained using

a GFP-LC3 reporter, this reporter showed an increase in the number of DsRed-LC3 puncta upon a PBS incubation or amino acid deprivation. Moreover, the reporter GFP separated from the C-terminus of LC3 by a recognition site for the autophagic protease, ATG4, and loss of GFP fluorescence can be monitored by decrease of GFP fluorescence or by flow cytometry (Fig. 11) [243].

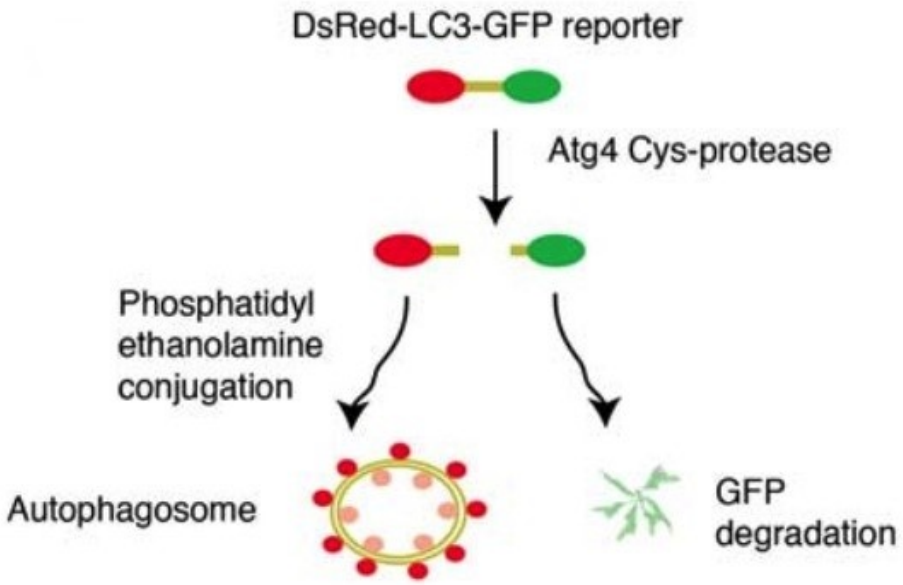


Figure 11: Schematic diagram showing the concept behind the DsRed-LC3-GFP autophagy reporter. When autophagy is activated, LC3 is cleaved to protease Atg4 in LC3II. Complex DsRed-LC3II is transported in the autophagosome membrane where is able to resist the acid pH, while the GFP is degraded.

### *1.9.4 CFP-DEVD-GFP: FRET (Fluorescent Resonance Energy Transfer) reporter.*

Caspase-3 is a crucial component of apoptotic machinery in many cell type. Apoptosis, or programmed cell death, is responsible for many normal development processes. For example, it is crucial during embryonic development, in shaping the adult organism, in surveillance of the cell cycle, and in some forms of chemically induced cell death. Inappropriate apoptosis has been implicated in many human disease such as neoplasia, in acute organ failure and also neurodegeneration and evidences support the opinion that dysregulation of apoptotic pathway might be a key event for ALS pathogenesis [244].

The development of mutants of GFP with distinct spectral properties, has allowed *in vivo* measurement of protein-protein interaction to be performed by measuring fluorescent resonance energy transfer (FRET). For example the emission spectrum of cyan fluorescent protein (CFP: GFP with mutations Y66W, F64L, S65T, N146I, M153T and V163A) overlaps significantly with the excitation spectrum of yellow fluorescent protein (YFP: a particular GFP variant called Venus with mutations F64L, M153T, V163A and S175G); placing CFP in close proximity to YFP (i.e. <5nm) allows FRET between the two fluorescent moieties to occur. Therefore, FRET between this two

spectrally distinct GFP mutants, fused with a peptide containing the sequence DEVD, which is cleaved by capsase-3 (Fig. 12) is a good sensor to monitor in living cells the activity of caspasi-3 [245,246].

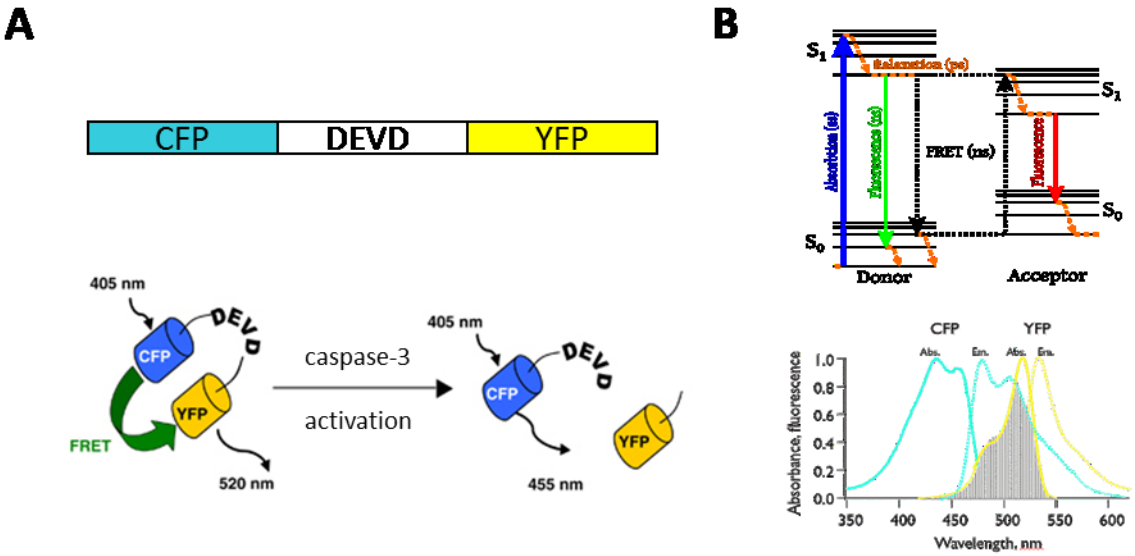


Figure 12: Structure and function of FRET reporter. A) Schematic diagram of CFP-DEVD-YFP fusion protein containing an 18 amino acid linker possessing the caspasi-3 specific cleavage sequence (DEVD). B) Schematic representation of electron vibrational energy states that occur during FRET and of the excitation spectrum overlap between fluorescent protein CFP and YFP cause of FRET.

# *CHAPTER 2:*

# *AIMS OF THE PROJECT.*

Up to date, hypotheses on biology underlying both sporadic and familiar ALS forms in humans outline a model in which non-competing mechanisms are likely to converge in various unsuccessful patterns to mediate selective motoneuron degeneration. Unfortunately these significant progresses in understanding the pathological mechanisms in ALS have not been matched with an effective disease-modifying pharmacotherapy. Moreover, in recent years the identification of TDP43 and FUS as ALS causative genes brought attention to the problems involved in RNA metabolism and protein aggregation.

For this reason, I decided to focus my PhD project on two objectives:

*AIM 1: GFP-based reporters to monitor biochemical alteration in cellular models for ALS: a possible and straightforward read-out for high-throughput screening (HTS) assay.*

This objective is focused on the development of different cellular models expressing high sensitive fluorescent probes suitable for the HTS analysis of cell toxicity upon expression of ALS-causative genes (SOD1, TDP43 and FUS in their wild type or mutant form) driven by adenoviral system.

*AIM 2: Study of the pathophysiological mechanisms responsible for cellular toxicity of pathological forms of two RNA-binding protein, FUS and TDP43, in familial forms of ALS.*

Identification of TD43 and FUS as ALS causative genes and their strong structural and functional similarities suggest a common mechanism of pathogenicity. Therefore, I decided to explore the molecular mechanisms of toxicity induced by the expression of pathological forms of TDP43 and FUS in two directions:

1) Identification of the RNA target of FUS.
2) Study of the relationship between aggregation, alterations of the proteasome and autophagy as well as cell death in the presence of pathological forms of TDP43 and FUS.

# *CHAPTER 3:*

# *MATERIALS AND METHODS.*

## *3.1 MATERIALS.*

***Bacterial strain.***

Competent cells used are E. coli DH5 $\alpha$. Bacterial cells are defective for the restriction and have mutations in relA1 and recA1 genes, to improve the stability and quality of recombinant plasmids.

***Cell lines.***

*SH-SY5Y cell line* [247]: SH-SY5Y cells (ATCC number CRL-2266) are human cells derived from neuroblastoma cell line.

*Adeno-X 293 cell line*: Adenovirus 5-transformed Human Embryonic Kidney 293 cell line (HEK 293; ATCC, Rockville, MD, CRL 1573) is used to package and propagate the recombinant adenoviral-based vectors produced with the BD Adeno-X Expression System.

***Plasmid constructions and oligonucleotides.***

*hFUS*$^{WT/R495X/H517G/R521G/P525L}$: Human cDNA coding for FUS (NM_004960.3) was cloned by reverse transcription-PCR from human SH-SY5Y neuroblastoma cells cDNA, using the forward primer 5'-AATTCTCGAGCCGCCTCAAACGATTATACCCA-3' and the reverse primer 5'-AATTCTCGAGTTAATACGGCCTCTCCCTG-3'. The resulting PCR fragment was inserted into XhoI restriction site of pCS2-MTK vector. Mutants were obtained by mutagenesis starting from hTDP-43, using the Quickchange site-directed mutagenesis kit (Stratagene) and primers indicated in the following table:

| NAME | SEQUENCE |
|---|---|
| hFUS$^{R495X}$ | 5'GGGACCGTGGAGGCTTCTAACTCGAGAATT3' |
| hFUS$^{H517G}$ | 5'TGCAGGGGTGAGCAGAGACAGGATCGC3' |
| hFUS$^{R521G}$ | 5'GAGCACAGACAGGATGGCAGGGAGAGG3' |
| hFUS$^{P525L}$ | 5'GAGAGGCTGTATTAACTCGAGAATT |

Table 2: Primer list used for mutagenesis of FUS cDNA.

*hTDP43*$^{WT/Q331K/M337V/A382T}$: Human cDNA coding for TDP43 (NM_007375.3) was cloned by reverse transcription-PCR from human SH-SY5Y neuroblastoma cells cDNA, using the forward primer 5'-AATTCTCGAGCCTCTGAATATATTCGGGTAACC-3' and the reverse primer 5'-AATTCTCGAGCTACATTCCCCAGCCAGAA-3'. The resulting PCR fragment was inserted downstream to 5xMyc repeats into XhoI restriction site of the pCS2-MTK vector. Mutants were obtained by

mutagenesis starting from hTDP43, using the Quickchange site-directed mutagenesis kit (Stratagene) and primers indicated in the following table:

| NAME | SEQUENCE |
|---|---|
| hTDP-43$^{Q331K}$ | 5'CCAGGCAGCACTAAAGAGCAGTTGGGG3' |
| hTDP-43$^{M337V}$ | 5'CAGTTGGGGTATGGTGGGCATGTTAGC3' |
| hTDP-43$^{A382T}$ | 5'AATTCTGGTGCAACAATTGGTTGGG3' |

Table 3: Primer list used for mutagenesis of TDP43 cDNA.

*roGFP*: cDNA coding for roGFP was cloned by restriction reactions or PCR from pCVU55762-roGFP (kindly provided by Dr. Andreas J. Meyer, University of Heidelberg, Germany). The resulting fragment was insert into BamHI/NotI sites of pcDNA3, into PstI/XhoI sites of pCMV/myc/mito (mito: mitochondrial matrix localization signal) and into BamHI/EcoRV sites of pcDNA3-IMS (IMS: mitochondrial intermembrane space targeting sequence from mouse cyt-C1). All the plasmid constructions were verified by automated sequencing.

*YFP$^{U}$*: the pEYFP-C1 plasmid was kindly provided by Prof. Rusmini (University of Milan, Italy) [248].
*DsRed-LC3-GFP*: the pQCXI Neo DsRed-LC3-GFP plasmid was purchased from Addgene company (cod. 31183).
*CFP-DEVD-YFP*: the pECFP-DEVDR-Venus plasmid was purchased from Addgene company (cod. 24537).

***Adenoviral vectors.***

All adenoviral vector (*pAdenoX-hFUS$^{WT/R495X/H517Q/R521G/P525L}$*; *pAdenoX-hTDP43$^{WT/Q331K/M337V/A382T}$* and *pAdenoX-hSOD1$^{WT/H80R/G93A}$*) were generated using the Adeno-X Expression System 1 (Clontech). Their production is completed in two stages. First, generation of mammalian expression cassette by cloning gene of interest into pShuttle2. Second, excision of expression cassette from pShuttle2 and insertion into I-Ceu I and PI-Sce I sites of BD Adeno-X Viral DNA. All constructions were verified by automated sequencing.

***Antibodies.***

In the present study we used the following antibodies: mouse anti-myc (clone 9E10 Sigma-Aldrich, 1:5000 for western and 1:20000 for immunofluorescence), rabbit anti-Cu/Zn SOD1 (Enzo Life Science, 1:2000 final dilution), rabbit TARDBP (Proteintech, 1:1500 final dilution), mouse FUS/TLS (Santa Cruz Biotechnology, 1:1000 final dilution), rabbit anti-GFP (Enzo Life Science, 1:1000 final

dilution), rabbit anti-CREB (Santa Cruz Biotechnology, 1:1000 final dilution), mouse anti-β-actin (Sigma-Aldrich, 1:5000 final dilution), rabbit anti-PARP (Cell Signaling, 1:1000 for western and 1:500 for immunofluorescence), rabbit antiLC3 (Cell Signaling, 1:1000 final dilution), Alexa Fluor®488 goat anti-mouse IgG (Life Technologies, 1:2000 final dilution), Alexa Fluor®647 goat anti-rabbit IgG (Life Technologies, 1:2000 final dilution), Goat anti-Mouse IgG Peroxidase conjugated (Millipore, 1:2500 final dilution), Goat anti-Rabbit IgG Peroxidase conjugated (Millipore, 1:2500 final dilution).

## *3.2 METHODS.*

***Standard technique of molecular biology.***

All standard technique of molecular biology were performed according to *Molecular Cloning–A Laboratory Manual* [249].

***DNA purification from agarose gel.***

Whenever it was necessary to purify DNA from agarose gel was used the commercial *Kit Wizard ® SV Gel and PCR Clean-Up System* (Promega) according to the manual instructions.

***Plasmid DNA purification.***

When it has been requested a greater quality of plasmidic DNA (i.e. sequence analysis or cell's transfection), was used the commercial kit *Wizard® Plus SV Minipreps DNA Purification System* (Promega) and *PureLink® HiPure Plasmid Midiprep Kit* (Life Technologies) according to the manual instructions.

***Cell cultures.***

SH-SY5Y are cultured in Dulbecco MEM/F12 ground (Gibco BRL), HEK293 in Dulbecco MEM (Gibco BRL), always in the presence of 10% fetal calf serum, free of tetracycline contamination (Tet-free FCS, Clontech) and inactivated at 56 °C for 30'. Medium contains 100 units/ml penicillin G and 100 µg/ml streptomycin (Gibco BRL). The cells are grown in an incubator at 37 °C in a humidified atmosphere containing 5% $CO_2$. Trypsin (0.5 g/ml, 68 mM EDTA) is added to split cells, then diluted in fresh medium.

***Transfection of eukaryotic cells.***

Transient expression of each plasmid (1.5 µg DNA/5–7×$10^5$ cells) is obtained transfecting cells with LipofectAMINE LTX and PLUS reagent (Life Technologies). Dilute the optimized amount of plasmid DNA in OPTIMEM (Gibco BRL) and add the optimized volume of PLUS™ Reagent directly to the diluted DNA. Mix gently and incubate for 5' at room temperature. Add the optimized volume of Lipofectamine™ LTX directly to the diluted DNA, incubate for 30' at room temperature. DNA-lipid complexes are stable for 6 hours at room temperature. Add DNA-lipid complex dropwise to the well containing cells, mixing gently. Medium may be changed after 4–6 hours.

***Production of recombinant adenovirus.***

Plate HEK 293 cells at a density of 1–2 x $10^6$ cells per 60-mm culture plate 12–24 hours before transfection and incubate the plate(s) at 37°C in a humidified atmosphere maintained at 5% CO2. Transfect each 60-mm culture plate with 5 µg of Pac I-digested BD Adeno-X DNA using standard transfection method. One day later, and periodically thereafter, check for cytopathic effect (CPE). One week later, transfer cells to a sterile 15-ml conical centrifuge tube (do not use trypsin: infected cells that still adhere to the bottom or sides of the culture plate can be dislodged into the medium by gentle agitation). Centrifuge the suspension at 1,500 x g for 5 min at room temperature. Resuspend the pellet in 500 µl sterile PBS. Lyse cells with three consecutive freeze-thaw cycles: freeze cells in a dry ice/ethanol bath; thaw cells by placing the tube in a 37°C water bath (do not allow the suspension to reach 37°C). Vortex cells after each thaw. After the third cycle, briefly centrifuge to pellet debris. Transfer the lysate to a clean, sterile centrifuge tube and use immediately to infect a fresh 60-mm culture by adding 250 µl (50%) of the cell lysate directly to the medium, then incubate as normal. CPE should be evident within one week. Repeat these steps two or three time until get a high titer viral preparation.

***Determination of adenoviral titer: End-Point dilution assay.***

Approximately 24 hours before beginning the titration protocol, plate HEK 293 cells in two 96-well plates. Carefully seed all wells at the same density (~$10^4$ cells per well) in 100 µl of growth medium. Prepare serial dilutions of your virus as follows:

- Make a 1:100 dilution by adding 10 µl virus stock to 990 µl sterile growth medium.
- Starting with the 1:100 dilution, prepare serial 1:10 dilutions by transferring 100 µl diluted virus to 900 µl sterile growth medium.

In general, an appropriate range of dilutions for testing is $10^{-3}$–$10^{-10}$. Remove the 96-well culture plate from the incubator and inspect the wells to ensure that the cells have attached to form an even monolayer. Add 100 µl diluted virus to each well in columns 1–10 and add 100 µl of virus-free growth medium to wells in columns 11–12, these wells serve as controls for the viability of non-infected cells. Cover the plate and incubate in a humidified CO2 (5%) incubator for 10 days at 37°C. Using a microscope, check each well for cytopathic effect (CPE). For each row, count the number of wells having CPE. A well is scored as CPE positive even if only a few cells show cytopathic effects. If you are uncertain, compare the infected well with the non-infected control wells. Calculate the fraction of CPE-positive wells in each row. Finally, calculate Viral Titer:

- Titer (pfu/ml) = $10^{(x + 0.8)}$

x = the sum of the fractions of CPE-positive wells.

The assay is a reliable indicator of viral titer only if the following three conditions are met: i) the negative control wells show no visible signs of CPE or growth inhibition. ii) wells infected with the least dilute virus ($10^{-3}$) are all CPE-positive. iii) wells infected with the most dilute virus ($10^{-10}$) are all CPE-negative.

***Adenoviral infection of eukaryotic target cells.***

Plate target cells (SH-SY5Y cells or SH-SY5Y stably espressing $YFP^{u}$, roGFP or mitochondrial targeted roGFP) 12–24 hours before infection in the culture plates desired. The next day, remove the growth medium and infect target cells diluting viruses at a multiplicity of between 5–30 pfu/cell in OPTIMEM (Gibco BRL). Cover the plates and incubate the cells in a humidified CO2 (5%) incubator at 37°C for 1 hour to allow the virus to infect the cells. Add fresh complete growth medium and incubate in a humidified 5% CO2 at 37°C. Analyze gene expression at different time points required then proceed to further experimental manipulations.

***CLIP (CrossLinking Immunoprecipitation).***

To identify potential RNA target of FUS, SH-SY5Y cells were subjected to CLIP method:

*Crosslink proteins-RNA, cell lysis and sonication.*

24h after infection with recombinant adenoviruses encoding for $FUS^{WT}$, SH-SY5Y infected or uninfected cells ($3.5x10^{6}$ cells) were fixed in formaldehyde 4% for 10 minutes then lysed in 1,5ml of RIPA buffer [Tris HCl pH 7.5 50mM, NP-40 1%, DOC 0.5%, SDS 0.05%, EDTA 1mM, NaCl 150mM, protease inhibitors cocktail (Sigma-Aldrich) and RNasin (Promega)] and incubated for 20 minutes on ice. The lysate was sonicated for three cycles of 20 seconds and after centrifugation at 12,000xg for 10 minutes at 4 °C, recover the supernatants.

*Immunoprecipitation.*

Pre-clear the supernatants at 4 °C for 1 h with protein A-Sepharose (Sigma-Aldrich). Add the anti-Myc antibody at 1:1000 dilution, and after an overnight incubation at 4 °C, collect the immunoprecipitates by adding 20 µl of protein A-Sepharose (Sigma-Aldrich). Wash the beads five times in RIPA buffer, at last wash remove 100 µl of sample to control the immunoprecipitation then add Laemmli Buffer 5X and analyze by Western blotting.

*Reverse crosslink.*

After centrifugation of immunoprecipitates, resuspend the beads in 300 µl of RIPA buffer [Tris HCl pH 7.5 50mM, NP-40 1%, DOC 0.5%, SDS 1%, EDTA 1mM, NaCl 150mM, protease inhibitors

cocktail (Sigma-Aldrich) and RNasin (Promega)] and incubate the supernatants for 45 minutes at 70°C. Centrifuge at 400xg at 4°C for 3 minutes and recover the supernatants.

*RNA extraction*.

After treatment for 15 minutes at 37 °C with Dnase (1U/µl, Promega) and RNase OUT (Promega, 40U/µl), add to the samples Na-acetate pH4 (1/10 volume), phenol acid (1/2 volume) and chloroform (1/5 volume), shake tubes vigorously and incubate for 10 minutes on ice. Centrifuge the samples at 12,000 ×*g* for 10 minutes at 4°C. Following centrifugation, the mixture is separated into a lower phenol-chloroform phase, an interphase, and a colorless upper aqueous phase. RNA remains exclusively in the aqueous phase. Transfer the aqueous phase to a fresh tube. Precipitate the RNA from the aqueous phase by mixing with two volumes of absolute ethyl alcohol . Incubate samples overnight at -20°C and centrifuge at 12,000 ×*g* for 10' at 4°C. Remove the supernatant and wash the RNA pellet once with 80% ethanol. Mix the sample by vortex and centrifuge at 12000 ×*g* for 5' at 4°C. At the end of the procedure, briefly dry the RNA pellet and dissolve RNA in 10µl od RNase-free water and use its half for RT-PCR reaction.

*RT-PCR.*

Add 2µl of random hexamers (100ng/µl), heat at 65 °C for 5min to denature RNA secondary structure. Add 2,5µl of 2mM dNTPs, 2,5µl of 0.1M DTT, 0,5µl of SuperScript II RT (200 U/µl), 0,5 µl od RNase OUT (40 U/µl) and incubate at room temperature for 5min, at 37°C for one hour and 95°C for 5min to inactivate reverse transcriptase. PCR settings as control to amplify C-terminal fragment of FUS sequence was set up as follows: 5min 95°C; 30 cycles of (30 s for 95 °C, 30 s for 58 °C, and 40 s for 72 °C); and 10min 72 °C. Run the entire PCR and visualize amplified DNA.

*Cloning and screening of colonies.*

After RT-PCR, to generate dsDNA add random hexamers (100ng/µl), dNTPs (2mM) and Klenow (5U/µl, Promega) and incubate for 30min at 25°C then add T4 polymerase (10U/ µl, Promega) and incubate for 10min at 37°C. Phosphorylate dsDNA by treatment with T4 polynucleotide kinase (10U/µl, BioLabs) for 30min at 37°C with ATP as phosphate donor. Finally, clone all obtained dsDNA into EcoRV restriction site of pBluescript II SK (-) vector and transform in *E.coli* DH5α cells. Grow singularly all colonies and extract plasmidic DNA. Analyse presence of CLIP-insert by PCR using T3 and T7 primers (reaction settings was described previously). All positive samples was sequenced availing an external company.

***Assessment of apoptosis and cell viability.***

Quantification of apoptotic cells was obtained by direct visual counting after nuclear staining of 4% paraformaldehyde-fixed cells with the fluorescent probe Hoechst 33342 (1 mg/ml) (Sigma-Aldrich). One hundred cells were examined for each field at a magnification of 200× and eight randomly chosen fields for each experimental condition were counted. Only the cells containing clearly picnotic or fragmented nuclei were considered apoptotic.

The viability of control SH-SY5Y cells or SH-SY5Y cells infected with adenoviruses encoding for fALS causative genes was calculated after 72 hours through an MTS assay. Cell viability was assessed by a colorimetric assay using the 3(4,5-dimethylthiazol-2yl)-5-(3-carboxymethoxyphenyl)-2-(4-sulfophenyl)-2H-tetrazolium (MTS) assay (CellTiter 96 Aqueous One Solution Assay, Promega), according to the manufacturer's instructions. Absorbance at 490 nm was measured in a multilabel counter (Victor X5, PerkinElmer).

***Nuclear-cytoplasmic separation.***

$1\times10^6$ SH-SY5Y cells were transfected or not (-) with a plasmid coding for $TDP43^{WT}$ or $TDP43^{M337V}$ and $TDP43^{A382T}$ mutants. 72 h after transfection cells were wash twice with cold PBS 1X, harvested in 500 µl of PBS 1X and centrifuged at 1000 xg for 3 min at 4 °C. The pellet were resuspended gently in 500 µl of S1 buffer (10mM Hepes pH 7.9, 10mM KCl, 1.5mM $MgCl_2$, 0.1mM EGTA pH 7.0, 1M DTT (1 µl/2ml), and protease inhibitors mixture, Sigma-Aldrich). Syringe ten times at 4 °C and centrifuge at 1000 xg for 3' at 4 °C, supernatant (cytoplasmic fraction) was collected and the pellet was resuspended gently in 500 µl of S1 buffer. Centrifuge at 3000 rpm for 3' at 4 °C, the pellet was resuspended with 30µl of S2 (10mM Hepes pH 7.9, o.4M NaCl, 1.5mM $MgCl_2$, 0.1mM EGTA pH 7.0, 5% glycerol 1M DTT (1 µl/2ml), and protease inhibitors mixture, Sigma-Aldrich). Shake for 30 min at 4 °C, centrifuge for 10 min at 4 °C at 12,000xg and collect the supernatant (nuclear fraction).

***Solubility assay.***

$5\text{-}7\times10^5$ SH-SY5Y cells were transfected or not (-) with a plasmid coding for $TDP43^{WT}$ or $TDP43^{M337V}$ and $TDP43^{A382T}$ mutants. 72 h after transfection cells were scraped off the plate in culture medium, collected by centrifugation, washed with PBS 1X, and resuspended in 150µl of buffer A (10mM Tris-HCl pH 8.0, 1mM EDTA pH 8.0, 100mM NaCl, 0.5% Nonidet-P40, and protease inhibitors mixture, Sigma-Aldrich). After 10 min of ice incubation, the lysates were centrifuged at 20,000 xg for 10 min, and the supernatants were collected as detergent soluble fractions, whereas the pellet (insoluble fractions) was washed in PBS 1X and resuspended in 150µl of Laemmli sample

buffer (62mM Tris-HCl pH 6.8, 10% glycerol, 2% SDS, 5% β-mercaptoethanol, and 0.05% bromophenol blue).

***Immunofluorescence.***

Wash $1\times10^5$ SH-SY5Y cells, grown on a cover-glass, twice with PBS 1X and then fix with 1 ml of 4% paraformaldehyde/PBS 1X for 10'. Permeabilize cells with 0.1% Triton X-100 in PBS and block non-specific binding with 5% bovine serum albumin, 0.1% Triton X-100 diluted in PBS for 1 h at room temperature. Incubate cells with primary antibodies diluted in blocking solution, overnight at 4 °C and then with secondary antibodies and nuclear marker (TO-PRO3, Life Technologies or Hoechst 33342, Sigma-Aldrich), diluted in blocking solution for 1 h at room temperature. Analyze cells with a Leica TCS SP5 confocal microscopy with LAS lite 170 image software.

# *CHAPTER 4:*

# *RESULTS.*

### *4.1 GFP-based reporters to monitor biochemical alteration in cellular models for ALS: a possible and straightforward read-out for high-throughput screening (HTS) assay.*

A critical step in designing more effective therapies for the treatment of neurodegenerative disorders, such as Amyotrophic Lateral Sclerosis (ALS), is the identification of drugs able to interfere with the first cellular alterations, prior to the onset of motoneuronal death. High−throughput experimental strategies (HTS) aimed at finding pharmacological compounds that might slow, stop or reverse disease progression may provide a unique and powerful tool to identify new active drugs for treating ALS. Such technologies rely on the availability of automated cell-based assays and screening protocols to fulfill all the requirements needed for HTS procedures.

To this purpose, we have generated different cellular models where specific markers of cell toxicity, induced by expression of ALS-causative genes, would be used as a straightforward read-out for high-throughput screening of compound libraries of different nature. In particular, the general strategy showed in figure 13 has been proposed.

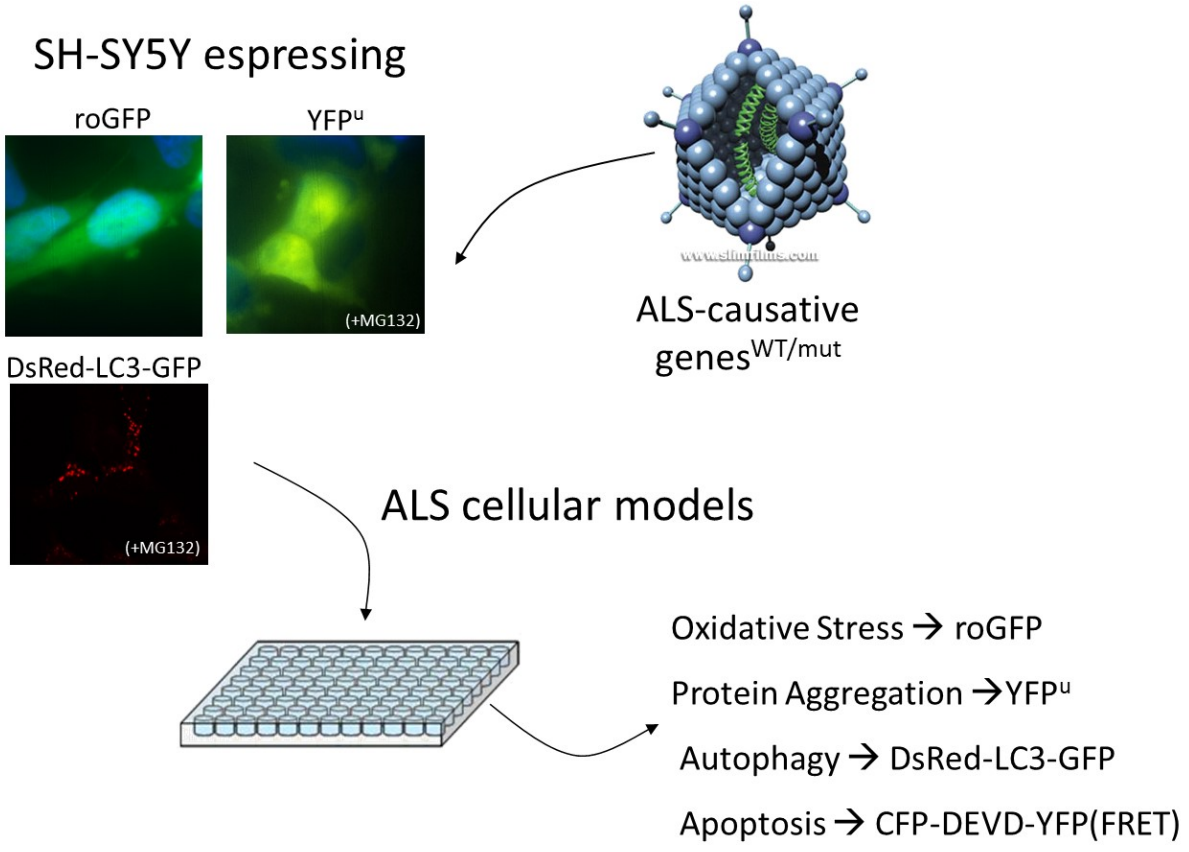


Figure 13: ALS cellular models experimental strategy.

As shown in figure 13 neuronal SH-SY5Y cells expressing high sensitive fluorescent probes suitable for measurement of i) oxidative stress; ii) ubiquitin proteasome system impairment; iii) autophagy activation; iv) caspasi-3 activation, which have been described to be key events during ALS disease progression. These biological effects have been evaluated upon adenoviral delivery of ALS disease causative genes SOD1, TDP43 and FUS in wilt type or mutant form.

### *4.1.1 Adenoviral delivery of ALS-causative genes.*

In order to identify molecules able to intercept the cellular damage generated by the expression of ALS causative genes, different cellular models able to mimic the genetic alterations that cause fALS were built by the overexpression of SOD1 (OMIM # 105400), TDP43 (OMIM # 612069) and FUS (OMIM # 608030), respectively. In particular, both WT and mutant variants of the mentioned genes (Table 4) were expressed, described to be pathological mutations.

| fALS | OMIM | Gene | Pathological mutations |
|---|---|---|---|
| ALS1 | # 105400 | SOD1 | G93A, H80R |
| ALS6 | # 608030 | FUS | R495X, H517G, R521G, P525L |
| ALS10 | # 612069 | TDP-43 | Q331K, M337V, A382T |

Table 4: fALS associated genes chosen for adenoviral delivery. Data extracted from the web site OMIM (Online Mendel Inheritance in Man).

To drive the expression of ALS causative genes, the recombinant adenoviruses encoding for hTDP43 (WT or mutant) and hFUS (WT or mutant) genes were produced, since adenoviral driven expression of WT or mutant SOD1 in neuronal cell lines have been demonstrated to provide a good ALS-cellular model [250] and Ad hSOD1 particles were already available in the laboratory. Recombinant adenoviruses, in fact, provide a versatile system for gene expression studies and therapeutic applications. Since infection by adenovirus is not cell-cycle dependent, it is possible to deliver the gene of interest to primary as well as to transformed cell lines. Following infection, target gene was transiently expressed at high levels since many cells received multiple copies of the recombinant genome. Expression is transient because adenoviral DNA normally does not integrate into the cellular genome.

The assembly of recombinant adenoviruses is completed in few stages: first the cDNA coding for TDP43 and FUS cDNA WT or bearing a pathological mutation was cloned into pShuttle2 vector, in fusion with five repeats of myc epitope (5xMyc). Second the expression cassette was excised from recombinant pShuttle2 plasmid DNA by digesting with I-Ceu I and PI-Sce I and ligated to Adeno-X

Viral DNA. Recombinants were selected with kanamycin and screened by restriction endonuclease digestion as shown in figure 14.

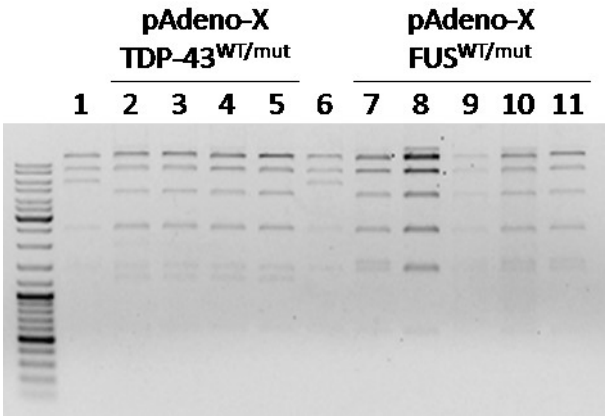


Figure 14: Production of recombinant adenoviruses with the BD Adeno-X™ Expression System 1 (Clontech). Control digestion with XhoI of positive recombinant adenoviruses. M = molecular weight marker; 1,6 = pAdeno-X vector; 2 = $TDP43^{WT}$; 3 = $TDP43^{Q331K}$; 4 = $TDP43^{M337V}$; 5 = $TDP43^{A382T}$; 7 = $FUS^{WT}$; 8 = $FUS^{R495X}$; 9 = $FUS^{H517G}$; 10 = $FUS^{R521G}$; 11 = $FUS^{P525L}$.

Third, the recombinant adenoviral construct was cleaved with PacI to expose its inverted terminal repeats and transfected into a packaging cell line HEK293. After 7–10 days, viruses were harvested and amplified by infecting packaging cells for three times to obtain high titer virus stock. By performing an end-point dilution assay, the final yields were evaluated generally around $10^8$ plaque-forming particles per ml (Tab. 5).

| | **x = the sum of the fractions of CPE-positive wells** | **Titer (pfu/ml) = $10^{(x + 0.8)}$** |
|---|---|---|
| $AdSOD1^{WT}$ | 5 | 3.2 x $10^8$ pfu/ml |
| $AdSOD1^{G93A}$ | 9.9 | 6.3 x $10^8$ pfu/ml |
| $AdSOD1^{H80R}$ | 7.9 | 5 x $10^8$ pfu/ml |
| $AdTDP43^{WT}$ | 9.9 | 6.3 x $10^8$ pfu/ml |
| $AdTDP43^{Q331K}$ | 4.9 | 3.1 x $10^8$ pfu/ml |
| $AdTDP43^{M337V}$ | 3.9 | 2.5 x $10^8$ pfu/ml |
| $AdTDP43^{A382T}$ | 2.4 | 1.5 x $10^8$ pfu/ml |
| $AdFUS^{WT}$ | 7,1 | 4.5 x $10^8$ pfu/ml |
| $AdFUS^{R495X}$ | 4.9 | 3.1 x $10^8$ pfu/ml |
| $AdFUS^{H517G}$ | 4.9 | 3.1 x $10^8$ pfu/ml |
| $AdFUS^{R521G}$ | 12 | 7.9 x $10^8$ pfu/ml |
| $AdFUS^{P525L}$ | 5 | 3.2 x $10^8$ pfu/ml |

Table 5: Determination of viral titer for all infectious recombinant adenoviruses encoding for fALS causative genes.

Recombinant adenoviruses were finally used to infect neuronal SH-SY5Y with a multiplicity of infection (M.O.I.) of 30 pfu/cell. Forty-eight hours after infection cells were harvested and protein extracts analyzed by Western Blot (Fig. 15).

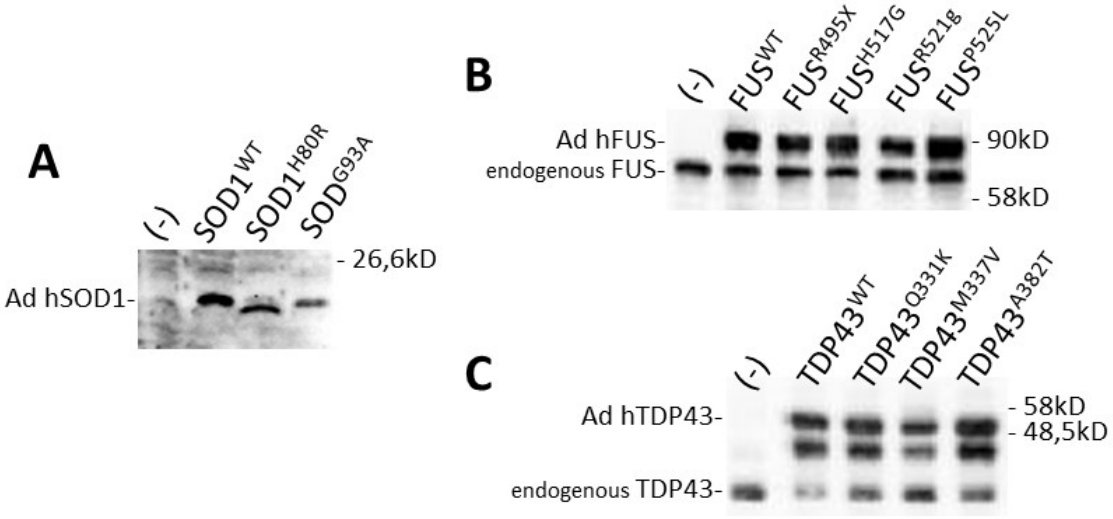


Figure 15: Cell lysates of SH-SY5Y cells after 48 hour following infection with 30 pfu/cell of infectious recombinant adenoviruses. Expression levels of genes of interest were evaluated by western blot analysis with anti-SOD1 antibody (A), anti-FUS antibody (B) and with anti-TDP43 antibody (C).

As shown in figure 15 we were able to produce successfully an high titer of infectious recombinant adenoviruses for all fALS genes.

### *4.1.2 Characterization of fALS cellular models.*

As an initial step to characterize the effects of adenoviral delivery of fALS genes into neuronal cells we evaluated metabolism and morphology of SH-SY5Y cells after infection with scalar concentration of infectious adenoviruses encoding for WT or mutant fALS genes through western blot analysis on total lysates or by immunofluorescence experiments. The cellular viability was analyzed performing a viability assay using a commercial kit (CellTiter 96® AQueous One Solution Cell Proliferation Assay, Promega). Neuronal SH-SY5Y cells were infected with increasing concentrations of adenoviruses encoding for WT or mutant fALS genes and 72 hours post-infection the MTS assay was performed, according to the manual instruction (Fig. 16).

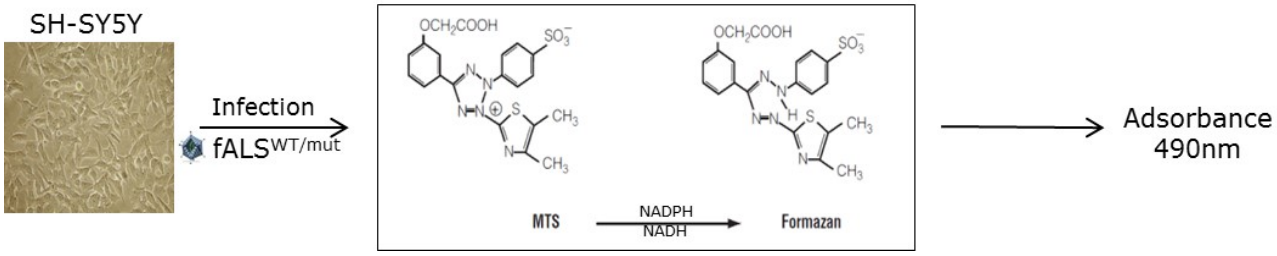

Figure 16: SH-SY5Y cells were infected with increasing concentrations of recombinant adenoviruses encoding wild type or mutant fALS genes. After 72h, MTS tetrazolium compound (Owen's reagent) was added to the cells and the plate was incubated at 37°C for 1–4 hours in a humidified, 5% $CO_2$ atmosphere and then the absorbance was recorded at 490nm. The quantity of formazan product is directly proportional to the number of living cells in culture.

As shown in figure 17A, the western blot analysis in neuronal cells after 72 hours of infection showed that recombinant adenoviruses are able to drive expression of human TDP43 in WT form or carrying the mutations Q331K, M337V and A382T, despite slightly different levels. The immunofluorescence experiments showed that $TDP43^{WT}$ and $TDP43^{Q331K}$ mutant are normally localized to the nucleus, however both mutants, $TDP43^{M337V}$ and especially $TDP43^{A382T}$ showed a redistribution in the cytoplasm associated with apoptotic nuclei (Fig. 17B). Finally, the overexpression of both wild type and mutant forms of TDP43 induced a drastic reduction of cell proliferation in a dose-dependent manner, according with data so far available in literature [120] (Fig 17C).

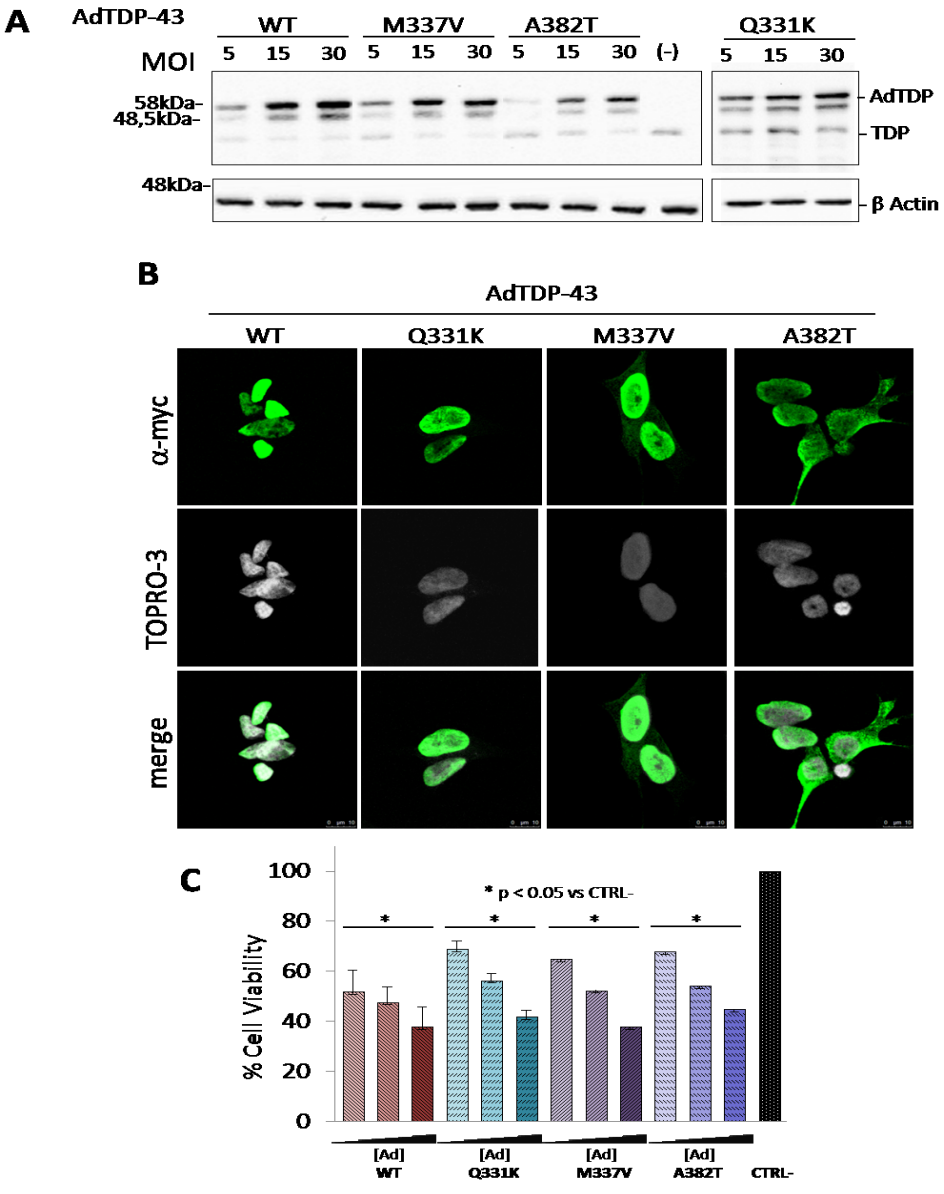

Figure 17: Effects of overexpression of wild type or mutant TDP43 gene on neuronal cells. A) Neuronal SH-SY5Y cells infected with increasing concentrations (5-15-30 pfu/cell) of adenoviruses encoding for WT or mutant TDP43 were analyzed 72h post-infection by western blot to evaluate expression levels of TDP43 (wild type or mutants). B) 72 hours post infection SH-SY5Y cells were subjected to immunofluorescence analysis with anti-myc (green) antibody to verify expression levels and localization of protein, anti-TOPRO-3 (grey) was used as nuclear marker. C) Neuronal SH-SY5Y cells infected with the indicated adenoviruses were analyzed 72h post-infection for quantity of formazan product directly proportional to the number of living cells in culture.

Similarly, figure 18A showed that also infectious recombinant adenoviruses are able to drive expression of human FUS in WT form or carrying the mutations R495X, H517G, R521G and P525L, 72 hours post-infection in neuronal cells. The immunofluorescence experiments showed that $FUS^{WT}$ is typically localized to the nucleus, and that all mutants, although in different ways, show a redistribution in the cytoplasm. This cytoplasmic relocation is particularly clear in $FUS^{R495X}$ and $FUS^{P525L}$ (Fig. 18B). Furthermore, the overexpression of $FUS^{R495X}$, but not of wild-type FUS and other mutants, induces a significant reduction of cell proliferation, as assessed by MTS assay, which becomes evident at 72 hours after infection and only with the increase of recombinant adenovirus concentration (Fig. 18C).

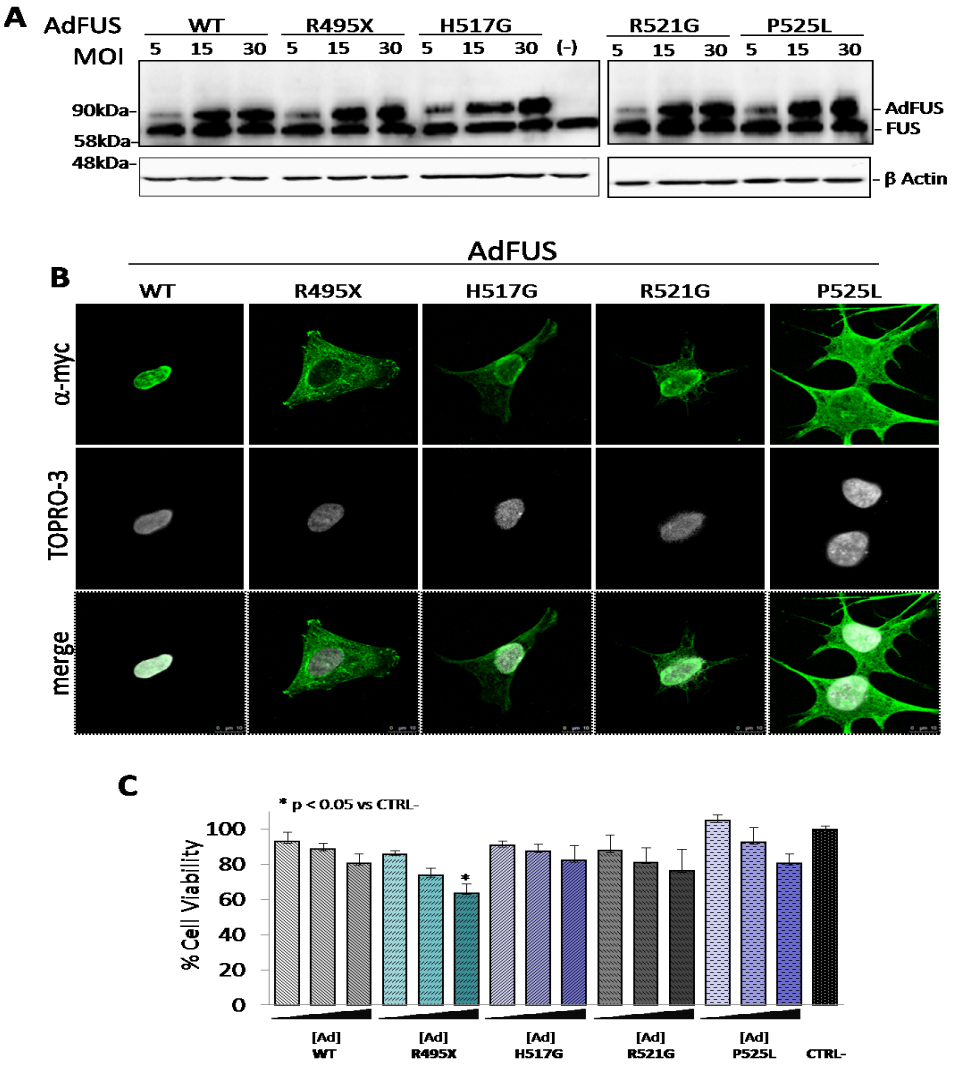

Figure 18: Effects of overexpression of wild type or mutant FUS gene on neuronal cells. A) Neuronal SH-SY5Y cells infected with increasing concentrations (5-15-30 pfu/cell) of adenoviruses encoding for WT or mutant FUS were analyzed 72h post-infection by western blot analysis to evaluate expression levels of FUS (wild type or mutants). B) 72 hours post infection SH-SY5Y cells were subjected to immunofluorescence analysis with anti-myc (green) antibody to verify expression levels and localization of protein, anti-TO-PRO-3 (grey) was used as nuclear marker. C) Neuronal SH-SY5Y cells infected with the indicated adenoviruses were analyzed 72h post-infection for quantity of formazan product directly proportional to the number of living cells in culture.

The effects of expression of WT or mutant SOD1 in neuronal cell lines through adenoviral delivery have been already demonstrated [250]. However, as shown in figure 19 we were able to produce recombinant adenoviruses to drive expression of human SOD1 in WT form or with pathological mutations H80R and G93A. Moreover, 48 and 72 hours after infection with infectious adenoviruses encoding for SOD1 mutants, as expected, we detected increase in accumulation of fragmented nuclei, suggestive of an ongoing apoptotic process.

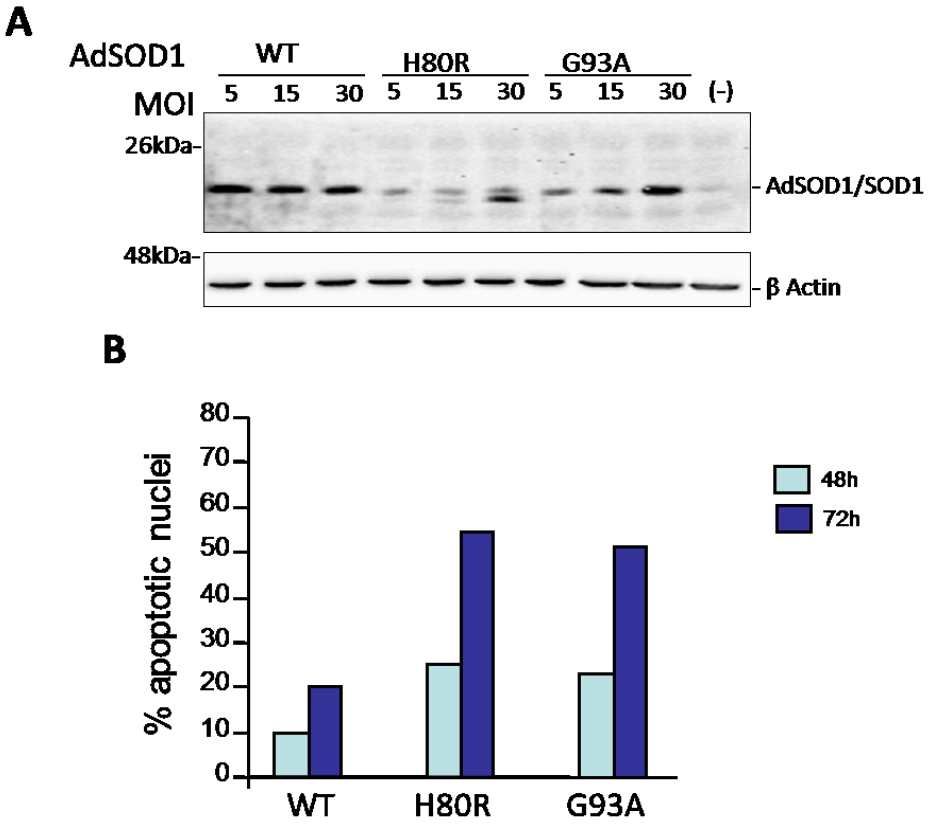


Figure 19: Mutants of human SOD1 induce accumulation of fragmented nuclei in SH-SY5Y cells. (A) Neuronal cells infected with increasing concentrations (5-15-30 pfu/cell) of adenoviruses encoding for WT or mutant SOD1 were analyzed 72h post-infection by western blot to evaluate expression levels of SOD1 (wild type or mutants). B) SH-SY5Y cells were infected with adenoviruses coding for wild-type SOD1 or H80R and G93A-SOD1 mutants. After 48-72 h, nuclei of cells were stained with Hoechst 33342, and apoptotic nuclei were quantified as described in Materials and Methods.

### *4.1.3 Construction and characterization of neuronal cell lines stably expressing fluorescent reporter genes to assess in vivo different parameters of cell toxicity induced by ALS−causative genes.*

As mentioned in the Introduction, motoneurons in both sporadic and familiar ALS degenerate with overlapping molecular mechanisms that involve oxidative stress, alteration of proteasome activity and, ultimately, autophagy and apoptosis. Major advances in biotechnology have provided powerful tools to monitor in vivo all these markers of cell damage. In particular, we planned to use:

− redox−sensitive GFP (roGFP) to monitor oxidative stress [251].

− $YFP^u$ to monitor alterations in the activity of ubiquitin−proteasome system [248].

− DsRed-LC3-GFP to monitor alterations of autophagy pathway [243].

− FRET−based caspase−3 biosensors to follow apoptosis [252].

#### *4.1.3.1 SHSY5Y cells stably expressing redox−sensitive GFP (roGFP) to monitor oxidative stress either in the cytoplasm or in the mitochondria.*

As reported in the Introduction, disruption in cellular oxidation/reduction (redox) regulation is implicated in the pathogenesis of neurodegenerative disorders, including ALS. To monitor oxidative stress induced by overexpression of ALS causative genes, stable clones of neuronal SHSY5Y cells expressing the roGFP or mitochondrial targeted (mito and IMS) roGFP reporter have been produced. Stable cell lines were selected and the expression levels of cytosolic and mitochondria-targeted roGFP were evaluated by western blot analysis and autofluorescence (Fig. 20).

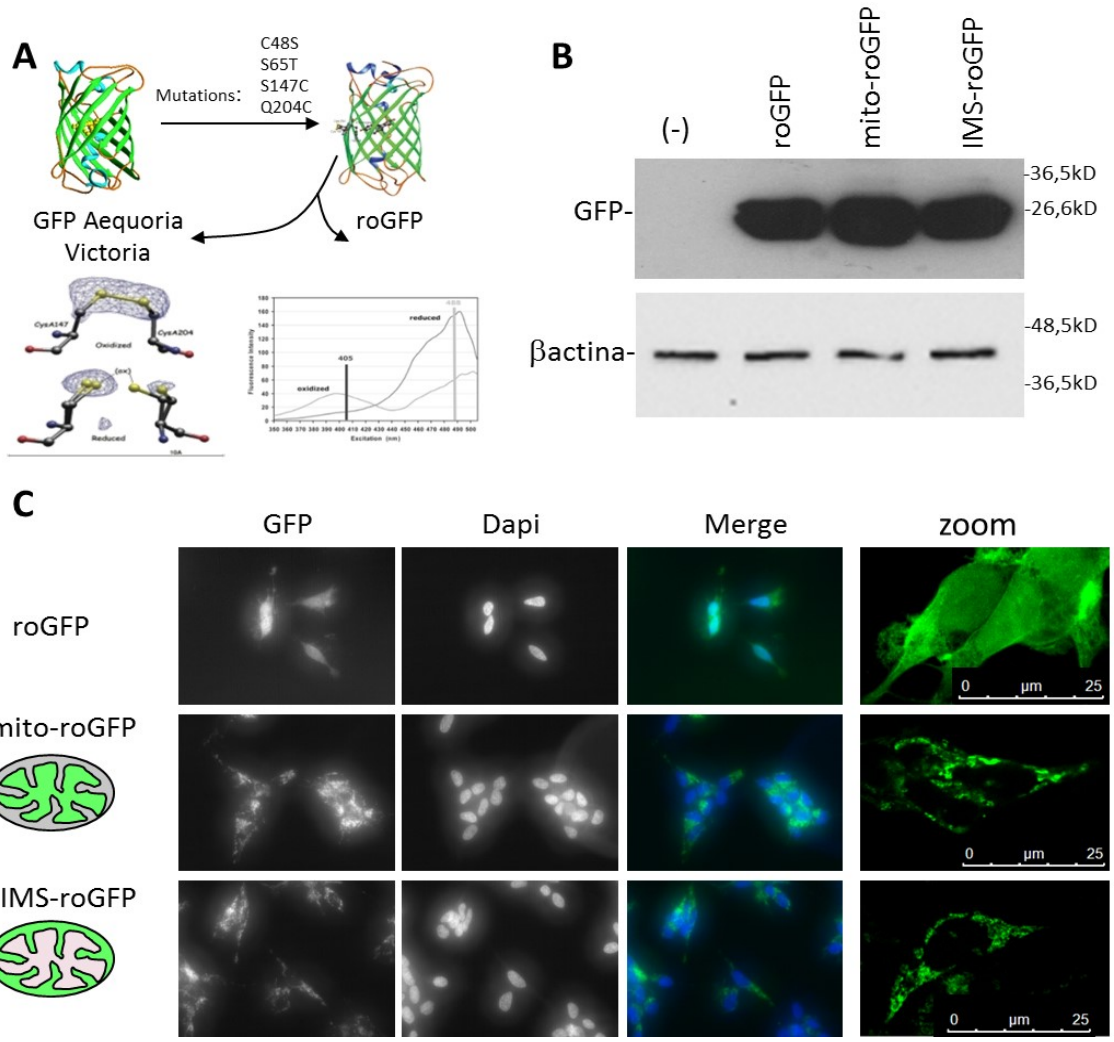


Figure 20: A) Structural features of roGFP. This reporter was constructed by engineering four aminoacid residues of $GFP^{WT}$. The cysteines Q204C and S147C form a disulfide cross-link between adjacent β-strands near the chromophore, which causes a internal structural rearrangements, so that the neutral chromophore is favored over the anionic. Therefore, as a population of roGFP is oxidized, disulfide formation leads to an increase in the excitation peak at 405nm at the expense of the 480nm peak, the 405/480 excitation ratio is an indicator of the ambient cellular redox potential [231 253]. Cell lysates of SH-SY5Y cell line stably expressing roGFP or mitochondrial targeted (mito and IMS) roGFP were subjected to western blot (B) with anti-GFP antibodies and autofluorescence analysis (C) to evaluate expression level and localization of roGFP.

To evaluate ability of these stable clones to monitor in vivo cellular redox state, the 405/480nm excitation ratio (with emission measured at 508nm) was measured in the presence of excess exogenous membrane permeable oxidants ($H_2O_2$) or reductants (DTT). Fluorescent emission was detected through a microplates reader (Victor X5, Perkin Elmer) (Fig. 21).

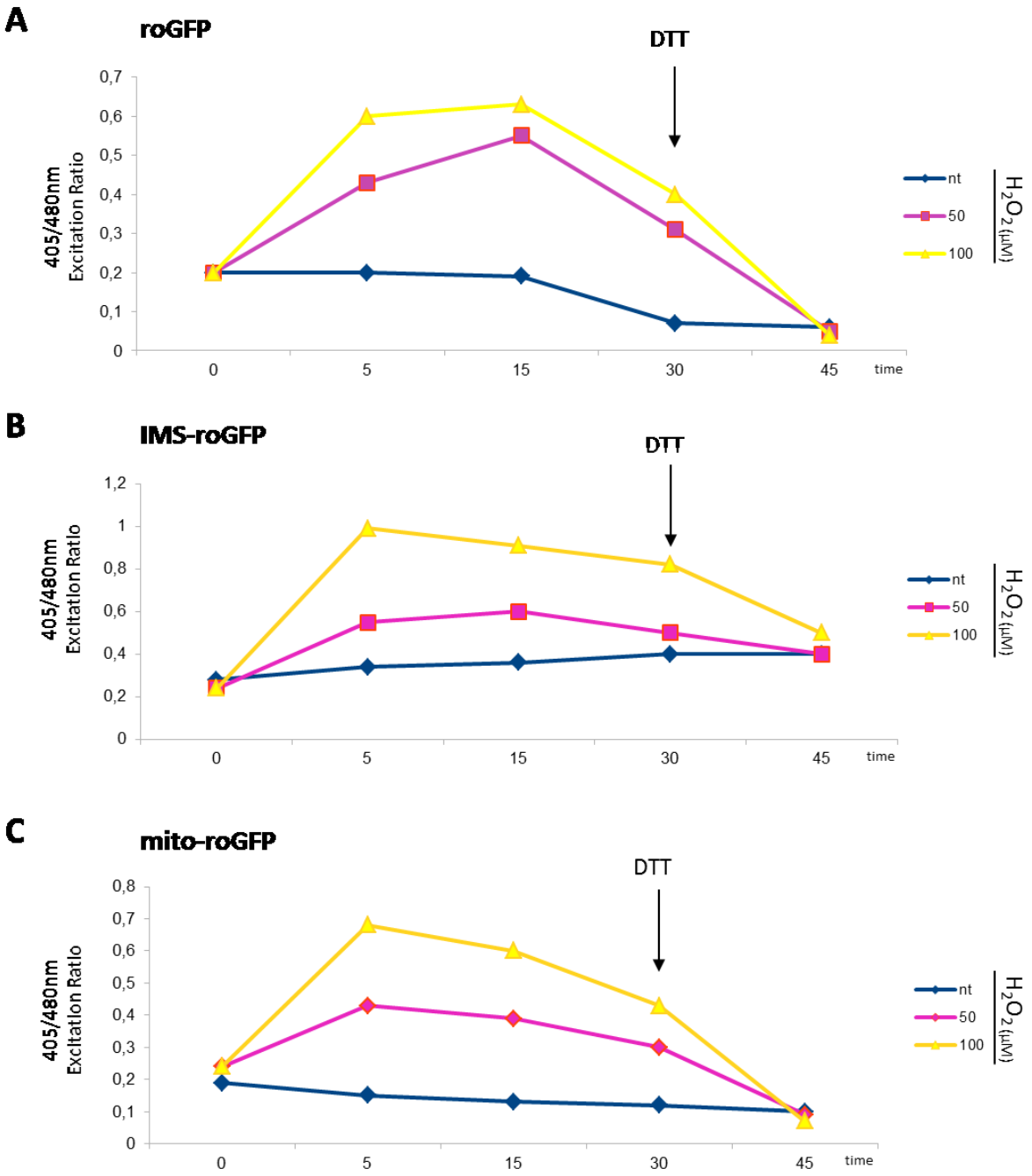


Figure 21: Validation of the probe: variations of cellular redox state in living SH-SY5Y cells expressing roGFP (A), IMS-roGFP (B) and mito-roGFP (C) after treatment for 30' with scalar concentrations of exogenous oxidants and subsequent treatment for 15' with reductants (DTT 10mM). Cellular redox state was expressed as 405/480nm excitation ratio (with emission measured at 508nm).

As expected, the addition of $H_2O_2$ determined immediate oxidation of roGFP, detectable by increase of 405/480nm excitation ratio. Over time a slight decrease in oxidation level could be observed, although only the addition of DTT 10mM took it back to basal level.

### *4.1.3.2 Construction and characterization of SHSY5Y cells stably expressing YFP$^u$ to monitor alterations in the activity of ubiquitin–proteasome system.*

Accumulation of aggregated proteins and impairment of ubiquitin/proteasome system (UPS) are a key feature of the pathology of all the major neurodegenerative diseases, included ALS. To measure the UPS function in living cells, neuronal SHSY5Y cells stably expressing the YFP$^u$ reporter (Fig. 22A) have been generated. Stable cell lines were selected and the expression levels of YFP$^u$, was evaluated by western blot analysis and autofluorescence after treatment with proteasome inhibitors MG132 or lactacystin (Fig. 22B and 22C).

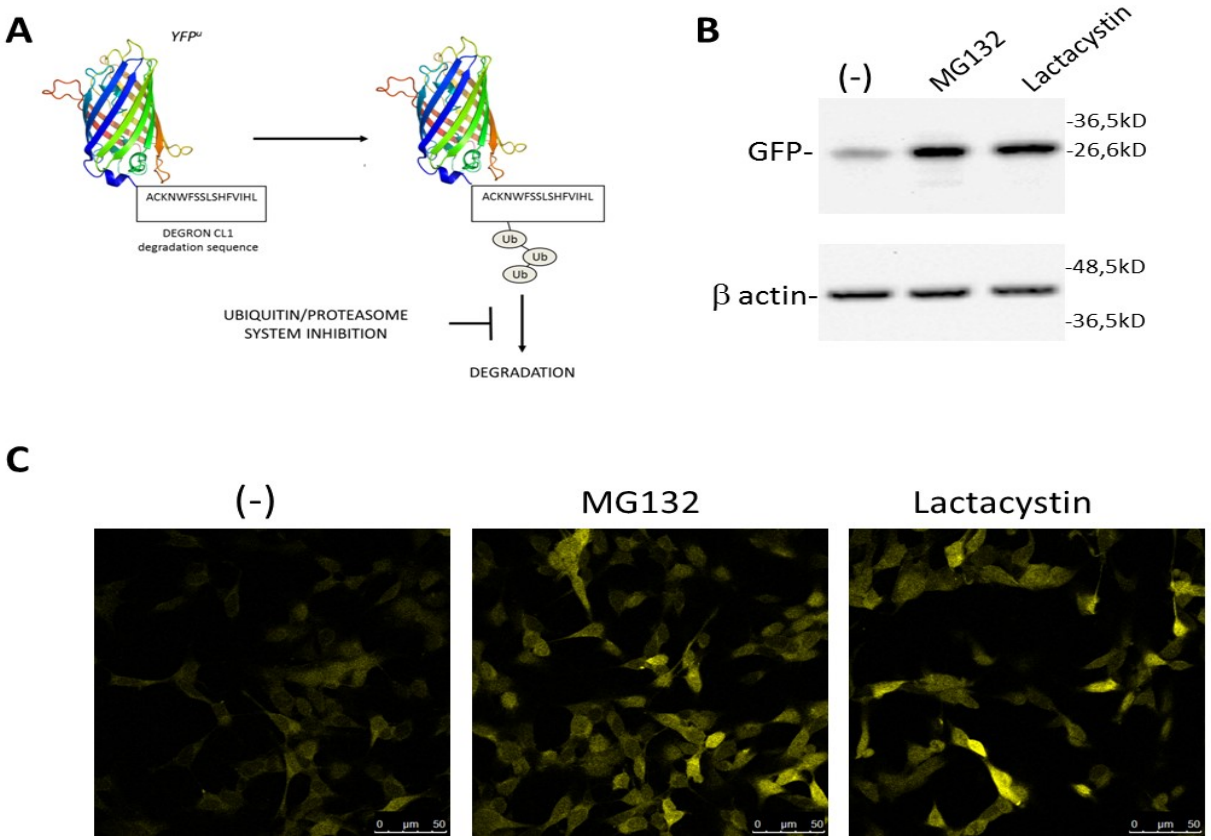


Figure 22: A) Structural features of YFP$^u$: This reporter was created by mutating Thr203 of GFPWT to aromatic amino acids, typically Tyr, and by fusion of a short Degron, CL1, to the COOH-terminus of the protein, which sends the protein at degradation through UPS system. Cell lysates of SH-SY5Y cell line stably expressing YFP$^u$ were analyzed treating the cells with proteasome inhibitors (MG132 and lactacystin 15μM for 4 hours). The accumulation of YFP$^u$ was analyzed by western blot (B) with anti-GFP antibodies and autofluorescence experiments (C)

As predictable, treatment with proteasome inhibitors determined accumulation of YFP$^u$, suggesting impairment of UPS system.

### *4.1.3.3 Construction and characterization of SHSY5Y cells stably expressing DsRed-LC3-GFP to monitor autophagy.*

Autophagy is an intracellular lysosomal degradation process, which plays an important role in cell growth and development, and keeps cellular homeostasis in all eukaryotes (Fig. 23A). Emerging evidences support the notion that dysregulation of autophagy might be critical for pathogenesis of ALS. To monitor autophagy activation, stable clones of neuronal SHSY5Y cells expressing DsRed-LC3-GFP reporter have been produced (Fig. 23B). Stable cell lines were selected and the expression levels of DsRed-LC3-GFP were evaluated by autofluorescence experiments (Fig. 23C) after treatment of 4 hours with proteasome inhibitor MG132.

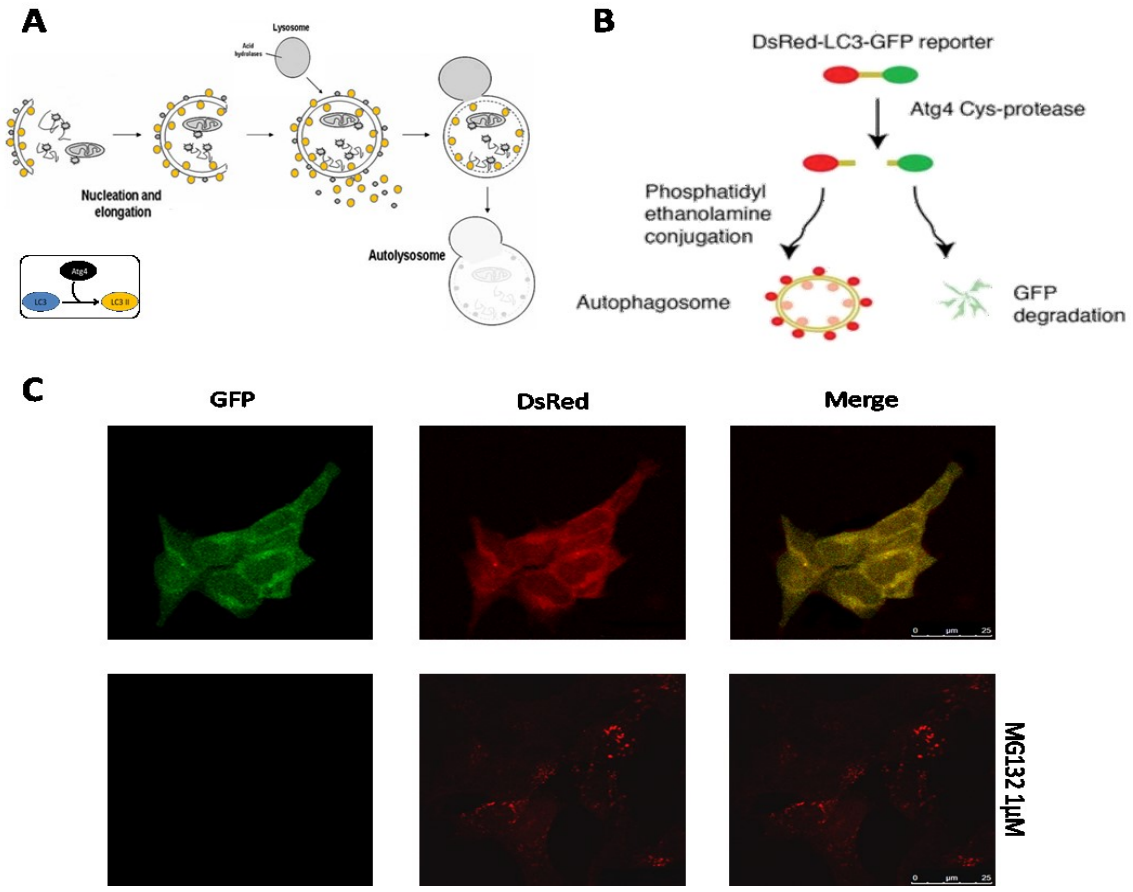


Figure 23: A) The autophagic process: Autophagy is characterized by the formation of a double-membrane delivery vesicle, the autophagosome. At present, microtubule-associated light chain 3-II (LC3-II) is the major protein marker specifically associated with the autophagosome in eukaryotes [242]. B) Schematic diagram showing the concept behind the DsRed-LC3-GFP autophagy reporter: when autophagy is activated, LC3 is cleaved to protease Atg4 in LC3II. Complex DsRed-LC3II is transported in the autophagosome membrane where is able to resist to the acid pH, while the GFP is degraded. C) SH-SY5Y cell line stably expressing DsRed-LC3-GFP was analyzed by autofluorescence experiments before and after treatment with inhibitor proteasome (MG132 1µM for 4 hours).

As expected, treatment with proteasome inhibitor determined cleavage of LC3 and the resulting red autofluorescence accumulation in the autophagosome membrane while the GFP is degraded, suggesting activation of autophagy pathway.

### *4.1.3.4 Construction and characterization of SHSY5Y cells stably expressing CFP-DEVD-YFP to monitor caspase-3 activation.*

Apoptosis is responsible for many normal development processes as embryonic development, in shaping the adult organism, in surveillance of the cell cycle, and in some forms of chemically induced cell death. Inappropriate apoptosis has been implicated in many human disease such as neurodegeneration and evidences support the opinion that dysregulation of apoptotic pathway might be a key event for ALS pathogenesis. The activation of caspasi-3 is a central event in the apoptotic process. To monitor apoptosis activation through cleavage of capsase-3, stable clones of neuronal SHSY5Y cells expressing CFP-DEVD-YFP reporter (FRET: fluorescence resonance energy transfer) have been produced. Stable cell lines were selected and the expression levels of CFP-DEVD-YFP were evaluated by western blot experiments (Fig. 24C) after induction of apoptosis through nutrients deprivation (HBSS: Hank's Balanced Salt Solution) or stausporine.

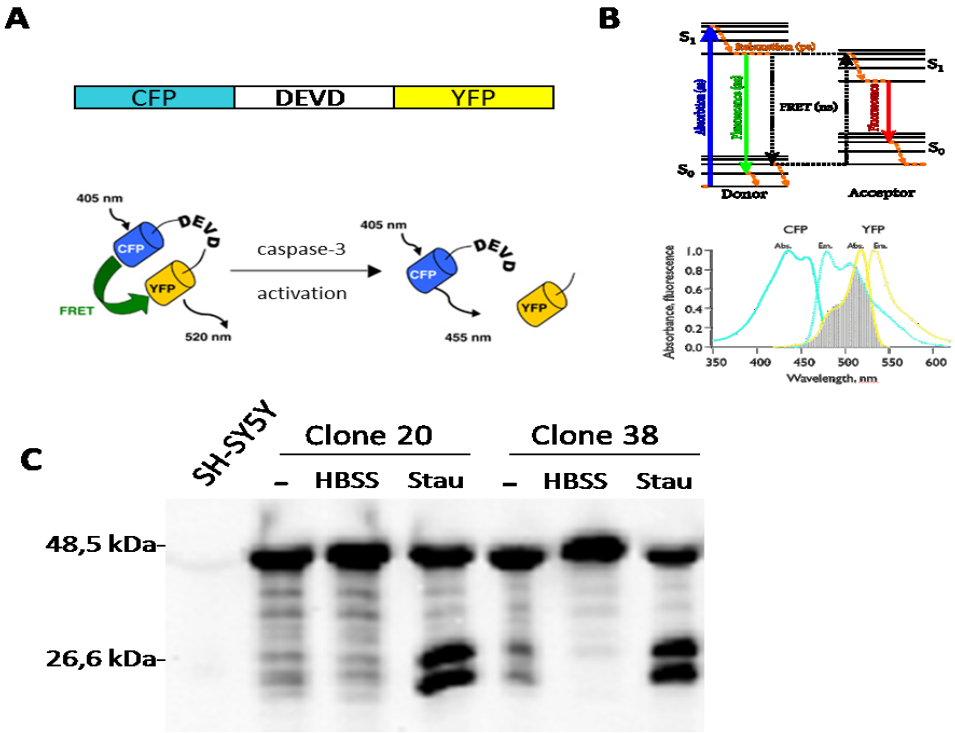


Figure 24: A) Schematic diagram showing the concept behind the CFP-DEVD-YFP reporter: the emission spectrum of cyan fluorescent protein (CFP) overlaps with the excitation spectrum of yellow fluorescent protein (YFP), placing CFP in proximity to YFP (i.e. <5nm) allows FRET between the two fluorescent moieties to occur. When induced apoptosis occurs the cleavage of DEVD sequence through caspase-3 protease and the decrease in FRET signal. B) SH-SY5Y stable

clones expressing CFP-DEVD-YFP were analyzed by western blot before or after induction of apoptosis through nutrients deprivation (HBSS for 2 hours) or treatment with stausporine (Stau 1μM for 2 hours).

As shown in figure 24B, treatment with stausporine determined cleavage of DEVD target sequence and the resulting separation of two fluorescent protein, suggesting a probable activation of caspasi-3.

### *4.1.4 Measure cell toxicity induced by ALS causative genes expression using fluorescent markers.*

In order to evaluate the possibility of using neuronal cell lines expressing roGFP, cytoplasmic or mitochondrial, or $YFP^u$ such as cellular system in HTS assays (see Introduction), several *in vivo* experiments have been performed using different cellular models to monitor the biological damage induced by the expression ALS-causative genes driven by adenoviral system.

Firstly, to set out the *in vivo* experiments, stable cell lines espressing roGFP or mitochondrial targeted (mito and IMS) roGFP were infected with recombinant adenoviruses (M.O.I. of 30 pfu/cell) encoding for wild type SOD1 or with the pathological mutations H80R and G93A. After 24, 48 or 72 hours of infection, the cells were analyzed in a microplates reader (Victor X5 - PerkinElmer) to evaluate the cellular redox state as 405/480nm excitation ratio and the same cells were lysed and analyzed by western blot to verify expression levels of SOD1 genes and roGFP.

As shown in figure 25A, after 24 or 48 hours of infection the overexpression of SOD1 with H80R pathological mutation induced a significant increase in the 405/480nm excitation ratio in stable cells espressing cytoplasmic roGFP when compared to wild type SOD1 or G93A mutant, to indicate that H80R mutant is able to induce oxidative stress in cellular environment. 72 hours post-infection, a drastic fall in the 405/480nm excitation ratio was observed in all samples likely to indicate a general state of cellular impairment. Also in neuronal cells stably espressing the mitochondrial variant mito-roGFP (Fig. 25B) only the overexpression of H80R mutant increased the 405/480nm excitation ratio after 24 or 48 hours of infection. Instead any significant change in the 405/480 nm excitation ratio was observed in stable cells expressing the other mitochondrial variant IMS-roGFP (Fig. 25C), to indicate that this system probably is not able to detect changes in the cellular redox state. Figure XD shows the increase in SOD1 expression over time (24-48-72 hours) and the expression levels of cytoplasmic roGFP in stable clone, similar results were also obtained on neuronal SH-SY5Y cells stably expressing two mitochondrial variants of roGFP (mito-roGFP and IMS-roGFP) (data not shown).

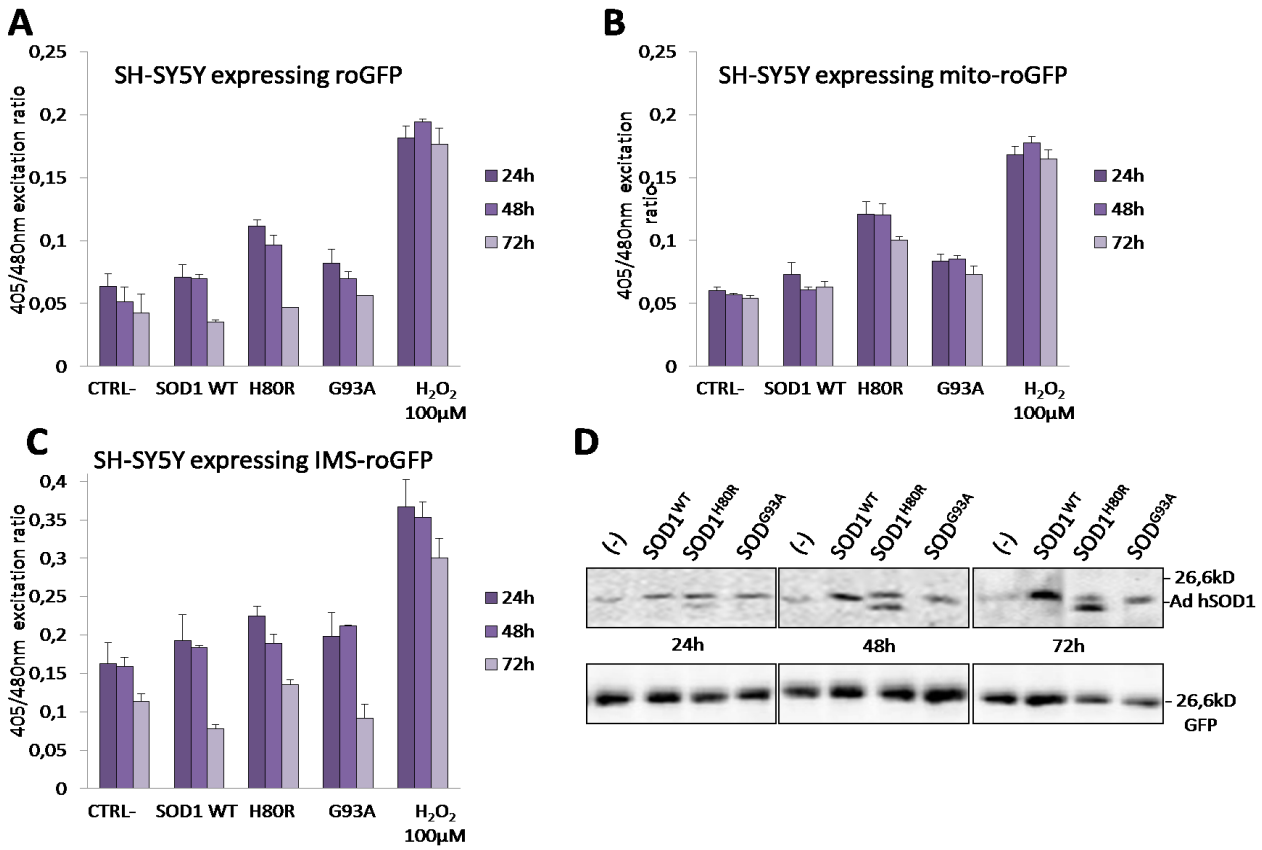


Figure 25: Time course on SH-SY5Y stably expressing roGFP cytoplasmic or mitochondrial (mito-roGFP or IMS-roGFP), to monitor the biological damage induced by the expression of SOD1 gene driven by adenoviral system. The graphs show the changes in the cellular redox state in the cells (SHSY5Y) expressing (A) roGFP, (B) mito-roGFP and (C) IMS-roGFP after exposure for 24-48-72 hours to the proper concentration of adenoviruses encoding for SOD1 gene in wild type form or with pathological mutations indicated. The fluorescence intensity was assessed using a microplates reader (Victor X5, Perkin Elmer), and the cellular redox state expressed as the ratio between the emission following excitation at 405nm and 480nm (with emission at 535nm). D) Representative western blot analysis using antibodies anti-SOD1 to verify comparable expression levels of SOD1 gene wild type or mutants over time. Antibody anti-GFP was used to verify the presence of roGFP reporter in stable cell expressing cytoplasmic roGFP and as a control of protein concentration.

At this point of the study, similar experiments were carried out by choosing the optimal conditions found from previous experiments. Therefore neuronal cells stably espressing cytoplasmic roGFP and mito-roGFP were infected with 30 pfu/cell of recombinant adenoviruses encoding for the other fALS genes, wild type TDP43 or with pathological mutations Q331K and M337V and wild type FUS or with pathological mutations H517G and R521G. After 48 hours of infection, neuronal cells were analyzed in a microplates reader (Victor X5 PerkinElmer) and expressed cellular redox state as the 405/480nm excitation ratio. Then, the same cells were lysed and analyzed by western blot to verify expression levels of ALS-causative genes and roGFP.

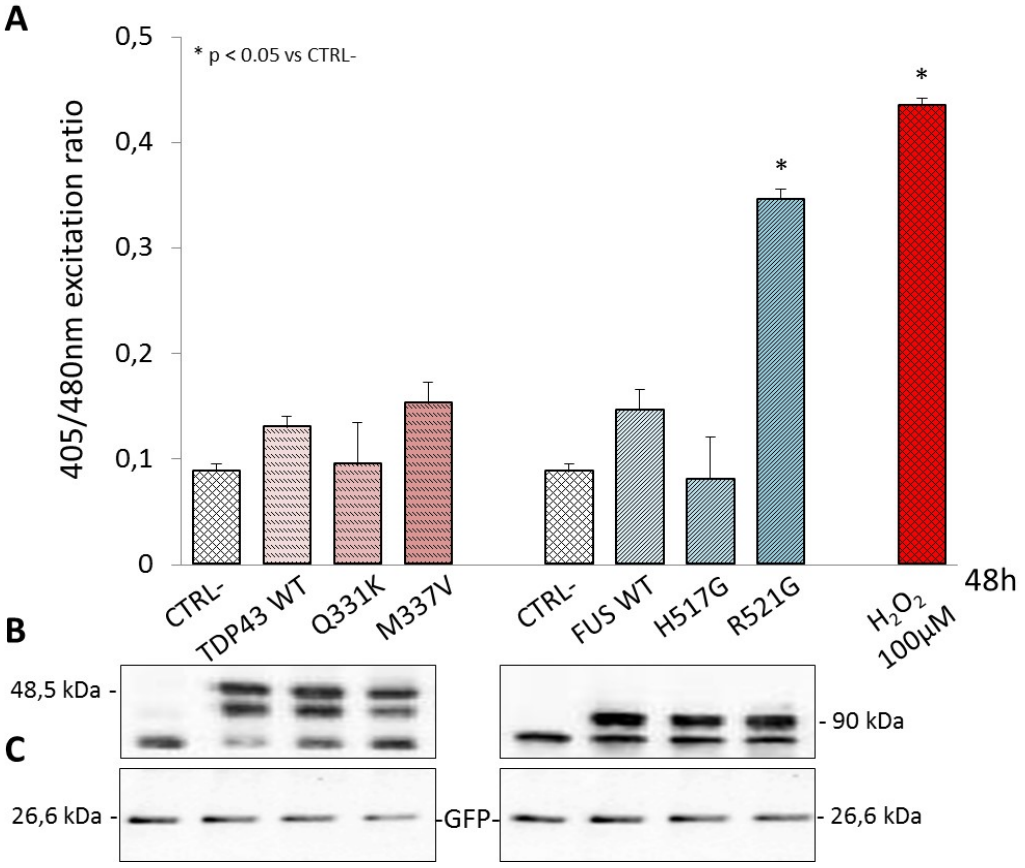


Figure 26: In vivo assay on SH-SY5Y stably expressing roGFP to monitor the biological damage induced by the expression of fALS-causative genes driven by adenoviral system. A) The graph shows the changes in the cellular redox state in the cells (SHSY5Y) expressing roGFP after exposure for 48 hours to the proper concentration of adenoviruses encoding for all three ALS-causative genes in their wild type or with pathological mutations indicated. The fluorescence intensity was assessed using a microplates reader (Victor X5, Perkin Elmer), and the cellular redox state expressed as the ratio between the emission following excitation at 405nm and 480nm (with emission at 535nm). B) Western blot analysis using antibodies anti-TDP43 and anti-FUS to verify comparable expression levels of all two ALS-causative genes wild type or mutants. Antibody anti-GFP was used to verify the presence of roGFP reporter and as a control of protein concentration (C).

As shown by the graph in figure 26A, the overexpression of FUS with pathological mutation R521G, induced a significant increase in the 405/480nm excitation ratio when compared with expression of the wild type FUS or H517G mutant, to indicate that R521G mutant is able to induce oxidative stress in cellular environment. Instead the overexpression of wild type TDP43 or with the pathological mutations, Q331K and M337V, did not induced any alteration of 405/480nm excitation ratio, to indicate that this cellular model probably is not able to evaluate oxidative stress induced by overexpression of this gene. Similar results were also obtained on neuronal SH-SY5Y cells stably expressing the mitochondrial variants mito-roGFP, while stable clones expressing IMS-roGFP are not able to detect changes in the cellular redox state (data not shown).

Using the same experimental strategy described in the experiment of roGFP, 48 hours post-infection the neuronal SH-SY5Y cells stably espressing $YFP^u$ reporter, able to monitor UPS activity,

were analyzed in a microplates reader (Victor X5 -PerkinElmer) to evaluate the fluorescence. Then, the same cells were lysed and analyzed by western blot to verify expression levels of ALS-causative genes and accumulation of $YFP^u$.

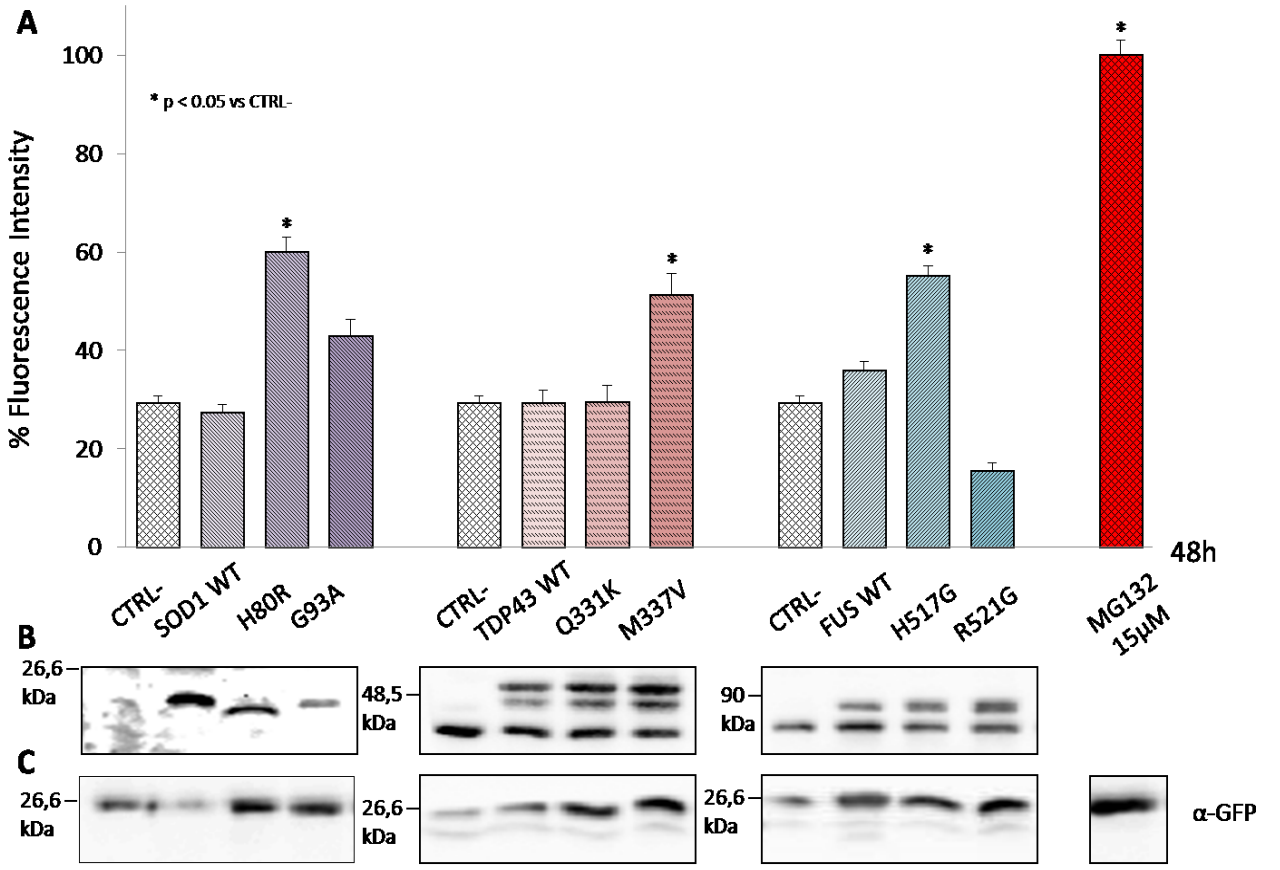


Figure 27: In vivo assay on SH-SY5Y stably expressing $YFP^u$ to monitor the biological damage induced by the expression of ALS-causative genes driven by adenoviral system. A) The graph shows the changes in fluorescence intensity in the cells (SHSY5Y) expressing $YFP^u$ after exposure for 48 hours to the proper concentration of adenoviruses encoding for all three ALS-causative genes in their wild type or with pathological mutations indicated. The fluorescence intensity was assessed using a microplates reader (Victor X5, Perkin Elmer), with excitation at 500nm. B) Western blot analysis using antibodies anti-SOD1, anti-TDP43 and anti-FUS to verify comparable expression levels of all three ALS-causative genes wild type or mutants. Antibody anti-GFP was used to verify the accumulation of $YFP^u$ reporter (C).

As shown by the graph in figure 27A, the overexpression of SOD1 with pathological mutation H80R induced a significant increase in fluorescence intensity when compared with expression of the wild type SOD1 or G93A mutant, suggesting that the presence of H80R mutation is probably able to impair the UPS activity resulting in accumulation of the protein. Also the overexpression of TDP43 with the pathological mutation M337V and the overexpression of FUS with pathological mutation H517G increased the fluorescence intensity when compared with expression of the respective wild type or the other mutants. But when the $YFP^u$ accumulation was evaluated by western blot analysis (Fig. 27C), it has been showed that even the expression of the other mutants G93A of

SOD1, Q331K of TDP43 and H517G of FUS, as well as the overexpression of TDP43 and FUS in their wild type form caused the $YFP^u$ accumulation. This mismatch between data obtained by microplates reader and those obtained by western blot analysis is probably due to the pro-aggregative properties of both wild type or mutant FUS and TDP43. The possible presence of these aggregates may interfere with the instrumental reading of fluorescence.

Finally, we decided to monitor $YFP^u$ accumulation through autofluorescence experiments. 48 hours after infection with adenoviruses encoding for all fALS genes, neuronal cells stable espressing $YFP^u$ were analyzed by confocal microscopy.

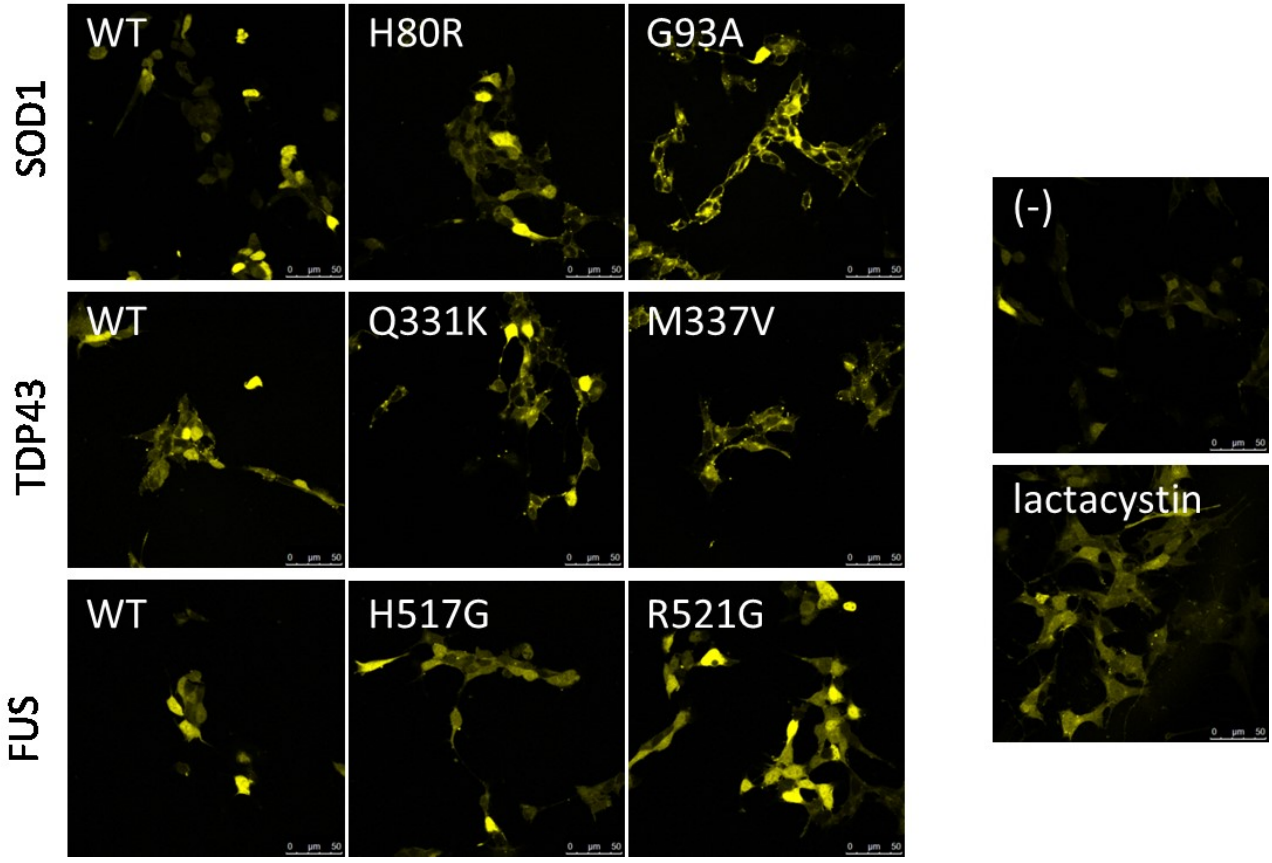


Figure 28: Autofluorescence analysis on SH-SY5Y stably expressing $YFP^u$ to monitor the biological damage induced by the expression of ALS-causative genes driven by adenoviral system. Cells (SHSY5Y) expressing $YFP^u$ were infected adenoviruses encoding for all three ALS-causative genes in their wild type or with pathological mutations indicated. 48 hours after infection the autofluorescence accumulation was detected by confocal microscopy. All images were acquired using the laser at the same power.

Figure 28, in agreement with the western blot analysis data (Fig. 27C), shows that overexpression of all fALS causative genes is able to induce $YFP^u$ accumulation although in different ways. In fact, expression of wild type form of SOD1, TDP43 and FUS as well as of some mutants (H80R-SOD1, Q331K and M337V-TDP43 and H517G-FUS) induces a slight fluorescence accumulation in most cells and only a 10-20% of cells showed a marked and generalized fluorescence accumulation if

compared with the same cells untreated or treated with UPS inhibitor (lactacystin). Instead, G93A-SOD1 and R521G-FUS expression induced on at least 80% of cells a more marked fluorescence accumulation.

Probably, this cellular models is not suitable for an instrumental reading of the assay.

## *4.2 Study of the pathophysiological mechanisms responsible for cellular toxicity of pathological forms of two RNA-binding protein, FUS and TDP-43, in familial forms of ALS.*

In recent years the identification of TDP43[92] and FUS[70,71] as ALS causative genes drew attention on two problems closely linked to each other: (i) the presence of protein aggregates linked and/or caused by the proteolytic systems alteration; (ii) the RNA metabolism alteration, resulting in the relocation TDP43 and/or FUS in the cytoplasm.

The strong structural and functional similarities between TDP43[254] and FUS[255], which are both proteins able to bind DNA and RNA , suggested a common mechanism of pathogenicity. The two current hypotheses involve both an abnormal RNA metabolism[60] and an accumulation in cytoplasmic insoluble aggregates of mutant TDP43 and/or FUS with the consequent neuronal death. However, the mRNA targets of these two genes as well as the functional role of the aggregates in neurodegeneration are still unknown. Therefore, this project aims to explore the molecular mechanisms of toxicity induced by the expression of pathological forms of TDP- 43 and FUS in two main directions:

1. Identification of the RNA target of FUS.
2. Study of the relationship between aggregation, proteins localization, autophagy and cell death alterations in the presence of pathological forms of TDP43.

### *4.2.1 Identification of the RNA target of FUS.*

Several lines of evidence suggested an involvement of FUS in multiple steps of RNA metabolism including transcription, splicing or transport of mRNA[60], as well as microRNA metabolism[66]. Misregulation of RNA processing has been described in a growing number of neurological diseases[256]. The recognition of FUS as a central player in neurodegeneration, and the recent identification of ALS-causing mutations in TDP43[92], another RNA/DNA binding protein, has reinforced a crucial role for RNA processing regulation in neuronal integrity. However, a comprehensive protein-RNA interaction map for FUS and identification of post-transcriptional events that may be crucial for neuronal survival remains to be established.

#### *4.2.1.1 CLIP (CrossLinking ImmunoPrecipitation) to identify RNA partners of FUS.*

To identify potential RNA target of FUS protein I set out to develop a variant of CLIP (Cross-Linking Immune-Precipitation) technique on SH-SY5Y cells infected with adenovirus encoding for this ALS causative gene in wild-type form or with pathological mutations (Fig.29).

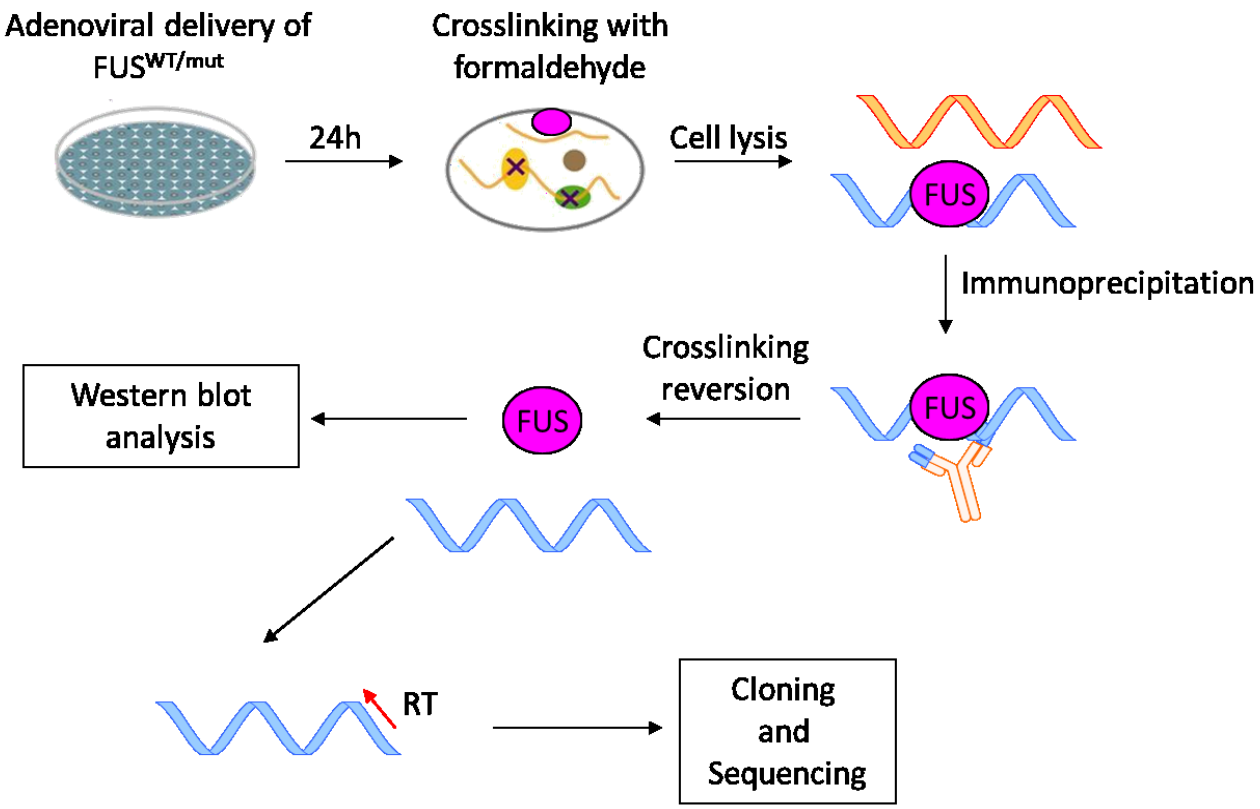


Figure 29: A schematic representation of CLIP procedure for identification of RNA partners of FUS protein in the context of intact cells. Neuronal SH-SY5Y cells adherent are treated with formaldehyde, leading to formation of a interactions between protein and RNA. Cells were lysed in RIPA buffer and the lysate was subjected of sonication (three cycles of 30 seconds on ice), then the lysate was immunoprecipitated and after reversion of crosslinking (heat treatment for 45 minutes at 75°C), the protein fraction was analyzed by western blot and RNA fraction was amplified by RT-PCR. The obtained cDNA was cloned and positive colonies was sequenced to identify the mRNA targets.

In particular, neuronal SH-SY5Y cells were infected with adenoviruses encoding for wild type FUS (CLIP-FUS), using as negative control of CLIP experiment SH-SY5Y uninfected cells (CLIP-NEG). After 24 hours of infection, protein-RNA interactions were fixed on intact cells by treatment with formaldehyde 0,5% and then cells were lysed in RIPA buffer, sonicated and immunoprecipitated with anti-myc antibody directed against myc epitope in fusion with C-terminal sequence of FUS. As shown in figure 30A, after reversion of crosslinks, in the protein fraction, analyzed by western blot, FUS protein has been detected.

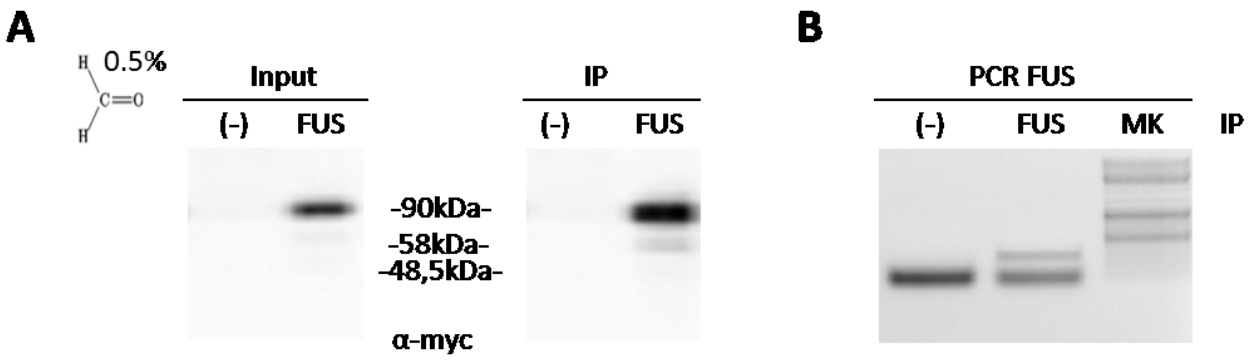

Figure 30: Analysis of protein and RNA fractions after immunoprecipitation of RNA-protein complexes. After reversion of crosslinks between RNA and proteins, the presence of FUS in protein fraction, before (Input) and after (IP) the immunoprecipitation, was assessed by Western blot analysis using antibody anti-myc (A). As positive control of CLIP experiment, the RNA fraction was amplified by RT-PCR with random hexamers and cDNA was subjected a PCR reaction to amplify a fragment of about 250bp at C-terminus of FUS sequence (B).

The RNA fraction was amplified by RT-PCR with random hexamers to obtain cDNA. At this point, to control the presence of FUS RNA after immunoprecipitation, we made a PCR to amplify a fragment of the C-terminus of FUS sequence. Presence of the amplified expected has been found only after immunoprecipitation of FUS but not in CLIP-NEG sample (Fig. 30B).

Then, we went ahead by creating double-stranded DNA (dsDNA) which was phosphorylated and cloned into the pBluescript II SK(-) vector.

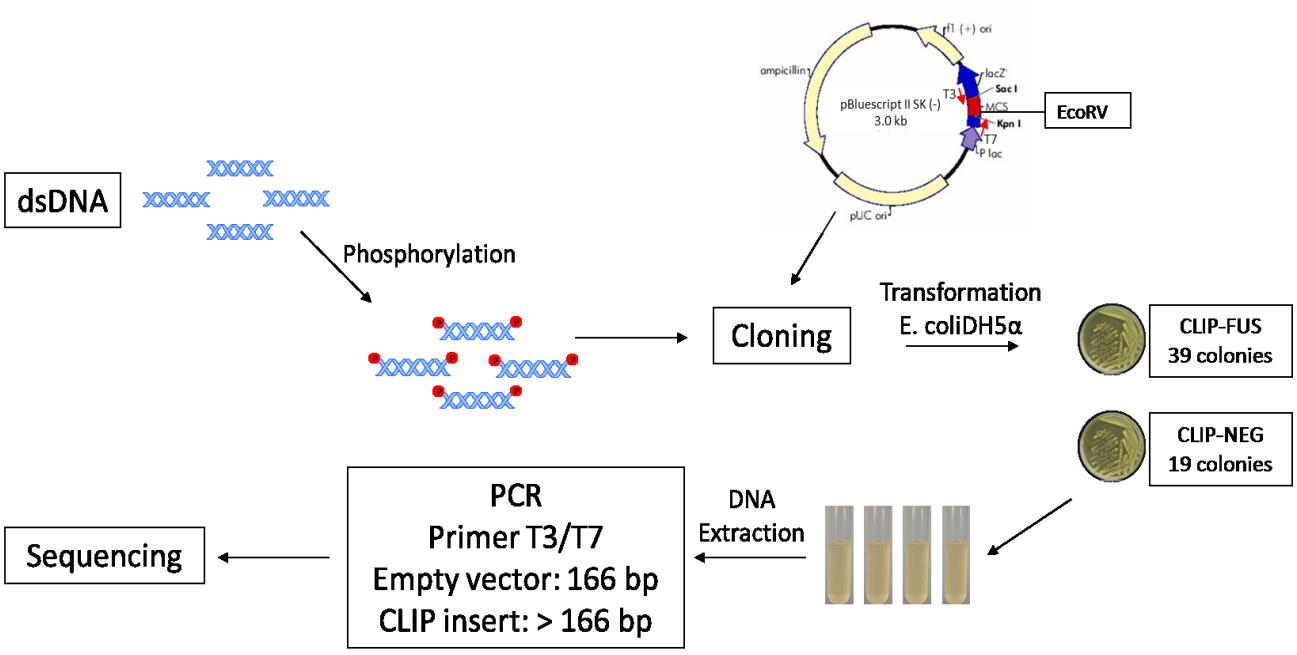


Figure 31: A schematic representation of the final steps of CLIP procedure. The dsDNA obtained was subjected to Klenow reaction (30 minutes at 25°C) and T4 polymerase reaction (10 minutes at 37°C) with respectively random hexamers and dNTPs to generate double strand DNA which was phosphorylated by treatment with T4 polynucleotide kinase (30 minutes at 37°C) with ATP as phosphate donor. The fragments of dsDNA obtained were cloned into EcoRV restriction site of pBluescript II SK (-) vector and transformed in *E.coli* DH5α cells. All colonies were grown singularly and then plasmid DNA was extracted. The presence of CLIP-insert was analyzed by PCR using T3 and T7 primers, empty vectors presented an amplified of 166bp while vector with CLIP-insert present an amplified >166bp. All positive samples was sequenced availing an external company.

The recombinant plasmids obtained were transformed in *E. coli* DH5α cells, all colonies were grown individually and then was performed the extraction of the plasmid DNA. Eventual CLIP-insert present were analyzed by performing a PCR reaction using T3 and T7 primers able to discriminate empty vectors from CLIP-insert vectors (Fig. 31).

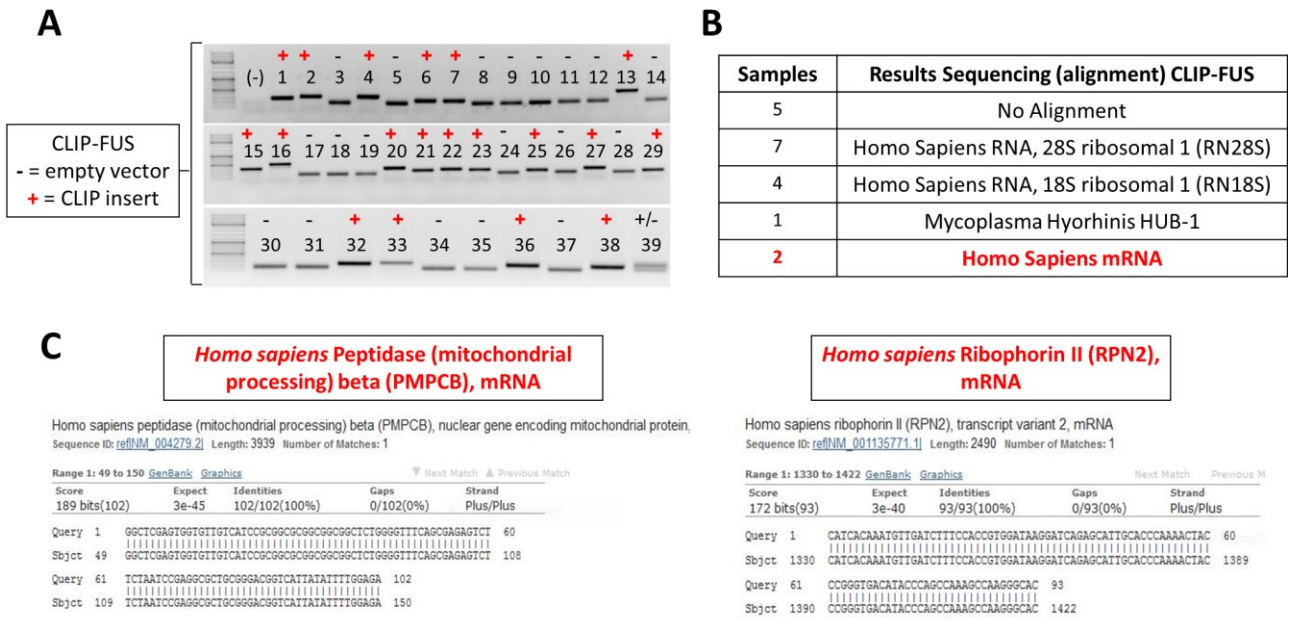


| Samples | Results Sequencing (alignment) CLIP-FUS |
|---|---|
| 5 | No Alignment |
| 7 | Homo Sapiens RNA, 28S ribosomal 1 (RN28S) |
| 4 | Homo Sapiens RNA, 18S ribosomal 1 (RN18S) |
| 1 | Mycoplasma Hyorhinis HUB-1 |
| 2 | Homo Sapiens mRNA |

Figure 32: FUS interacts with two human mRNA. A) 19 positive colonies were identified by PCR using T3 and T7 primers. (-) negative control of PCR reaction; - = empty vector, the amplified 166bp; + = CLIP-insert vector, the amplified >166bp. B) Summary table of results of sequence analysis on the 19 positive samples for CLIP-insert. C) The two human mRNA which interact with FUS protein.

As shown in figure 32A, 19 positive vectors have been identified for CLIP-insert in CLIP-FUS sample by PCR reaction, while it has not been identified any positive vector in CLIP-NEG samples (data not shown). These PCR products were subjected to sequence analysis availing an external company and only two of these samples showed an alignment with human mRNA (Fig. 32B and 32C): (i) *Homo sapiens* Ribophorin II (RPN2), mRNA. RPN2 is a multi-pass membrane protein localized in the endoplasmic reticulum membrane, essential subunit of OST (OligoSaccharylTransferase) complex which catalyses the transfer of a high mannose oligosaccharide from a lipid-linked oligosaccharide donor to an asparagine residue within an Asn-X-Ser/Thr consensus motif in nascent polypeptide chains; (ii) *Homo sapiens* Peptidase (mitochondrial processing) beta (PMPCB), mRNA. PMPCB is an heterodimeric enzyme localized in mitochondrion matrix which cleaves presequences (N-terminal transit peptides) from mitochondrial protein precursors, typically with Arg in position P2.

Given the positive results obtained at this point we would have wanted to apply this CLIP method on neuronal SH-SY5Y cells infected with adenovirus encoding for FUS with pathological mutations ALS associated. But we decided to abandon this aim of my PhD, following the identification of global RNA targets for wild type and mutant FUS proteins ($FUS^{R521G}$ and $FUS^{R521H}$) using PAR-CLIP method [257].

We want to emphasize that the mRNAs identified through my CLIP method were also identified in the publication above mentioned.

### *4.2.1.2 R521G-FUS mutant does not mediates alternative splicing of its mRNA targets.*

In order to evaluate if expression of mutant FUS was able to mediate alternative splicing of its mRNA target, we chose to use experimental strategy shown in figure 33.

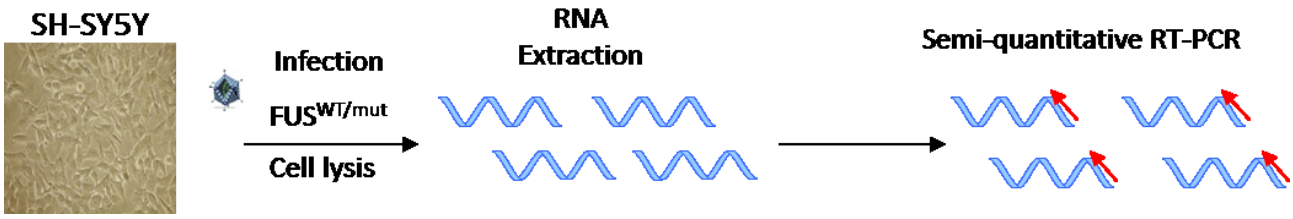


Figure 33: Experimental strategy to evaluate alternative splicing.

Neuronal cells were infected with recombinant adenoviruses encoding for wild type FUS or with pathological mutation R521G. 48 hours after infection, cells were harvested and then was extracted total mRNA which was subjected to a semi-quantitative RT-PCR of selected targets, RPN2 and PMPCB mRNAs, using primer pairs including the exon-exon junction nearest to binding site FUS-mRNA (Fig. 34).

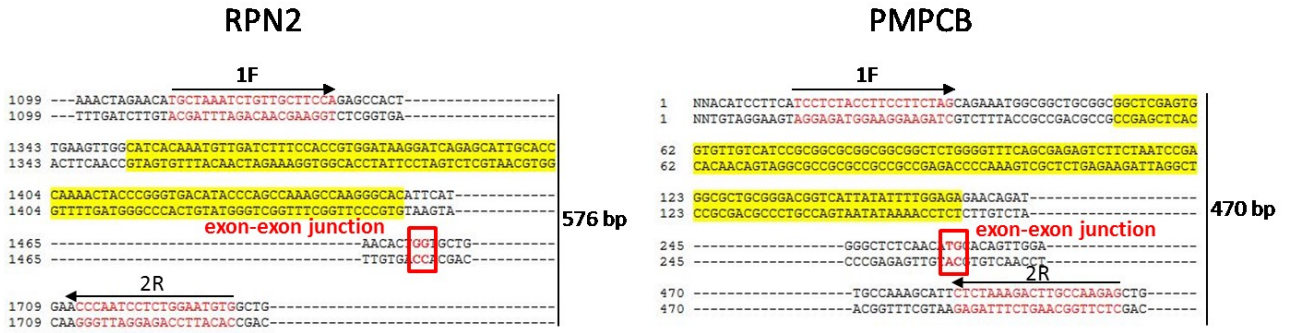


Figure 34: Schematic representation of primer pairs to evaluate alternative splicing. The black arrows depict the position of the primers used for RT-PCR. Yellow highlighted sequences indicate FUS binding sites as defined by CLIP-assay and red boxes define exon-exon junctions.

As shown in figure 35, expression of $FUS^{R521G}$ does not influence alternative splicing of both mRNA targets.

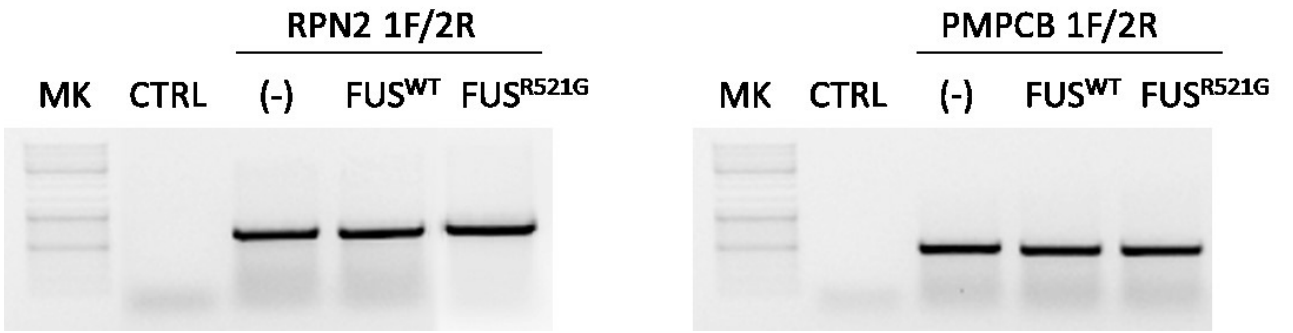


Figure 35: R521G-FUS mutant does not mediates alternative splicing of its mRNA targets. Semi-quantitative RT-PCR of selected targets showing any splice changes in samples with $FUS^{R521G}$ compared to $FUS^{WT}$ and to controls.

### *4.2.2 Study of the relationship between aggregation, proteins localization, autophagy and cell death alterations in the presence of pathological forms of TDP43.*

As stated before, protein aggregation is a key event of all of the major neurodegenerative diseases. In recent years, discovery of TDP43 mutations in familial form of ALS and identification of TDP43 aggregates as major component in nearly all ALS patients, has led to the hypothesis that altered TDP43 function can be a primary cause of the disease. However, the mechanism through which TDP43 promotes motor neurons death is still under investigation. To date we know that some pathological mutations cause aberrant modification of the protein that generates, for proteolysis, a C-terminal fragment of about 25 kDa, and one N-terminal approximately 18 kDa. These fragments combine to form cytoplasmic aggregates, resulting in dysfunctions of neuronal cells, probably related to loss of function of TDP-43 at the nuclear level [258].

Several dominantly inherited mutations in TARDBP have been reported in more than one patient and by more than one group, which corroborates their causative role in disease pathogenesis [86], but it remains to be proved whether these mutants can induce a motor neuronal phenotype and to determine the mechanism of toxicity. The aim of this work is the understanding of the relationship between TDP43 aggregation/delocalization and neurodegeneration, focusing on TDP43 A382T missense mutation responsible for about thirty percent of all ALS cases in Sardinian population [93].

#### *4.2.2.1 TDP43 A382T is delocalized into the cytoplasm.*

In order to get more insight into the pathogenic mechanism of both WT or mutant TDP43 overexpression (Fig. 36) we perform a more detailed confocal microscopy investigation.

According to the literature, when $TDP43^{WT}$ is overexpressed, either by transfection or infection, is largely localized to the nucleus as well as $TDP43^{M337V}$ mutant. In most cells, however, the A382T mutant shows a clear redistribution in the cytoplasm and presents small aggregates both

cytoplasmic and intra-nuclear conversely absent in TDP43$^{WT}$ and TDP43$^{M337V}$. The import defects of TDP43$^{A382T}$ is likely to be one of the key steps that are involved in the pathological cascade, and that the full blown pathology, namely protein deposition within insoluble inclusions, requires a second hit or even multiple hits [259]. Since cytoplasmic redistribution of TDP43$^{A382T}$ is more evident in transfection experiments (may be due to TDP43 level for single cell) we decided to favor this experimental approach instead of infection. In order to test this hypothesis we used a combination of a nuclear transport defect (first hit) and cellular stress (second hit) could be necessary to lead to the typical TDP-43 pathology. 72 hours post-transfection (first hit) neuronal SH-SY5Y cells were subjected to heat shock for 4 hours (second hit). Figure 36B shows that heat shock exacerbate TDP43$^{A382T}$ phenotype and big cytoplasmic and intra-nuclear aggregates can be observed. Interestingly after the second hit we observed the occurrence of small aggregates also in TDP43$^{WT}$ and TDP43$^{M337V}$ mutant.

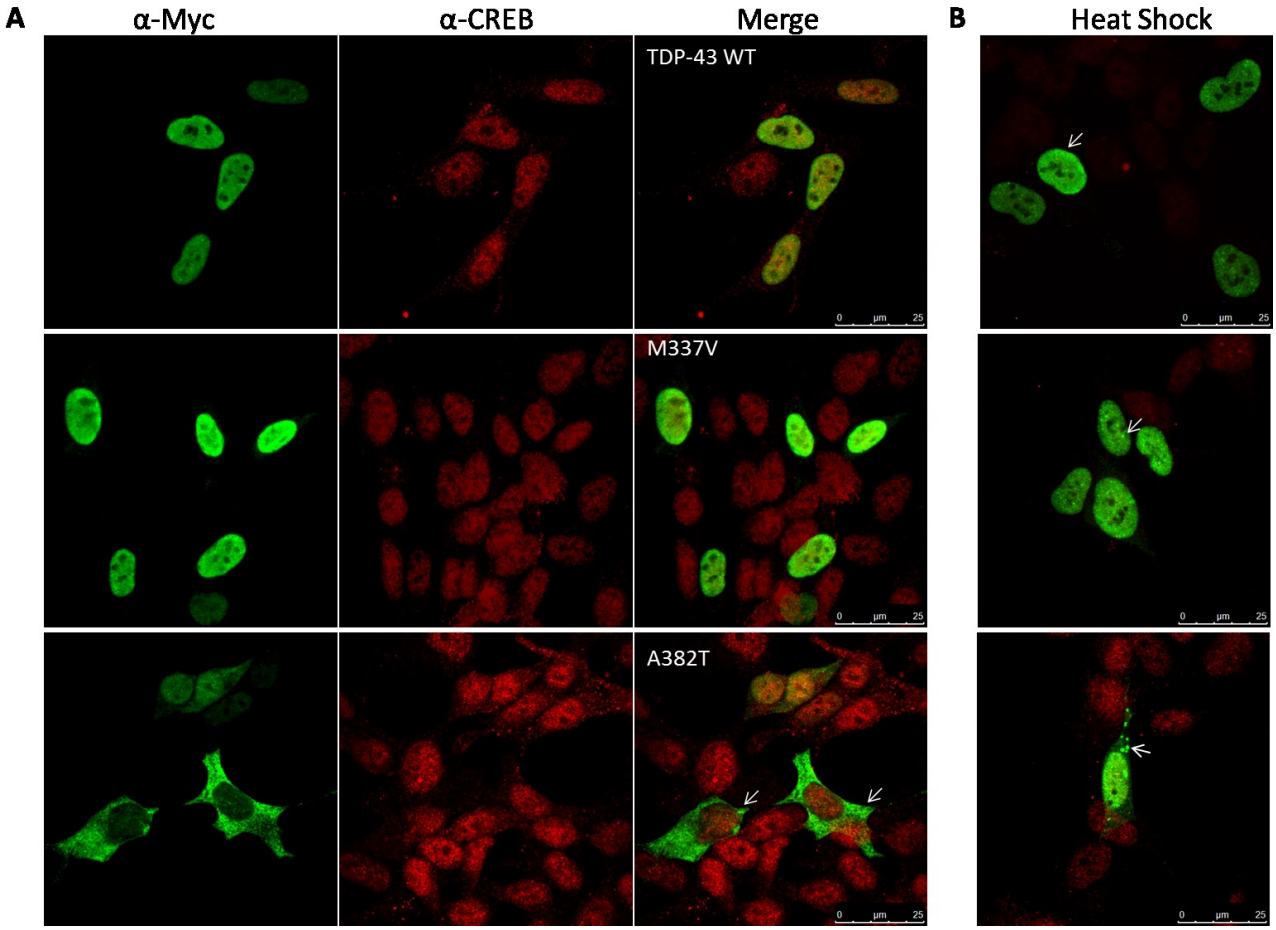


Figure 36: Confocal microscopy analysis of SH-SY5Y cells transfected with human TDP43$^{WT}$ wild type or TDP43$^{M337V}$, TDP43$^{A382T}$. The immunofluorescence was performed after 72 h of transient transfection (A) and after additional 4 hours of heat shock (B). Antibody anti-myc was used to show the localization of the TDP43 protein and antibody anti-CREB was used as nuclear marker. The white arrows show the presence of cytoplasmic and intra-nuclear aggregates.

### *4.2.2.2 Mutation A382T induces shuttling nucleus/cytoplasm.*

To confirm the remarks obtained by immunofluorescence experiments, we extended analysis using a biochemical approach to evaluate localization and aggregation properties of wild type and mutant TDP43.

In particular, to investigate the subcellular distribution of wild type and mutant TDP43, experiments of cellular fractionation have been carried out. As shown in figure 37, neuronal SH-SY5Y cells espressing TDP43$^{A382T}$ displayed a significant redistribution of the protein in the cytoplasm (red rectangles) when compared to the TDP$^{WT}$ or TDP$^{M337V}$ mutant, which are mostly localized in the nuclear fraction. This cytoplasmic accumulation corresponds to its nuclear decrease and perhaps in accumulation of its C-terminal fragments of 25kDa, as visible especially in total lysate. Similar results were obtained using neuronal SH-SY5Y cells infected with adenoviruses encoding for TDP43WT and both mutants analyzed (data not shown).

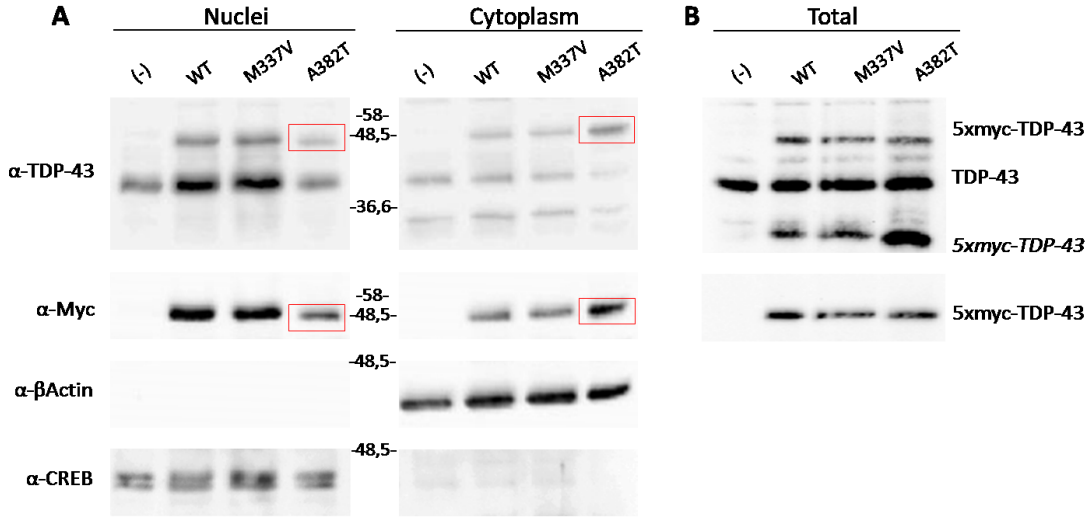


Figure 37: Mutation A382T induces shuttling nucleus/cytoplasm. Cytosolic and nuclear protein extracts were prepared after 72 h of transient transfection of SH-SY5Y. The presence of TDP43 protein in cellular fractions (A) and in total lysate (B) was assessed by Western blot analysis using antibody anti-TDP43 and anti-myc. Antibody anti-βactin and antibody anti-CREB were used respectively as cytoplasmic and nuclear fraction marker.

### *4.2.2.3 Mutation A382T promotes TDP43 aggregation.*

To better verify the aggregation properties of wild type and mutant TDP43, we transfected neuronal SH-SY5Y cells with the indicated plasmids, and the extracted proteins were separated according to their solubility.

As shown in figure 38, it has been observed difference only between TDP43$^{WT}$ and TDP43$^{A382T}$ mutant. In fact, as highlighted by red rectangles, TDP43$^{WT}$ and TDP43$^{M337V}$ are mostly present in the soluble fraction, almost 50% of TDP43$^{A382T}$ is present in the insoluble fraction. Similar results

were obtained using neuronal SH-SY5Y cells infected with adenoviruses encoding for TDP43$^{WT}$ and both mutants analyzed (data not shown).

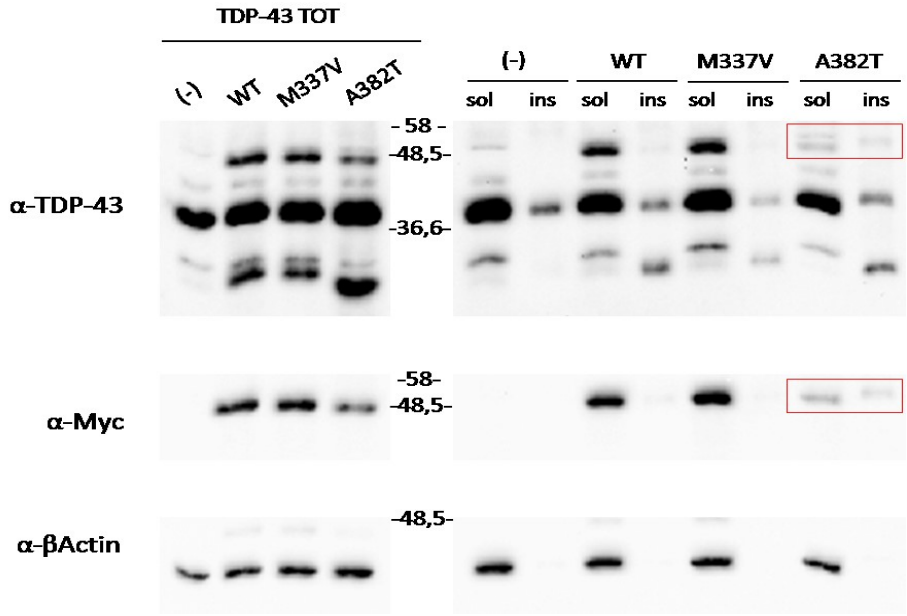


Figure 38: Mutation A382T promotes TDP43 aggregation. Total lysate (TOT), Soluble fraction (sol) and insoluble fraction (ins) protein were prepared after 72 h of transient transfection of SH-SY5Y cells. The relative abundance of TDP43 protein in respective fractions was detected by western blot analysis using antibody anti-TDP43 and anti-myc. Antibody anti-βactin was used as a control of protein concentration.

#### *4.2.2.4* Overexpression of WT or mutant TDP43 not induces PARP or LC3 cleavage.

In order to assess whether the relocation and protein aggregation of TDP43$^{A382T}$ mutant observed in previous experiments may be sufficient events to explain cellular toxicity detected by the MTS assay, we decided to evaluate activation of different cellular death markers.

In the first instance, we analyzed possible activation of PARP-1 (poly (ADP-ribose) polymerase-1) performing immunofluorescence and western blot experiments on neuronal SH-SY5Y transfected cells (data not shown).

As shown in figure 39B we did not observed any decrease of total PARP-1 in response to expression of TDP43$^{WT}$, TDP43$^{M337V}$ and TDP43$^{A382T}$ in neuronal SH-SY5Y cells when compared to SH-SY5Y cells where apoptosis was induced with staurosporine (Fig 39A). This result was confirmed by analyzing the level of cleaved PARP-1 in western blot (Fig 39C).

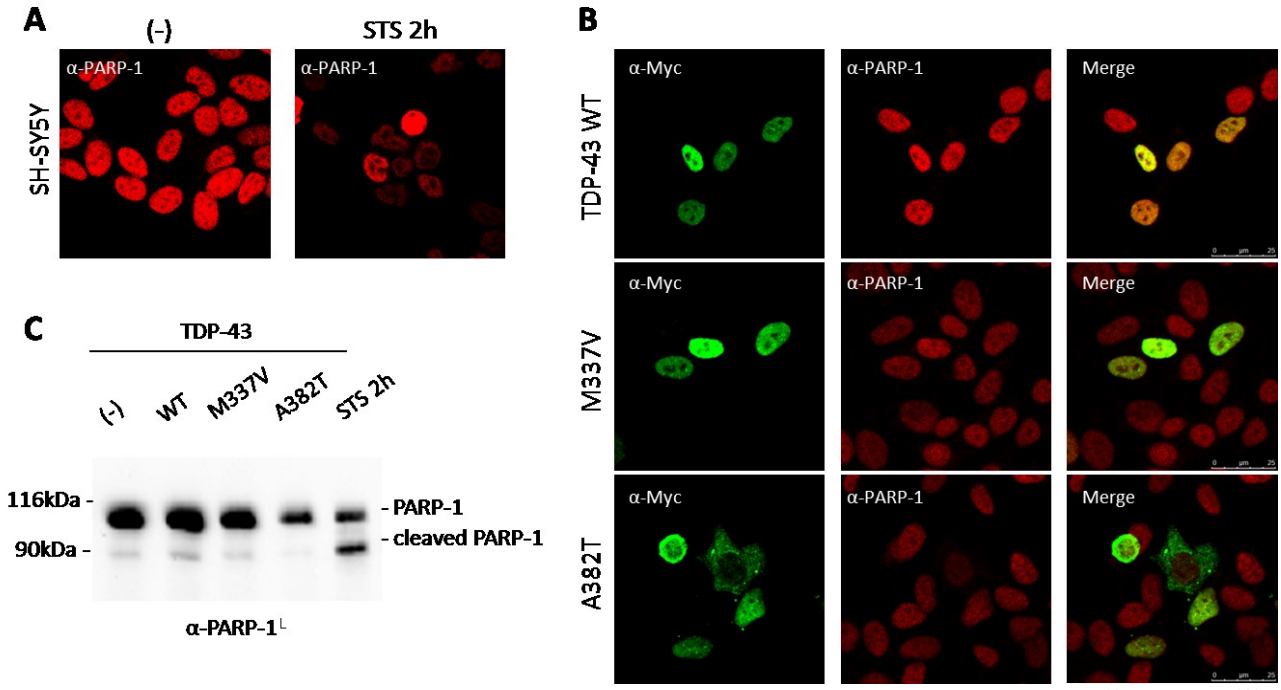


Figure 39: Confocal microscopy analysis of SH-SY5Y cells transfected with human TDP43$^{WT}$ or TDP43$^{M337V}$, TDP43$^{A382T}$. The immunofluorescence was performed after 2 h of treatment with STS (staurosporine 1µM) as control positive (A) and after 72 h of transient transfection (B). Antibody anti-myc was used to detect the TDP43 protein and antibody anti-PARP-1 was used to detect decrease of PARP-1 as apoptotic marker. Western blot analysis on total lysate of SH-SY5Y cells transfected with human TDP43$^{WT}$ wild type or TDP43$^{M337V}$, TDP43$^{A382T}$, was performed in the same experimental conditions indicated in immunofluorescence experiment (C). Antibody anti-PARP-1 was used to detect increase of cleaved-PARP-1 as apoptotic marker.

Finally we decided to verify eventual activation of autophagy performing western blot experiments on neuronal SH-SY5Y transfected with the indicated plasmids to evaluate LC3 cleavage.

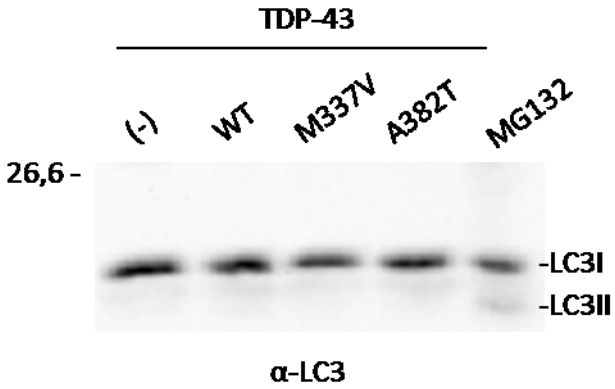


Figure 40: Western blot analysis on total lysate of SH-SY5Y cells after 72 h of transient transfection with human TDP43$^{WT}$ wild type or TDP43$^{M337V}$, TDP43$^{A382T}$. Antibody anti-LC3 was used to detect increase of LC3-II levels as autophagy marker.

Even in this case we did not observed any increase in LC3-II levels as result of TDP-43$^{WT}$, TDP43$^{M337V}$ and TDP43$^{A382T}$ expression in neuronal SH-SY5Y cells when compared to SH-SY5Y cells where autophagy was induced with MG132 (Fig. 40).

# *CHAPTER 5:*

# *DISCUSSION.*

### *5.1 ALS cellular models for high-throughput screening (HTS) assay.*

A critical step in designing more effective therapies for the treatment of neurodegenerative disorders, such as ALS, is the identification of drugs able to interfere with the first cellular alterations, prior to the onset of motoneuronal death. High−throughput experimental strategies (HTS) aimed at finding pharmacological compounds that might slow, stop or reverse disease progression may provide a unique and powerful tool to identify new active drugs for treating ALS. However, such technologies rely on the availability of automated cell-based assays as well as screening protocols to fulfill all the requirements needed for HTS procedures. In addition, this kind of approach requires the availability of efficient robotic platforms to execute the screening on large scale according to high levels of standardization. To this purpose, we have generated different cellular models where specific markers of cell toxicity, induced by expression of ALS-causative genes, may be used as a straightforward read-out for high-throughput screening of compound libraries of different nature. In particular, we have developed four different cellular models expressing high sensitive fluorescent probes, roGFP, $YFP^u$, DsRed-LC3-GFP and CFP-DEVD-YFP, suitable for oxidative stress measurement, proteasomal impairment, autophagy defects or caspase 3 activation respectively, which have been described to be key-events during ALS disease progression. These biological effects have been evaluated upon adenoviral delivery of ALS disease causative genes SOD1, FUS and TDP43 in wild type form or with pathological mutations.

Firstly, we have dealt with generating and characterizing neuronal cell lines stably expressing fluorescent reporter genes and we have found that all stable clones, in particular roGFP and $YFP^u$, are able to monitor in vivo the redox cellular state, expressed as 405/480 excitation ratio, and the ubiquitin-proteasome system activity, expressed as fluorescent accumulation (Fig. 21, 22); further experiments will be conducted to evaluate ability of stable clones espressing DsRed-LC3-GFP and CFP-DEVD-YFP to monitor in vivo LC3 or caspase-3 activation.

After production of an high titer of infectious recombinant adenoviruses to drive expression of all fALS genes, we carried out several in vivo experiments using different cellular models to monitor the biological damage induced by expression of fALS-causative genes.

#### *5.1.1 Oxidative stress, roGFP and ALS-causative genes.*

A significant body of literature indicates that oxidative stress in neurons is a common marker of various adult-onset neurodegenerative diseases including Alzheimer's Disease (AD), Parkinson's disease (PD) and ALS. The exact mechanisms involved into the events leading to disease initiation and progression are still quite obscure, thus preventing the individuation of early and suitable

targets for treatment. In fact, despite increasing efforts in research, effective therapies for ND are still to be found because of the complexity of pathogenic mechanisms and the nature of cellular events initiating the loss of specific neuron populations (cortical, dopaminergic or motor neurons) as well as the alteration of neighboring glial cells, which remains a mystery. One of the common tracts of the pathological mechanisms underlying ND is an increase of reactive oxygen species (ROS). Although the role of ROS in initiating neurodegenerative diseases is still debated, it is known that they clearly contribute to events associated with neurodegeneration in different ways and they can be used as specific and straightforward markers of the degeneration process. roGFPs have been widely used as tools for monitoring neuronal degeneration in the most common NDs. roGFP probes were, in fact successfully used to monitor mitochondrial oxidant stress in the dopaminergic neurons of the Substantia Nigra, in animal [260,261] and cellular model of PD [262], in cellular model for AD [263,264].

We have demonstrated that stable clones espressing cytoplasmic roGFP or its mitochondrial variant mito-roGFP, are able to monitor in vivo oxidative stress induced in cellular environment after expression of pathological mutants of ALS causative gene SOD1 (Fig. 25, 26).

Both WT or mutant TDP43 do not seem to induce oxidative stress measurable by roGFP, while, between the FUS mutant tested, only the one bearing the R521G mutation induces oxidation of roGFP. This data is of particular interest because underlines that different pathological mutants can perturb cellular homeostasis in different ways that are converging on cell death induction.

### *5.1.2 Protein aggregation, YFP$^u$ and ALS-causative genes.*

A common aspect of different familial forms of ALS, beside a common clinical manifestation, is that they all are characterized by genetic mutations leading to misfolding proteins with formation of intracellular protein aggregates or inclusions. Misfolded proteins may also delocalize and interfere in several ways with the mRNA processing system.

We tried to monitor the impairment of the degradative ubiquitin-proteasome (UPS) by using a YFP fused to the CL1 degron (YFP$^u$), since it has been already used in different paradigms of neurodegeneration included ALS [141,248,265-267].

According to previous reports [141,266,267], we found that YFP$^u$ is accumulated in SH-SY5Y cells expressing mutant SOD1 (Fig 27C, 28). Moreover we were able to demonstrate also upon mutant TDP43 and FUS expression a defect in YFP$^u$ clearance (Fig. 27C, 28). By contrast under the same experimental conditions we were not able to measure a statistically significant and reproducible accumulation of YFP$^u$ using a microplates reader. In fact we observed a problematic instrumental

evaluation of fluorescence accumulation probably due to the pro-aggregative properties of both wild type or mutant FUS and TDP43 (Fig. 27A).

The $YFP^{u}$ cellular models, although useful to analyse and compare the effects due to fALS causative genes expression and to discriminate between different pathological mutants, do not seem to be available for HTS assay to perform the screening of a large number of compounds (libraries of natural molecules, peptides and pharmacological drugs) and discover new therapeutical approaches able to alter the course of ALS. In fact, the system has not proved to be very sensitive and it is hard to standardize.

Recent evidence indicates that endoplasmic reticulum (ER) stress plays a central role in ALS pathogenesis. ER stress activates the unfolded protein response (UPR), a homeostatic response to misfolded proteins. The UPR has initially a protective effect through up-regulation of specific ER stress-regulated genes and inhibition of general protein translation. However, long-term ER stress leads to cell death via apoptotic signaling, thus providing a link to neurodegeneration [268]. One of the mechanisms of ER stress-induced cell death involves induction of CHOP/GADD153 [269], a recent study has suggested that CHOP expression is a signal required for ER stress-induced cell death [270].

In the future, we may generate high sensitive probes, previously described, under CHOP-promoter control to analyse the effects due to fALS causative genes expression and to obtain a potential cell-based assay suitable for HTS analysis.

### *5.2 TDP43 A382T pathological mutation: relationship between aggregation, localization and cell death.*

It has been recently demonstrated that approximately one third of ALS cases on the Mediterranean island of Sardinia show a single mutation, namely the c.1144G>A (p.A382T) missense mutation, probably due to a founder effect, indicating that these patients had a common ancestor and were part of a larger kindred [93,271]. It has also been demonstrated a wide phenotypic spectrum associated to A382T mutation, spanning from patient with ALS, PD, frontotemporal lobar degeneration and neurologically healthy subjects [271,272]. Moreover, as stated in the introduction, several dominantly inherited mutations in TDP43 in more than one patient and identification of TDP43 aggregates as major component in nearly all ALS patients, has led to the hypothesis that altered TDP43 function can be a primary cause of disease pathogenesis [86].

In this respect is of particular interest the possibility of dissecting the pathological mechanisms beside the different TDP43 pathological mutants, also to test patient-targeted therapies.

Firstly, using SH-SY5Y cell line, we have demonstrated that overexpression of both wild type and mutant forms of TDP43 induced a severe reduction of cell proliferation in a dose-dependent manner, according with data so far available in literature [120] (Fig. 17C). Immunofluorescence experiments have showed that $TDP43^{WT}$ and $TDP43^{M337V}$ mutants, when overexpressed, are largely localized to the nucleus, instead the A382T mutant shows a clear cytoplasmic redistribution and presents small aggregates both intra-nuclear and cytoplasmic (Fig. 17B, 36A). This phenotype was exacerbated when we used a combination of pathological hit (Fig. 36B).

These remarks have been confirmed through biochemical approaches. In particular, we have observed that $TDP43^{WT}$ and $TDP43^{M337V}$ mutant are mostly localized in the nuclear fraction while $TDP43^{A382T}$ revealed a significant redistribution in the cytoplasmic fraction that corresponds to its nuclear decrease and perhaps in accumulation of its C-terminal fragments of 25kDa (Fig. 37). This pro-aggregative ability has been confirmed through solubility assays, where only $TDP43^{A382T}$ has displayed a significant accumulation (about 50%) in the insoluble fraction of the proteins, when compared to the $TDP43^{WT}$ or $TDP43^{M337V}$ mutants, which are mostly present in the soluble fraction (Fig. 38).

Finally, we have observed that relocation and protein aggregation are events not sufficient to induce cell death activation. In particular, we did not observe cleaved PARP-1 or LC3-II accumulation in response to expression of $TDP\text{-}43^{WT}$, $TDP43^{M337V}$ and $TDP43^{A382T}$ in neuronal SH-SY5Y (Fig. 39, 40), to indicate that the observed toxicity does not lead to activation of apoptotic pathways or autophagy.

In conclusion, ALS-linked mutation A382T is itself able to alter the localization and to amplify the pro-aggregative ability of TDP43, but the molecular mechanism through which this mutant leads to motor neurons degeneration is still not understood.

We will need further analysis in order to clarify relationship between TDP-43 aggregation, inclusion formation and neurodegeneration, since protein aggregation may represent a potential therapeutic target for ALS.

## *CHAPTER 6:*

## *BIBLIOGRAFY.*

1 Rowland, L. P. & Shneider, N. A. Amyotrophic lateral sclerosis. *The New England journal of medicine* **344**, 1688-1700, doi:10.1056/NEJM200105313442207 (2001).
2 Pasinelli, P. & Brown, R. H. Molecular biology of amyotrophic lateral sclerosis: insights from genetics. *Nature reviews. Neuroscience* **7**, 710-723, doi:10.1038/nrn1971 (2006).
3 Cozzolino, M., Pesaresi, M. G., Gerbino, V., Grosskreutz, J. & Carri, M. T. Amyotrophic lateral sclerosis: new insights into underlying molecular mechanisms and opportunities for therapeutic intervention. *Antioxidants & redox signaling* **17**, 1277-1330, doi:10.1089/ars.2011.4328 (2012).
4 Hand, C. K. & Rouleau, G. A. Familial amyotrophic lateral sclerosis. *Muscle & nerve* **25**, 135-159 (2002).
5 Bendotti, C. & Carri, M. T. Lessons from models of SOD1-linked familial ALS. *Trends in molecular medicine* **10**, 393-400, doi:10.1016/j.molmed.2004.06.009 (2004).
6 Andersen, P. M. & Al-Chalabi, A. Clinical genetics of amyotrophic lateral sclerosis: what do we really know? *Nature reviews. Neurology* **7**, 603-615, doi:10.1038/nrneurol.2011.150 (2011).
7 Miller, R. G., Mitchell, J. D., Lyon, M. & Moore, D. H. Riluzole for amyotrophic lateral sclerosis (ALS)/motor neuron disease (MND). *Amyotroph Lateral Scler Other Motor Neuron Disord* **4**, 191-206 (2003).
8 Volonte, C., Apolloni, S., Carri, M. T. & D'Ambrosi, N. ALS: Focus on purinergic signalling. *Pharmacol Ther* **132**, 111-122 (2011).
9 Rothstein, J. D. Current hypotheses for the underlying biology of amyotrophic lateral sclerosis. *Annals of neurology* **65 Suppl 1**, S3-9, doi:10.1002/ana.21543 (2009).
10 Boillee, S., Vande Velde, C. & Cleveland, D. W. ALS: a disease of motor neurons and their nonneuronal neighbors. *Neuron* **52**, 39-59, doi:10.1016/j.neuron.2006.09.018 (2006).
11 Schmidt, S., Kwee, L. C., Allen, K. D. & Oddone, E. Z. Association of ALS with head injury, cigarette smoking and APOE genotypes. *Journal of the neurological sciences* **291**, 22-29, doi:10.1016/j.jns.2010.01.011 (2010).
12 Sutedja, N. A. *et al.* Exposure to chemicals and metals and risk of amyotrophic lateral sclerosis: a systematic review. *Amyotrophic lateral sclerosis : official publication of the World Federation of Neurology Research Group on Motor Neuron Diseases* **10**, 302-309, doi:10.3109/17482960802455416 (2009).
13 Steele, A. J. *et al.* Detection of serum reverse transcriptase activity in patients with ALS and unaffected blood relatives. *Neurology* **64**, 454-458, doi:10.1212/01.WNL.0000150899.76130.71 (2005).
14 Rowland, L. P. Amyotrophic lateral sclerosis and autoimmunity. *The New England journal of medicine* **327**, 1752-1753, doi:10.1056/NEJM199212103272411 (1992).
15 Ferri, A. *et al.* Cell death in amyotrophic lateral sclerosis: interplay between neuronal and glial cells. *FASEB journal : official publication of the Federation of American Societies for Experimental Biology* **18**, 1261-1263, doi:10.1096/fj.03-1199fje (2004).
16 Gallo, V. *et al.* Smoking and risk for amyotrophic lateral sclerosis: analysis of the EPIC cohort. *Ann Neurol* **65**, 378-385 (2009).
17 Cox, P. A. & Sacks, O. W. Cycad neurotoxins, consumption of flying foxes, and ALS-PDC disease in Guam. *Neurology* **58**, 956-959 (2002).
18 Golomb, B. A., Kwon, E. K., Koperski, S. & Evans, M. A. Amyotrophic lateral sclerosis-like conditions in possible association with cholesterol-lowering drugs: an analysis of patient reports to the University of California, San Diego (UCSD) Statin Effects Study. *Drug Saf* **32**, 649-661 (2009).
19 Kamel, F. *et al.* Lead exposure as a risk factor for amyotrophic lateral sclerosis. *Neurodegener Dis* **2**, 195-201 (2005).
20 Burns, C. J., Beard, K. K. & Cartmill, J. B. Mortality in chemical workers potentially exposed to 2,4-dichlorophenoxyacetic acid (2,4-D) 1945-94: an update. *Occupational and environmental medicine* **58**, 24-30 (2001).
21 Bendotti, C. & Carri, M. T. Amyotrophic lateral sclerosis: mechanisms and countermeasures. *Antioxidants & redox signaling* **11**, 1519-1522, doi:10.1089/ARS.2009.2620 (2009).

22 Barbeito, A. G. *et al.* Lead exposure stimulates VEGF expression in the spinal cord and extends survival in a mouse model of ALS. *Neurobiology of disease* **37**, 574-580, doi:10.1016/j.nbd.2009.11.007 (2010).
23 Chen, Y. Organophosphate-induced brain damage: mechanisms, neuropsychiatric and neurological consequences, and potential therapeutic strategies. *Neurotoxicology* **33**, 391-400, doi:10.1016/j.neuro.2012.03.011 (2012).
24 Chio, A. *et al.* ALS in Italian professional soccer players: the risk is still present and could be soccer-specific. *Amyotrophic lateral sclerosis : official publication of the World Federation of Neurology Research Group on Motor Neuron Diseases* **10**, 205-209, doi:10.1080/17482960902721634 (2009).
25 Wicks, P. *et al.* Three soccer playing friends with simultaneous amyotrophic lateral sclerosis. *Amyotrophic lateral sclerosis : official publication of the World Federation of Neurology Research Group on Motor Neuron Diseases* **8**, 177-179, doi:10.1080/17482960701195220 (2007).
26 Kasarskis, E. J. *et al.* Clinical aspects of ALS in Gulf War veterans. *Amyotrophic lateral sclerosis : official publication of the World Federation of Neurology Research Group on Motor Neuron Diseases* **10**, 35-41, doi:10.1080/17482960802351029 (2009).
27 Vanacore, N., Cocco, P., Fadda, D. & Dosemeci, M. Job strain, hypoxia and risk of amyotrophic lateral sclerosis: Results from a death certificate study. *Amyotrophic lateral sclerosis : official publication of the World Federation of Neurology Research Group on Motor Neuron Diseases* **11**, 430-434, doi:10.3109/17482961003605796 (2010).
28 Chen, H., Richard, M., Sandler, D. P., Umbach, D. M. & Kamel, F. Head injury and amyotrophic lateral sclerosis. *American journal of epidemiology* **166**, 810-816, doi:10.1093/aje/kwm153 (2007).
29 Trojsi, F., Monsurro, M. R. & Tedeschi, G. Exposure to environmental toxicants and pathogenesis of amyotrophic lateral sclerosis: state of the art and research perspectives. *International journal of molecular sciences* **14**, 15286-15311, doi:10.3390/ijms140815286 (2013).
30 Migliore, L. & Coppede, F. Genetics, environmental factors and the emerging role of epigenetics in neurodegenerative diseases. *Mutation research* **667**, 82-97, doi:10.1016/j.mrfmmm.2008.10.011 (2009).
31 Ryu, H. *et al.* Sodium phenylbutyrate prolongs survival and regulates expression of anti-apoptotic genes in transgenic amyotrophic lateral sclerosis mice. *Journal of neurochemistry* **93**, 1087-1098, doi:10.1111/j.1471-4159.2005.03077.x (2005).
32 Rouaux, C. *et al.* Sodium valproate exerts neuroprotective effects in vivo through CREB-binding protein-dependent mechanisms but does not improve survival in an amyotrophic lateral sclerosis mouse model. *The Journal of neuroscience : the official journal of the Society for Neuroscience* **27**, 5535-5545, doi:10.1523/JNEUROSCI.1139-07.2007 (2007).
33 Huntemann, M. *et al.* Genome sequence of the phylogenetically isolated spirochete Leptonema illini type strain (3055(T)). *Standards in genomic sciences* **8**, 177-187, doi:10.4056/sigs.3637201 (2013).
34 Pardo, C. A. *et al.* Superoxide dismutase is an abundant component in cell bodies, dendrites, and axons of motor neurons and in a subset of other neurons. *Proceedings of the National Academy of Sciences of the United States of America* **92**, 954-958 (1995).
35 Shaw, P. J. Molecular and cellular pathways of neurodegeneration in motor neurone disease. *Journal of neurology, neurosurgery, and psychiatry* **76**, 1046-1057, doi:10.1136/jnnp.2004.048652 (2005).
36 Banci, L. *et al.* SOD1 and amyotrophic lateral sclerosis: mutations and oligomerization. *PloS one* **3**, e1677, doi:10.1371/journal.pone.0001677 (2008).
37 Valentine, J. S., Doucette, P. A. & Zittin Potter, S. Copper-zinc superoxide dismutase and amyotrophic lateral sclerosis. *Annual review of biochemistry* **74**, 563-593, doi:10.1146/annurev.biochem.72.121801.161647 (2005).
38 Dion, P. A., Daoud, H. & Rouleau, G. A. Genetics of motor neuron disorders: new insights into pathogenic mechanisms. *Nature reviews. Genetics* **10**, 769-782, doi:10.1038/nrg2680 (2009).
39 Turner, M. R. *et al.* Controversies and priorities in amyotrophic lateral sclerosis. *Lancet neurology* **12**, 310-322, doi:10.1016/S1474-4422(13)70036-X (2013).

40 Rosen, D. R. *et al.* Mutations in Cu/Zn superoxide dismutase gene are associated with familial amyotrophic lateral sclerosis. *Nature* **362**, 59-62, doi:10.1038/362059a0 (1993).
41 Turner, B. J. & Talbot, K. Transgenics, toxicity and therapeutics in rodent models of mutant SOD1-mediated familial ALS. *Progress in neurobiology* **85**, 94-134, doi:10.1016/j.pneurobio.2008.01.001 (2008).
42 Shaw, B. F. & Valentine, J. S. How do ALS-associated mutations in superoxide dismutase 1 promote aggregation of the protein? *Trends Biochem Sci* **32**, 78-85 (2007).
43 Tiwari, A. & Hayward, L. J. Mutant SOD1 instability: implications for toxicity in amyotrophic lateral sclerosis. *Neuro-degenerative diseases* **2**, 115-127, doi:10.1159/000089616 (2005).
44 Yamanaka, K. & Cleveland, D. W. Determinants of rapid disease progression in ALS. *Neurology* **65**, 1859-1860, doi:10.1212/01.wnl.0000192717.25980.b5 (2005).
45 Cudkowicz, M. E. *et al.* Epidemiology of mutations in superoxide dismutase in amyotrophic lateral sclerosis. *Annals of neurology* **41**, 210-221, doi:10.1002/ana.410410212 (1997).
46 Andersen, P. M. *et al.* Phenotypic heterogeneity in motor neuron disease patients with CuZn-superoxide dismutase mutations in Scandinavia. *Brain : a journal of neurology* **120 ( Pt 10)**, 1723-1737 (1997).
47 Andersen, P. M. Amyotrophic lateral sclerosis associated with mutations in the CuZn superoxide dismutase gene. *Current neurology and neuroscience reports* **6**, 37-46 (2006).
48 Hayward, C., Brock, D. J., Minns, R. A. & Swingler, R. J. Homozygosity for Asn86Ser mutation in the CuZn-superoxide dismutase gene produces a severe clinical phenotype in a juvenile onset case of familial amyotrophic lateral sclerosis. *Journal of medical genetics* **35**, 174 (1998).
49 Deng, H. X. *et al.* Amyotrophic lateral sclerosis and structural defects in Cu,Zn superoxide dismutase. *Science* **261**, 1047-1051 (1993).
50 Pasinelli, P., Borchelt, D. R., Houseweart, M. K., Cleveland, D. W. & Brown, R. H., Jr. Caspase-1 is activated in neural cells and tissue with amyotrophic lateral sclerosis-associated mutations in copper-zinc superoxide dismutase. *Proceedings of the National Academy of Sciences of the United States of America* **95**, 15763-15768 (1998).
51 Reaume, A. G. *et al.* Motor neurons in Cu/Zn superoxide dismutase-deficient mice develop normally but exhibit enhanced cell death after axonal injury. *Nature genetics* **13**, 43-47, doi:10.1038/ng0596-43 (1996).
52 Ticozzi, N. *et al.* Genetics of familial Amyotrophic lateral sclerosis. *Archives italiennes de biologie* **149**, 65-82, doi:10.4449/aib.v149i1.1262 (2011).
53 Beckman, J. S., Carson, M., Smith, C. D. & Koppenol, W. H. ALS, SOD and peroxynitrite. *Nature* **364**, 584, doi:10.1038/364584a0 (1993).
54 Crozat, A., Aman, P., Mandahl, N. & Ron, D. Fusion of CHOP to a novel RNA-binding protein in human myxoid liposarcoma. *Nature* **363**, 640-644, doi:10.1038/363640a0 (1993).
55 Prasad, D. D., Ouchida, M., Lee, L., Rao, V. N. & Reddy, E. S. TLS/FUS fusion domain of TLS/FUS-erg chimeric protein resulting from the t(16;21) chromosomal translocation in human myeloid leukemia functions as a transcriptional activation domain. *Oncogene* **9**, 3717-3729 (1994).
56 Tan, A. Y. & Manley, J. L. The TET family of proteins: functions and roles in disease. *Journal of molecular cell biology* **1**, 82-92, doi:10.1093/jmcb/mjp025 (2009).
57 Morohoshi, F. *et al.* Genomic structure of the human RBP56/hTAFII68 and FUS/TLS genes. *Gene* **221**, 191-198 (1998).
58 Iko, Y. *et al.* Domain architectures and characterization of an RNA-binding protein, TLS. *The Journal of biological chemistry* **279**, 44834-44840, doi:10.1074/jbc.M408552200 (2004).
59 Yang, S., Warraich, S. T., Nicholson, G. A. & Blair, I. P. Fused in sarcoma/translocated in liposarcoma: a multifunctional DNA/RNA binding protein. *The international journal of biochemistry & cell biology* **42**, 1408-1411, doi:10.1016/j.biocel.2010.06.003 (2010).
60 Lagier-Tourenne, C., Polymenidou, M. & Cleveland, D. W. TDP-43 and FUS/TLS: emerging roles in RNA processing and neurodegeneration. *Human molecular genetics* **19**, R46-64, doi:10.1093/hmg/ddq137 (2010).

61 Uranishi, H. *et al.* Involvement of the pro-oncoprotein TLS (translocated in liposarcoma) in nuclear factor-kappa B p65-mediated transcription as a coactivator. *The Journal of biological chemistry* **276**, 13395-13401, doi:10.1074/jbc.M011176200 (2001).
62 Bertolotti, A., Lutz, Y., Heard, D. J., Chambon, P. & Tora, L. hTAF(II)68, a novel RNA/ssDNA-binding protein with homology to the pro-oncoproteins TLS/FUS and EWS is associated with both TFIID and RNA polymerase II. *The EMBO journal* **15**, 5022-5031 (1996).
63 Rappsilber, J., Ryder, U., Lamond, A. I. & Mann, M. Large-scale proteomic analysis of the human spliceosome. *Genome research* **12**, 1231-1245, doi:10.1101/gr.473902 (2002).
64 Kameoka, S., Duque, P. & Konarska, M. M. p54(nrb) associates with the 5' splice site within large transcription/splicing complexes. *The EMBO journal* **23**, 1782-1791, doi:10.1038/sj.emboj.7600187 (2004).
65 Wu, S. & Green, M. R. Identification of a human protein that recognizes the 3' splice site during the second step of pre-mRNA splicing. *The EMBO journal* **16**, 4421-4432, doi:10.1093/emboj/16.14.4421 (1997).
66 Gregory, R. I. *et al.* The Microprocessor complex mediates the genesis of microRNAs. *Nature* **432**, 235-240, doi:10.1038/nature03120 (2004).
67 Zinszner, H., Immanuel, D., Yin, Y., Liang, F. X. & Ron, D. A topogenic role for the oncogenic N-terminus of TLS: nucleolar localization when transcription is inhibited. *Oncogene* **14**, 451-461, doi:10.1038/sj.onc.1200854 (1997).
68 Andersson, M. K. *et al.* The multifunctional FUS, EWS and TAF15 proto-oncoproteins show cell type-specific expression patterns and involvement in cell spreading and stress response. *BMC cell biology* **9**, 37, doi:10.1186/1471-2121-9-37 (2008).
69 Baechtold, H. *et al.* Human 75-kDa DNA-pairing protein is identical to the pro-oncoprotein TLS/FUS and is able to promote D-loop formation. *The Journal of biological chemistry* **274**, 34337-34342 (1999).
70 Kwiatkowski, T. J., Jr. *et al.* Mutations in the FUS/TLS gene on chromosome 16 cause familial amyotrophic lateral sclerosis. *Science* **323**, 1205-1208, doi:10.1126/science.1166066 (2009).
71 Vance, C. *et al.* Mutations in FUS, an RNA processing protein, cause familial amyotrophic lateral sclerosis type 6. *Science* **323**, 1208-1211, doi:10.1126/science.1165942 (2009).
72 Lagier-Tourenne, C. & Cleveland, D. W. Rethinking ALS: the FUS about TDP-43. *Cell* **136**, 1001-1004 (2009).
73 Dormann, D. *et al.* ALS-associated fused in sarcoma (FUS) mutations disrupt Transportin-mediated nuclear import. *The EMBO journal* **29**, 2841-2857, doi:10.1038/emboj.2010.143 (2010).
74 Corrado, L. *et al.* Mutations of FUS gene in sporadic amyotrophic lateral sclerosis. *Journal of medical genetics* **47**, 190-194, doi:10.1136/jmg.2009.071027 (2010).
75 Blair, I. P. *et al.* FUS mutations in amyotrophic lateral sclerosis: clinical, pathological, neurophysiological and genetic analysis. *Journal of neurology, neurosurgery, and psychiatry* **81**, 639-645, doi:10.1136/jnnp.2009.194399 (2010).
76 Da Cruz, S. & Cleveland, D. W. Understanding the role of TDP-43 and FUS/TLS in ALS and beyond. *Current opinion in neurobiology* **21**, 904-919, doi:10.1016/j.conb.2011.05.029 (2011).
77 Gourie-Devi, M., Nalini, A. & Sandhya, S. Early or late appearance of "dropped head syndrome" in amyotrophic lateral sclerosis. *Journal of neurology, neurosurgery, and psychiatry* **74**, 683-686 (2003).
78 Waibel, S., Neumann, M., Rabe, M., Meyer, T. & Ludolph, A. C. Novel missense and truncating mutations in FUS/TLS in familial ALS. *Neurology* **75**, 815-817, doi:10.1212/WNL.0b013e3181f07e26 (2010).
79 Banks, G. T., Kuta, A., Isaacs, A. M. & Fisher, E. M. TDP-43 is a culprit in human neurodegeneration, and not just an innocent bystander. *Mammalian genome : official journal of the International Mammalian Genome Society* **19**, 299-305, doi:10.1007/s00335-008-9117-x (2008).
80 Ou, S. H., Wu, F., Harrich, D., Garcia-Martinez, L. F. & Gaynor, R. B. Cloning and characterization of a novel cellular protein, TDP-43, that binds to human immunodeficiency virus type 1 TAR DNA sequence motifs. *Journal of virology* **69**, 3584-3596 (1995).

81 Wang, H. Y., Wang, I. F., Bose, J. & Shen, C. K. Structural diversity and functional implications of the eukaryotic TDP gene family. *Genomics* **83**, 130-139 (2004).
82 Warraich, S. T., Yang, S., Nicholson, G. A. & Blair, I. P. TDP-43: a DNA and RNA binding protein with roles in neurodegenerative diseases. *The international journal of biochemistry & cell biology* **42**, 1606-1609, doi:10.1016/j.biocel.2010.06.016 (2010).
83 Colombrita, C. *et al.* TDP-43 is recruited to stress granules in conditions of oxidative insult. *Journal of neurochemistry* **111**, 1051-1061, doi:10.1111/j.1471-4159.2009.06383.x (2009).
84 Sephton, C. F. *et al.* TDP-43 is a developmentally regulated protein essential for early embryonic development. *The Journal of biological chemistry* **285**, 6826-6834, doi:10.1074/jbc.M109.061846 (2010).
85 Ayala, Y. M., Misteli, T. & Baralle, F. E. TDP-43 regulates retinoblastoma protein phosphorylation through the repression of cyclin-dependent kinase 6 expression. *Proceedings of the National Academy of Sciences of the United States of America* **105**, 3785-3789, doi:10.1073/pnas.0800546105 (2008).
86 Sreedharan, J. *et al.* TDP-43 mutations in familial and sporadic amyotrophic lateral sclerosis. *Science* **319**, 1668-1672, doi:10.1126/science.1154584 (2008).
87 Daoud, H. *et al.* Contribution of TARDBP mutations to sporadic amyotrophic lateral sclerosis. *Journal of medical genetics* **46**, 112-114, doi:10.1136/jmg.2008.062463 (2009).
88 Luquin, N., Yu, B., Saunderson, R. B., Trent, R. J. & Pamphlett, R. Genetic variants in the promoter of TARDBP in sporadic amyotrophic lateral sclerosis. *Neuromuscular disorders : NMD* **19**, 696-700, doi:10.1016/j.nmd.2009.07.005 (2009).
89 Gitcho, M. A. *et al.* TARDBP 3'-UTR variant in autopsy-confirmed frontotemporal lobar degeneration with TDP-43 proteinopathy. *Acta neuropathologica* **118**, 633-645, doi:10.1007/s00401-009-0571-7 (2009).
90 Benajiba, L. *et al.* TARDBP mutations in motoneuron disease with frontotemporal lobar degeneration. *Annals of neurology* **65**, 470-473, doi:10.1002/ana.21612 (2009).
91 Borroni, B. *et al.* Mutation within TARDBP leads to frontotemporal dementia without motor neuron disease. *Human mutation* **30**, E974-983, doi:10.1002/humu.21100 (2009).
92 Kabashi, E. *et al.* TARDBP mutations in individuals with sporadic and familial amyotrophic lateral sclerosis. *Nature genetics* **40**, 572-574, doi:10.1038/ng.132 (2008).
93 Chio, A. *et al.* Large proportion of amyotrophic lateral sclerosis cases in Sardinia due to a single founder mutation of the TARDBP gene. *Archives of neurology* **68**, 594-598, doi:10.1001/archneurol.2010.352 (2011).
94 Orru, S. *et al.* High frequency of the TARDBP p.Ala382Thr mutation in Sardinian patients with amyotrophic lateral sclerosis. *Clinical genetics* **81**, 172-178, doi:10.1111/j.1399-0004.2011.01668.x (2012).
95 Lattante, S., Rouleau, G. A. & Kabashi, E. TARDBP and FUS mutations associated with amyotrophic lateral sclerosis: summary and update. *Human mutation* **34**, 812-826, doi:10.1002/humu.22319 (2013).
96 Yokoseki, A. *et al.* TDP-43 mutation in familial amyotrophic lateral sclerosis. *Annals of neurology* **63**, 538-542, doi:10.1002/ana.21392 (2008).
97 Giordana, M. T. *et al.* TDP-43 redistribution is an early event in sporadic amyotrophic lateral sclerosis. *Brain Pathol* **20**, 351-360, doi:10.1111/j.1750-3639.2009.00284.x (2010).
98 Neumann, M. *et al.* Ubiquitinated TDP-43 in frontotemporal lobar degeneration and amyotrophic lateral sclerosis. *Science* **314**, 130-133, doi:10.1126/science.1134108 (2006).
99 Igaz, L. M. *et al.* Enrichment of C-terminal fragments in TAR DNA-binding protein-43 cytoplasmic inclusions in brain but not in spinal cord of frontotemporal lobar degeneration and amyotrophic lateral sclerosis. *The American journal of pathology* **173**, 182-194, doi:10.2353/ajpath.2008.080003 (2008).
100 Mori, F. *et al.* Maturation process of TDP-43-positive neuronal cytoplasmic inclusions in amyotrophic lateral sclerosis with and without dementia. *Acta neuropathologica* **116**, 193-203, doi:10.1007/s00401-008-0396-9 (2008).

101 Neumann, M. *et al.* Phosphorylation of S409/410 of TDP-43 is a consistent feature in all sporadic and familial forms of TDP-43 proteinopathies. *Acta neuropathologica* **117**, 137-149, doi:10.1007/s00401-008-0477-9 (2009).
102 Rothstein, J. D., Bristol, L. A., Hosler, B., Brown, R. H., Jr. & Kuncl, R. W. Chronic inhibition of superoxide dismutase produces apoptotic death of spinal neurons. *Proceedings of the National Academy of Sciences of the United States of America* **91**, 4155-4159 (1994).
103 Troy, C. M. & Shelanski, M. L. Down-regulation of copper/zinc superoxide dismutase causes apoptotic death in PC12 neuronal cells. *Proceedings of the National Academy of Sciences of the United States of America* **91**, 6384-6387 (1994).
104 Liu, R. *et al.* Increased mitochondrial antioxidative activity or decreased oxygen free radical propagation prevent mutant SOD1-mediated motor neuron cell death and increase amyotrophic lateral sclerosis-like transgenic mouse survival. *Journal of neurochemistry* **80**, 488-500 (2002).
105 Kostic, V. *et al.* Midbrain dopaminergic neuronal degeneration in a transgenic mouse model of familial amyotrophic lateral sclerosis. *Annals of neurology* **41**, 497-504, doi:10.1002/ana.410410413 (1997).
106 Shibata, N. Transgenic mouse model for familial amyotrophic lateral sclerosis with superoxide dismutase-1 mutation. *Neuropathology : official journal of the Japanese Society of Neuropathology* **21**, 82-92 (2001).
107 Bendotti, C. *et al.* Transgenic SOD1 G93A mice develop reduced GLT-1 in spinal cord without alterations in cerebrospinal fluid glutamate levels. *Journal of neurochemistry* **79**, 737-746 (2001).
108 Kino, Y. *et al.* Intracellular localization and splicing regulation of FUS/TLS are variably affected by amyotrophic lateral sclerosis-linked mutations. *Nucleic acids research* **39**, 2781-2798, doi:10.1093/nar/gkq1162 (2011).
109 Bosco, D. A. *et al.* Mutant FUS proteins that cause amyotrophic lateral sclerosis incorporate into stress granules. *Human molecular genetics* **19**, 4160-4175, doi:10.1093/hmg/ddq335 (2010).
110 Fushimi, K. *et al.* Expression of human FUS/TLS in yeast leads to protein aggregation and cytotoxicity, recapitulating key features of FUS proteinopathy. *Protein & cell* **2**, 141-149, doi:10.1007/s13238-011-1014-5 (2011).
111 Sun, Z. *et al.* Molecular determinants and genetic modifiers of aggregation and toxicity for the ALS disease protein FUS/TLS. *PLoS biology* **9**, e1000614, doi:10.1371/journal.pbio.1000614 (2011).
112 Chen, Y. *et al.* Expression of human FUS protein in Drosophila leads to progressive neurodegeneration. *Protein & cell* **2**, 477-486, doi:10.1007/s13238-011-1065-7 (2011).
113 Wang, J. W., Brent, J. R., Tomlinson, A., Shneider, N. A. & McCabe, B. D. The ALS-associated proteins FUS and TDP-43 function together to affect Drosophila locomotion and life span. *The Journal of clinical investigation* **121**, 4118-4126, doi:10.1172/JCI57883 (2011).
114 Lanson, N. A., Jr. *et al.* A Drosophila model of FUS-related neurodegeneration reveals genetic interaction between FUS and TDP-43. *Human molecular genetics* **20**, 2510-2523, doi:10.1093/hmg/ddr150 (2011).
115 Kabashi, E. *et al.* FUS and TARDBP but not SOD1 interact in genetic models of amyotrophic lateral sclerosis. *PLoS genetics* **7**, e1002214, doi:10.1371/journal.pgen.1002214 (2011).
116 Hicks, G. G. *et al.* Fus deficiency in mice results in defective B-lymphocyte development and activation, high levels of chromosomal instability and perinatal death. *Nature genetics* **24**, 175-179, doi:10.1038/72842 (2000).
117 Kuroda, M. *et al.* Male sterility and enhanced radiation sensitivity in TLS(-/-) mice. *The EMBO journal* **19**, 453-462, doi:10.1093/emboj/19.3.453 (2000).
118 Huang, C. *et al.* FUS transgenic rats develop the phenotypes of amyotrophic lateral sclerosis and frontotemporal lobar degeneration. *PLoS genetics* **7**, e1002011, doi:10.1371/journal.pgen.1002011 (2011).
119 Winton, M. J. *et al.* Disturbance of nuclear and cytoplasmic TAR DNA-binding protein (TDP-43) induces disease-like redistribution, sequestration, and aggregate formation. *The Journal of biological chemistry* **283**, 13302-13309, doi:10.1074/jbc.M800342200 (2008).
120 Barmada, S. J. *et al.* Cytoplasmic mislocalization of TDP-43 is toxic to neurons and enhanced by a mutation associated with familial amyotrophic lateral sclerosis. *The Journal of neuroscience : the*

*official journal of the Society for Neuroscience* **30**, 639-649, doi:10.1523/JNEUROSCI.4988-09.2010 (2010).

121 Xu, Y. F. *et al.* Wild-type human TDP-43 expression causes TDP-43 phosphorylation, mitochondrial aggregation, motor deficits, and early mortality in transgenic mice. *The Journal of neuroscience : the official journal of the Society for Neuroscience* **30**, 10851-10859, doi:10.1523/JNEUROSCI.1630-10.2010 (2010).

122 Arnold, E. S. *et al.* ALS-linked TDP-43 mutations produce aberrant RNA splicing and adult-onset motor neuron disease without aggregation or loss of nuclear TDP-43. *Proceedings of the National Academy of Sciences of the United States of America* **110**, E736-745, doi:10.1073/pnas.1222809110 (2013).

123 Zhou, H. *et al.* Transgenic rat model of neurodegeneration caused by mutation in the TDP gene. *PLoS genetics* **6**, e1000887, doi:10.1371/journal.pgen.1000887 (2010).

124 Uchida, A. *et al.* Non-human primate model of amyotrophic lateral sclerosis with cytoplasmic mislocalization of TDP-43. *Brain : a journal of neurology* **135**, 833-846, doi:10.1093/brain/awr348 (2012).

125 Vaccaro, A. *et al.* Mutant TDP-43 and FUS cause age-dependent paralysis and neurodegeneration in C. elegans. *PloS one* **7**, e31321, doi:10.1371/journal.pone.0031321 (2012).

126 Hewamadduma, C. A. *et al.* Tardbpl splicing rescues motor neuron and axonal development in a mutant tardbp zebrafish. *Human molecular genetics* **22**, 2376-2386, doi:10.1093/hmg/ddt082 (2013).

127 Li, Y. *et al.* A Drosophila model for TDP-43 proteinopathy. *Proceedings of the National Academy of Sciences of the United States of America* **107**, 3169-3174, doi:10.1073/pnas.0913602107 (2010).

128 Zhang, Y. J. *et al.* Aberrant cleavage of TDP-43 enhances aggregation and cellular toxicity. *Proceedings of the National Academy of Sciences of the United States of America* **106**, 7607-7612, doi:10.1073/pnas.0900688106 (2009).

129 Wils, H. *et al.* TDP-43 transgenic mice develop spastic paralysis and neuronal inclusions characteristic of ALS and frontotemporal lobar degeneration. *Proceedings of the National Academy of Sciences of the United States of America* **107**, 3858-3863, doi:10.1073/pnas.0912417107 (2010).

130 Caccamo, A., Majumder, S. & Oddo, S. Cognitive decline typical of frontotemporal lobar degeneration in transgenic mice expressing the 25-kDa C-terminal fragment of TDP-43. *The American journal of pathology* **180**, 293-302, doi:10.1016/j.ajpath.2011.09.022 (2012).

131 Nishimoto, Y. *et al.* Characterization of alternative isoforms and inclusion body of the TAR DNA-binding protein-43. *The Journal of biological chemistry* **285**, 608-619, doi:10.1074/jbc.M109.022012 (2010).

132 Igaz, L. M. *et al.* Expression of TDP-43 C-terminal Fragments in Vitro Recapitulates Pathological Features of TDP-43 Proteinopathies. *The Journal of biological chemistry* **284**, 8516-8524, doi:10.1074/jbc.M809462200 (2009).

133 Levine, B. & Kroemer, G. Autophagy in the pathogenesis of disease. *Cell* **132**, 27-42, doi:10.1016/j.cell.2007.12.018 (2008).

134 Kraemer, B. C. *et al.* Loss of murine TDP-43 disrupts motor function and plays an essential role in embryogenesis. *Acta neuropathologica* **119**, 409-419, doi:10.1007/s00401-010-0659-0 (2010).

135 Wu, L. S., Cheng, W. C. & Shen, C. K. Targeted depletion of TDP-43 expression in the spinal cord motor neurons leads to the development of amyotrophic lateral sclerosis-like phenotypes in mice. *The Journal of biological chemistry* **287**, 27335-27344, doi:10.1074/jbc.M112.359000 (2012).

136 Chiang, P. M. *et al.* Deletion of TDP-43 down-regulates Tbc1d1, a gene linked to obesity, and alters body fat metabolism. *Proceedings of the National Academy of Sciences of the United States of America* **107**, 16320-16324, doi:10.1073/pnas.1002176107 (2010).

137 Barber, S. C. & Shaw, P. J. Oxidative stress in ALS: key role in motor neuron injury and therapeutic target. *Free radical biology & medicine* **48**, 629-641, doi:10.1016/j.freeradbiomed.2009.11.018 (2010).

138 Bogdanov, M. *et al.* Increased oxidative damage to DNA in ALS patients. *Free radical biology & medicine* **29**, 652-658 (2000).

139 Tohgi, H. *et al.* Increase in oxidized NO products and reduction in oxidized glutathione in cerebrospinal fluid from patients with sporadic form of amyotrophic lateral sclerosis. *Neuroscience letters* **260**, 204-206 (1999).
140 Karch, C. M., Prudencio, M., Winkler, D. D., Hart, P. J. & Borchelt, D. R. Role of mutant SOD1 disulfide oxidation and aggregation in the pathogenesis of familial ALS. *Proceedings of the National Academy of Sciences of the United States of America* **106**, 7774-7779, doi:10.1073/pnas.0902505106 (2009).
141 Sau, D. *et al.* Mutation of SOD1 in ALS: a gain of a loss of function. *Human molecular genetics* **16**, 1604-1618, doi:10.1093/hmg/ddm110 (2007).
142 Wiedau-Pazos, M. *et al.* Altered reactivity of superoxide dismutase in familial amyotrophic lateral sclerosis. *Science* **271**, 515-518 (1996).
143 Estevez, A. G. *et al.* Induction of nitric oxide-dependent apoptosis in motor neurons by zinc-deficient superoxide dismutase. *Science* **286**, 2498-2500 (1999).
144 Duan, W. *et al.* Mutant TAR DNA-binding protein-43 induces oxidative injury in motor neuron-like cell. *Neuroscience* **169**, 1621-1629, doi:10.1016/j.neuroscience.2010.06.018 (2010).
145 Braun, R. J. *et al.* Neurotoxic 43-kDa TAR DNA-binding protein (TDP-43) triggers mitochondrion-dependent programmed cell death in yeast. *J Biol Chem* **286**, 19958-19972 (2011).
146 Sen, I., Nalini, A., Joshi, N. B. & Joshi, P. G. Cerebrospinal fluid from amyotrophic lateral sclerosis patients preferentially elevates intracellular calcium and toxicity in motor neurons via AMPA/kainate receptor. *Journal of the neurological sciences* **235**, 45-54, doi:10.1016/j.jns.2005.03.049 (2005).
147 Van Den Bosch, L. & Robberecht, W. Different receptors mediate motor neuron death induced by short and long exposures to excitotoxicity. *Brain research bulletin* **53**, 383-388 (2000).
148 Rothstein, J. D., Martin, L. J. & Kuncl, R. W. Decreased glutamate transport by the brain and spinal cord in amyotrophic lateral sclerosis. *The New England journal of medicine* **326**, 1464-1468, doi:10.1056/NEJM199205283262204 (1992).
149 Howland, D. S. *et al.* Focal loss of the glutamate transporter EAAT2 in a transgenic rat model of SOD1 mutant-mediated amyotrophic lateral sclerosis (ALS). *Proceedings of the National Academy of Sciences of the United States of America* **99**, 1604-1609, doi:10.1073/pnas.032539299 (2002).
150 Kruman, II, Pedersen, W. A., Springer, J. E. & Mattson, M. P. ALS-linked Cu/Zn-SOD mutation increases vulnerability of motor neurons to excitotoxicity by a mechanism involving increased oxidative stress and perturbed calcium homeostasis. *Experimental neurology* **160**, 28-39, doi:10.1006/exnr.1999.7190 (1999).
151 Spalloni, A. *et al.* Cu/Zn-superoxide dismutase (GLY93-->ALA) mutation alters AMPA receptor subunit expression and function and potentiates kainate-mediated toxicity in motor neurons in culture. *Neurobiology of disease* **15**, 340-350, doi:10.1016/j.nbd.2003.11.012 (2004).
152 Wiedemann, F. R., Manfredi, G., Mawrin, C., Beal, M. F. & Schon, E. A. Mitochondrial DNA and respiratory chain function in spinal cords of ALS patients. *Journal of neurochemistry* **80**, 616-625 (2002).
153 Sasaki, S. & Iwata, M. Ultrastructural study of synapses in the anterior horn neurons of patients with amyotrophic lateral sclerosis. *Neuroscience letters* **204**, 53-56 (1996).
154 Menzies, F. M. *et al.* Mitochondrial dysfunction in a cell culture model of familial amyotrophic lateral sclerosis. *Brain : a journal of neurology* **125**, 1522-1533 (2002).
155 Collard, J. F., Cote, F. & Julien, J. P. Defective axonal transport in a transgenic mouse model of amyotrophic lateral sclerosis. *Nature* **375**, 61-64, doi:10.1038/375061a0 (1995).
156 Takeuchi, H., Kobayashi, Y., Ishigaki, S., Doyu, M. & Sobue, G. Mitochondrial localization of mutant superoxide dismutase 1 triggers caspase-dependent cell death in a cellular model of familial amyotrophic lateral sclerosis. *The Journal of biological chemistry* **277**, 50966-50972, doi:10.1074/jbc.M209356200 (2002).
157 Jaarsma, D. *et al.* CuZn superoxide dismutase (SOD1) accumulates in vacuolated mitochondria in transgenic mice expressing amyotrophic lateral sclerosis-linked SOD1 mutations. *Acta neuropathologica* **102**, 293-305 (2001).

158 Hong, K. *et al.* Full-length TDP-43 and its C-terminal fragments activate mitophagy in NSC34 cell line. *Neuroscience letters* **530**, 144-149, doi:10.1016/j.neulet.2012.10.003 (2012).
159 Bandy, B. & Davison, A. J. Mitochondrial mutations may increase oxidative stress: implications for carcinogenesis and aging? *Free radical biology & medicine* **8**, 523-539 (1990).
160 Figlewicz, D. A. *et al.* Variants of the heavy neurofilament subunit are associated with the development of amyotrophic lateral sclerosis. *Human molecular genetics* **3**, 1757-1761 (1994).
161 Borchelt, D. R. *et al.* Axonal transport of mutant superoxide dismutase 1 and focal axonal abnormalities in the proximal axons of transgenic mice. *Neurobiology of disease* **5**, 27-35, doi:10.1006/nbdi.1998.0178 (1998).
162 Murakami, T. *et al.* Impaired retrograde axonal transport of adenovirus-mediated E. coli LacZ gene in the mice carrying mutant SOD1 gene. *Neuroscience letters* **308**, 149-152 (2001).
163 Bosco, D. A. *et al.* Wild-type and mutant SOD1 share an aberrant conformation and a common pathogenic pathway in ALS. *Nature neuroscience* **13**, 1396-1403, doi:10.1038/nn.2660 (2010).
164 Chou, S. M., Wang, H. S. & Komai, K. Colocalization of NOS and SOD1 in neurofilament accumulation within motor neurons of amyotrophic lateral sclerosis: an immunohistochemical study. *Journal of chemical neuroanatomy* **10**, 249-258 (1996).
165 Foran, E. & Trotti, D. Glutamate transporters and the excitotoxic path to motor neuron degeneration in amyotrophic lateral sclerosis. *Antioxidants & redox signaling* **11**, 1587-1602, doi:10.1089/ars.2009.2444 (2009).
166 Ekestern, E. Neurotrophic factors and amyotrophic lateral sclerosis. *Neuro-degenerative diseases* **1**, 88-100, doi:10.1159/000080049 (2004).
167 Papadimitriou, D. *et al.* Inflammation in ALS and SMA: sorting out the good from the evil. *Neurobiology of disease* **37**, 493-502, doi:10.1016/j.nbd.2009.10.005 (2010).
168 Kaltschmidt, B., Widera, D. & Kaltschmidt, C. Signaling via NF-kappaB in the nervous system. *Biochimica et biophysica acta* **1745**, 287-299, doi:10.1016/j.bbamcr.2005.05.009 (2005).
169 Casciati, A. *et al.* Oxidative modulation of nuclear factor-kappaB in human cells expressing mutant fALS-typical superoxide dismutases. *Journal of neurochemistry* **83**, 1019-1029 (2002).
170 Pramatarova, A., Laganiere, J., Roussel, J., Brisebois, K. & Rouleau, G. A. Neuron-specific expression of mutant superoxide dismutase 1 in transgenic mice does not lead to motor impairment. *The Journal of neuroscience : the official journal of the Society for Neuroscience* **21**, 3369-3374 (2001).
171 Crosio, C., Valle, C., Casciati, A., Iaccarino, C. & Carri, M. T. Astroglial inhibition of NF-kappaB does not ameliorate disease onset and progression in a mouse model for amyotrophic lateral sclerosis (ALS). *PloS one* **6**, e17187, doi:10.1371/journal.pone.0017187 (2011).
172 Gonzalez-Scarano, F. & Baltuch, G. Microglia as mediators of inflammatory and degenerative diseases. *Annual review of neuroscience* **22**, 219-240, doi:10.1146/annurev.neuro.22.1.219 (1999).
173 Alexianu, M. E., Kozovska, M. & Appel, S. H. Immune reactivity in a mouse model of familial ALS correlates with disease progression. *Neurology* **57**, 1282-1289 (2001).
174 Hensley, K. *et al.* Temporal patterns of cytokine and apoptosis-related gene expression in spinal cords of the G93A-SOD1 mouse model of amyotrophic lateral sclerosis. *Journal of neurochemistry* **82**, 365-374 (2002).
175 Brooks, B. R. *et al.* Natural history of amyotrophic lateral sclerosis. Quantification of symptoms, signs, strength, and function. *Advances in neurology* **68**, 163-184 (1995).
176 D'Ambrosi, N. *et al.* The proinflammatory action of microglial P2 receptors is enhanced in SOD1 models for amyotrophic lateral sclerosis. *J Immunol* **183**, 4648-4656, doi:10.4049/jimmunol.0901212 (2009).
177 Cozzolino, M., Ferri, A. & Carri, M. T. Amyotrophic lateral sclerosis: from current developments in the laboratory to clinical implications. *Antioxid Redox Signal* **10**, 405-443 (2008).
178 Chattopadhyay, M. & Valentine, J. S. Aggregation of copper-zinc superoxide dismutase in familial and sporadic ALS. *Antioxid Redox Signal* **11**, 1603-1614 (2009).
179 Pasinelli, P. *et al.* Amyotrophic lateral sclerosis-associated SOD1 mutant proteins bind and aggregate with Bcl-2 in spinal cord mitochondria. *Neuron* **43**, 19-30, doi:10.1016/j.neuron.2004.06.021 (2004).

180 Allen, S. *et al.* Analysis of the cytosolic proteome in a cell culture model of familial amyotrophic lateral sclerosis reveals alterations to the proteasome, antioxidant defenses, and nitric oxide synthetic pathways. *The Journal of biological chemistry* **278**, 6371-6383, doi:10.1074/jbc.M209915200 (2003).
181 Mackenzie, I. R., Rademakers, R. & Neumann, M. TDP-43 and FUS in amyotrophic lateral sclerosis and frontotemporal dementia. *Lancet Neurol* **9**, 995-1007 (2010).
182 Johnson, B. S. *et al.* TDP-43 is intrinsically aggregation-prone, and amyotrophic lateral sclerosis-linked mutations accelerate aggregation and increase toxicity. *The Journal of biological chemistry* **284**, 20329-20339, doi:10.1074/jbc.M109.010264 (2009).
183 Blokhuis, A. M., Groen, E. J., Koppers, M., van den Berg, L. H. & Pasterkamp, R. J. Protein aggregation in amyotrophic lateral sclerosis. *Acta neuropathologica* **125**, 777-794, doi:10.1007/s00401-013-1125-6 (2013).
184 Gal, J., Strom, A. L., Kilty, R., Zhang, F. & Zhu, H. p62 accumulates and enhances aggregate formation in model systems of familial amyotrophic lateral sclerosis. *The Journal of biological chemistry* **282**, 11068-11077, doi:10.1074/jbc.M608787200 (2007).
185 Anderson, P. & Kedersha, N. Stress granules: the Tao of RNA triage. *Trends in biochemical sciences* **33**, 141-150, doi:10.1016/j.tibs.2007.12.003 (2008).
186 Ayala, Y. M. *et al.* Structural determinants of the cellular localization and shuttling of TDP-43. *Journal of cell science* **121**, 3778-3785, doi:10.1242/jcs.038950 (2008).
187 Li, Y. R., King, O. D., Shorter, J. & Gitler, A. D. Stress granules as crucibles of ALS pathogenesis. *The Journal of cell biology* **201**, 361-372, doi:10.1083/jcb.201302044 (2013).
188 Liu-Yesucevitz, L. *et al.* Tar DNA binding protein-43 (TDP-43) associates with stress granules: analysis of cultured cells and pathological brain tissue. *PloS one* **5**, e13250, doi:10.1371/journal.pone.0013250 (2010).
189 Buchan, J. R. & Parker, R. Eukaryotic stress granules: the ins and outs of translation. *Molecular cell* **36**, 932-941, doi:10.1016/j.molcel.2009.11.020 (2009).
190 Parker, S. J. *et al.* Endogenous TDP-43 localized to stress granules can subsequently form protein aggregates. *Neurochemistry international* **60**, 415-424, doi:10.1016/j.neuint.2012.01.019 (2012).
191 Aulas, A., Stabile, S. & Vande Velde, C. Endogenous TDP-43, but not FUS, contributes to stress granule assembly via G3BP. *Molecular neurodegeneration* **7**, 54, doi:10.1186/1750-1326-7-54 (2012).
192 Fujii, R. *et al.* The RNA binding protein TLS is translocated to dendritic spines by mGluR5 activation and regulates spine morphology. *Current biology : CB* **15**, 587-593, doi:10.1016/j.cub.2005.01.058 (2005).
193 Polymenidou, M. *et al.* Long pre-mRNA depletion and RNA missplicing contribute to neuronal vulnerability from loss of TDP-43. *Nature neuroscience* **14**, 459-468, doi:10.1038/nn.2779 (2011).
194 Lagier-Tourenne, C. *et al.* Divergent roles of ALS-linked proteins FUS/TLS and TDP-43 intersect in processing long pre-mRNAs. *Nature neuroscience* **15**, 1488-1497, doi:10.1038/nn.3230 (2012).
195 Komatsu, M. *et al.* Impairment of starvation-induced and constitutive autophagy in Atg7-deficient mice. *The Journal of cell biology* **169**, 425-434, doi:10.1083/jcb.200412022 (2005).
196 Scarlatti, F., Granata, R., Meijer, A. J. & Codogno, P. Does autophagy have a license to kill mammalian cells? *Cell death and differentiation* **16**, 12-20, doi:10.1038/cdd.2008.101 (2009).
197 Wong, E. & Cuervo, A. M. Autophagy gone awry in neurodegenerative diseases. *Nature neuroscience* **13**, 805-811, doi:10.1038/nn.2575 (2010).
198 Li, L., Zhang, X. & Le, W. Altered macroautophagy in the spinal cord of SOD1 mutant mice. *Autophagy* **4**, 290-293 (2008).
199 Banerjee, R., Beal, M. F. & Thomas, B. Autophagy in neurodegenerative disorders: pathogenic roles and therapeutic implications. *Trends in neurosciences* **33**, 541-549, doi:10.1016/j.tins.2010.09.001 (2010).
200 Zhang, X. *et al.* Rapamycin treatment augments motor neuron degeneration in SOD1(G93A) mouse model of amyotrophic lateral sclerosis. *Autophagy* **7**, 412-425 (2011).
201 Wang, X. *et al.* Degradation of TDP-43 and its pathogenic form by autophagy and the ubiquitin-proteasome system. *Neuroscience letters* **469**, 112-116, doi:10.1016/j.neulet.2009.11.055 (2010).

202 Caccamo, A. *et al.* Rapamycin rescues TDP-43 mislocalization and the associated low molecular mass neurofilament instability. *The Journal of biological chemistry* **284**, 27416-27424, doi:10.1074/jbc.M109.031278 (2009).
203 Gomes, C., Escrevente, C. & Costa, J. Mutant superoxide dismutase 1 overexpression in NSC-34 cells: effect of trehalose on aggregation, TDP-43 localization and levels of co-expressed glycoproteins. *Neuroscience letters* **475**, 145-149, doi:10.1016/j.neulet.2010.03.065 (2010).
204 Brady, O. A., Meng, P., Zheng, Y., Mao, Y. & Hu, F. Regulation of TDP-43 aggregation by phosphorylation and p62/SQSTM1. *Journal of neurochemistry* **116**, 248-259, doi:10.1111/j.1471-4159.2010.07098.x (2011).
205 Wegorzewska, I., Bell, S., Cairns, N. J., Miller, T. M. & Baloh, R. H. TDP-43 mutant transgenic mice develop features of ALS and frontotemporal lobar degeneration. *Proceedings of the National Academy of Sciences of the United States of America* **106**, 18809-18814, doi:10.1073/pnas.0908767106 (2009).
206 Schultz, D. R. & Harrington, W. J., Jr. Apoptosis: programmed cell death at a molecular level. *Seminars in arthritis and rheumatism* **32**, 345-369, doi:10.1053/sarh.2003.50005 (2003).
207 Monaghan, P. *et al.* Ultrastructural localization of bcl-2 protein. *The journal of histochemistry and cytochemistry : official journal of the Histochemistry Society* **40**, 1819-1825 (1992).
208 Antonsson, B. & Martinou, J. C. The Bcl-2 protein family. *Experimental cell research* **256**, 50-57, doi:10.1006/excr.2000.4839 (2000).
209 Pasinelli, P., Houseweart, M. K., Brown, R. H., Jr. & Cleveland, D. W. Caspase-1 and -3 are sequentially activated in motor neuron death in Cu,Zn superoxide dismutase-mediated familial amyotrophic lateral sclerosis. *Proceedings of the National Academy of Sciences of the United States of America* **97**, 13901-13906, doi:10.1073/pnas.240305897 (2000).
210 Guegan, C. & Przedborski, S. Programmed cell death in amyotrophic lateral sclerosis. *The Journal of clinical investigation* **111**, 153-161, doi:10.1172/JCI17610 (2003).
211 Cozzolino, M. *et al.* Apoptosome inactivation rescues proneural and neural cells from neurodegeneration. *Cell death and differentiation* **11**, 1179-1191, doi:10.1038/sj.cdd.4401476 (2004).
212 Crosio, C., Casciati, A., Iaccarino, C., Rotilio, G. & Carri, M. T. Bcl2a1 serves as a switch in death of motor neurons in amyotrophic lateral sclerosis. *Cell death and differentiation* **13**, 2150-2153, doi:10.1038/sj.cdd.4401943 (2006).
213 Iaccarino, C. *et al.* Bcl2-A1 interacts with pro-caspase-3: implications for amyotrophic lateral sclerosis. *Neurobiology of disease* **43**, 642-650, doi:10.1016/j.nbd.2011.05.013 (2011).
214 Suzuki, H., Lee, K. & Matsuoka, M. TDP-43-induced death is associated with altered regulation of BIM and Bcl-xL and attenuated by caspase-mediated TDP-43 cleavage. *J Biol Chem* **286**, 13171-13183 (2011).
215 Doble, A. The pharmacology and mechanism of action of riluzole. *Neurology* **47**, S233-241 (1996).
216 Miller, R. G., Mitchell, J. D., Lyon, M. & Moore, D. H. Riluzole for amyotrophic lateral sclerosis (ALS)/motor neuron disease (MND). *The Cochrane database of systematic reviews*, CD001447, doi:10.1002/14651858.CD001447.pub2 (2007).
217 Musaro, A. Understanding ALS: new therapeutic approaches. *The FEBS journal* **280**, 4315-4322, doi:10.1111/febs.12087 (2013).
218 Mazzini, L. *et al.* Stem cell therapy in amyotrophic lateral sclerosis: a methodological approach in humans. *Amyotrophic lateral sclerosis and other motor neuron disorders : official publication of the World Federation of Neurology, Research Group on Motor Neuron Diseases* **4**, 158-161 (2003).
219 Silani, V., Calzarossa, C., Cova, L. & Ticozzi, N. Stem cells in amyotrophic lateral sclerosis: motor neuron protection or replacement? *CNS & neurological disorders drug targets* **9**, 314-324 (2010).
220 Yamanaka, S. & Takahashi, K. [Induction of pluripotent stem cells from mouse fibroblast cultures]. *Tanpakushitsu kakusan koso. Protein, nucleic acid, enzyme* **51**, 2346-2351 (2006).
221 Karumbayaram, S. *et al.* Directed differentiation of human-induced pluripotent stem cells generates active motor neurons. *Stem Cells* **27**, 806-811, doi:10.1002/stem.31 (2009).
222 Mello, C. C. & Conte, D., Jr. Revealing the world of RNA interference. *Nature* **431**, 338-342, doi:10.1038/nature02872 (2004).

223 Dreyer, J. L. Lentiviral vector-mediated gene transfer and RNA silencing technology in neuronal dysfunctions. *Molecular biotechnology* **47**, 169-187, doi:10.1007/s12033-010-9334-x (2011).
224 Smith, R. A. *et al.* Antisense oligonucleotide therapy for neurodegenerative disease. *The Journal of clinical investigation* **116**, 2290-2296, doi:10.1172/JCI25424 (2006).
225 Nizzardo, M. *et al.* Research advances in gene therapy approaches for the treatment of amyotrophic lateral sclerosis. *Cellular and molecular life sciences : CMLS* **69**, 1641-1650, doi:10.1007/s00018-011-0881-5 (2012).
226 Azzouz, M. Gene Therapy for ALS: progress and prospects. *Biochimica et biophysica acta* **1762**, 1122-1127, doi:10.1016/j.bbadis.2006.05.003 (2006).
227 Davidson, B. L. & Breakefield, X. O. Viral vectors for gene delivery to the nervous system. *Nature reviews. Neuroscience* **4**, 353-364, doi:10.1038/nrn1104 (2003).
228 Lim, S. T., Airavaara, M. & Harvey, B. K. Viral vectors for neurotrophic factor delivery: a gene therapy approach for neurodegenerative diseases of the CNS. *Pharmacological research : the official journal of the Italian Pharmacological Society* **61**, 14-26, doi:10.1016/j.phrs.2009.10.002 (2010).
229 Mayr, L. M. & Bojanic, D. Novel trends in high-throughput screening. *Current opinion in pharmacology* **9**, 580-588, doi:10.1016/j.coph.2009.08.004 (2009).
230 Ostergaard, H., Henriksen, A., Hansen, F. G. & Winther, J. R. Shedding light on disulfide bond formation: engineering a redox switch in green fluorescent protein. *The EMBO journal* **20**, 5853-5862 (2001).
231 Hanson, G. T. *et al.* Investigating mitochondrial redox potential with redox-sensitive green fluorescent protein indicators. *The Journal of biological chemistry* **279**, 13044-13053, doi:10.1074/jbc.M312846200 (2004).
232 Dooley, C. T. *et al.* Imaging dynamic redox changes in mammalian cells with green fluorescent protein indicators. *The Journal of biological chemistry* **279**, 22284-22293 (2004).
233 Schwarzlander, M. *et al.* Confocal imaging of glutathione redox potential in living plant cells. *Journal of microscopy* **231**, 299-316 (2008).
234 Gilon, T., Chomsky, O. & Kulka, R. G. Degradation signals for ubiquitin system proteolysis in Saccharomyces cerevisiae. *The EMBO journal* **17**, 2759-2766, doi:10.1093/emboj/17.10.2759 (1998).
235 Griesbeck, O., Baird, G. S., Campbell, R. E., Zacharias, D. A. & Tsien, R. Y. Reducing the environmental sensitivity of yellow fluorescent protein. Mechanism and applications. *The Journal of biological chemistry* **276**, 29188-29194, doi:10.1074/jbc.M102815200 (2001).
236 Ormo, M. *et al.* Crystal structure of the Aequorea victoria green fluorescent protein. *Science* **273**, 1392-1395 (1996).
237 Tsien, R. Y. The green fluorescent protein. *Annual review of biochemistry* **67**, 509-544, doi:10.1146/annurev.biochem.67.1.509 (1998).
238 Wachter, R. M., Elsliger, M. A., Kallio, K., Hanson, G. T. & Remington, S. J. Structural basis of spectral shifts in the yellow-emission variants of green fluorescent protein. *Structure* **6**, 1267-1277 (1998).
239 Bence, N. F., Sampat, R. M. & Kopito, R. R. Impairment of the ubiquitin-proteasome system by protein aggregation. *Science* **292**, 1552-1555, doi:10.1126/science.292.5521.1552 (2001).
240 Baehrecke, E. H. Autophagy: dual roles in life and death? *Nature reviews. Molecular cell biology* **6**, 505-510, doi:10.1038/nrm1666 (2005).
241 Matz, M. V. *et al.* Fluorescent proteins from nonbioluminescent Anthozoa species. *Nature biotechnology* **17**, 969-973, doi:10.1038/13657 (1999).
242 Kabeya, Y. *et al.* LC3, a mammalian homologue of yeast Apg8p, is localized in autophagosome membranes after processing. *The EMBO journal* **19**, 5720-5728, doi:10.1093/emboj/19.21.5720 (2000).
243 Sheen, J. H., Zoncu, R., Kim, D. & Sabatini, D. M. Defective regulation of autophagy upon leucine deprivation reveals a targetable liability of human melanoma cells in vitro and in vivo. *Cancer cell* **19**, 613-628, doi:10.1016/j.ccr.2011.03.012 (2011).

244 Tyas, L., Brophy, V. A., Pope, A., Rivett, A. J. & Tavare, J. M. Rapid caspase-3 activation during apoptosis revealed using fluorescence-resonance energy transfer. *EMBO reports* **1**, 266-270, doi:10.1093/embo-reports/kvd050 (2000).
245 Xu, X. *et al.* Detection of programmed cell death using fluorescence energy transfer. *Nucleic acids research* **26**, 2034-2035 (1998).
246 Mahajan, N. P., Harrison-Shostak, D. C., Michaux, J. & Herman, B. Novel mutant green fluorescent protein protease substrates reveal the activation of specific caspases during apoptosis. *Chemistry & biology* **6**, 401-409 (1999).
247 Biedler, J. L., Roffler-Tarlov, S., Schachner, M. & Freedman, L. S. Multiple neurotransmitter synthesis by human neuroblastoma cell lines and clones. *Cancer research* **38**, 3751-3757 (1978).
248 Rusmini, P. *et al.* Aggregation and proteasome: the case of elongated polyglutamine aggregation in spinal and bulbar muscular atrophy. *Neurobiology of aging* **28**, 1099-1111, doi:10.1016/j.neurobiolaging.2006.05.015 (2007).
249 Maniatis, T., Fritsch, E. F. & Sambrook, J. *Molecular cloning : a laboratory manual*. (Cold Spring Harbor Laboratory, 1982).
250 Pesaresi, M. G. *et al.* Mitochondrial redox signalling by p66Shc mediates ALS-like disease through Rac1 inactivation. *Human molecular genetics* **20**, 4196-4208, doi:10.1093/hmg/ddr347 (2011).
251 Onoue, S., Igarashi, N., Yamada, S. & Tsuda, Y. High-throughput reactive oxygen species (ROS) assay: an enabling technology for screening the phototoxic potential of pharmaceutical substances. *Journal of pharmaceutical and biomedical analysis* **46**, 187-193, doi:10.1016/j.jpba.2007.09.003 (2008).
252 Nguyen, A. W. & Daugherty, P. S. Evolutionary optimization of fluorescent proteins for intracellular FRET. *Nature biotechnology* **23**, 355-360, doi:10.1038/nbt1066 (2005).
253 Cannon, M. B. & Remington, S. J. Redox-sensitive green fluorescent protein: probes for dynamic intracellular redox responses. A review. *Methods Mol Biol* **476**, 51-65 (2008).
254 Buratti, E. & Baralle, F. E. The multiple roles of TDP-43 in pre-mRNA processing and gene expression regulation. *RNA biology* **7**, 420-429 (2010).
255 Kovar, H. Dr. Jekyll and Mr. Hyde: The Two Faces of the FUS/EWS/TAF15 Protein Family. *Sarcoma* **2011**, 837474 (2010).
256 Cooper, T. A., Wan, L. & Dreyfuss, G. RNA and disease. *Cell* **136**, 777-793, doi:10.1016/j.cell.2009.02.011 (2009).
257 Hoell, J. I. *et al.* RNA targets of wild-type and mutant FET family proteins. *Nature structural & molecular biology* **18**, 1428-1431, doi:10.1038/nsmb.2163 (2011).
258 Chen, A. K. *et al.* Induction of amyloid fibrils by the C-terminal fragments of TDP-43 in amyotrophic lateral sclerosis. *Journal of the American Chemical Society* **132**, 1186-1187, doi:10.1021/ja9066207 (2010).
259 Dormann, D. & Haass, C. TDP-43 and FUS: a nuclear affair. *Trends in neurosciences* **34**, 339-348, doi:10.1016/j.tins.2011.05.002 (2011).
260 Guzman, J. N. *et al.* Oxidant stress evoked by pacemaking in dopaminergic neurons is attenuated by DJ-1. *Nature* **468**, 696-700, doi:10.1038/nature09536 (2010).
261 Goldberg, J. A. *et al.* Calcium entry induces mitochondrial oxidant stress in vagal neurons at risk in Parkinson's disease. *Nature neuroscience* **15**, 1414-1421, doi:10.1038/nn.3209 (2012).
262 Rodriguez-Rocha, H. *et al.* Compartmentalized oxidative stress in dopaminergic cell death induced by pesticides and complex I inhibitors: Distinct roles of superoxide anion and superoxide dismutases. *Free radical biology & medicine* **61C**, 370-383, doi:10.1016/j.freeradbiomed.2013.04.021 (2013).
263 Xie, H. *et al.* Rapid cell death is preceded by amyloid plaque-mediated oxidative stress. *Proceedings of the National Academy of Sciences of the United States of America* **110**, 7904-7909, doi:10.1073/pnas.1217938110 (2013).
264 Zhang, J. *et al.* 3-hydroxybutyrate methyl ester as a potential drug against Alzheimer's disease via mitochondria protection mechanism. *Biomaterials* **34**, 7552-7562, doi:10.1016/j.biomaterials.2013.06.043 (2013).

265 Cook, C. *et al.* Aging is not associated with proteasome impairment in UPS reporter mice. *PloS one* **4**, e5888, doi:10.1371/journal.pone.0005888 (2009).
266 Onesto, E. *et al.* Muscle cells and motoneurons differentially remove mutant SOD1 causing familial amyotrophic lateral sclerosis. *Journal of neurochemistry* **118**, 266-280, doi:10.1111/j.1471-4159.2011.07298.x (2011).
267 Crippa, V. *et al.* The small heat shock protein B8 (HspB8) promotes autophagic removal of misfolded proteins involved in amyotrophic lateral sclerosis (ALS). *Human molecular genetics* **19**, 3440-3456, doi:10.1093/hmg/ddq257 (2010).
268 Walker, A. K. & Atkin, J. D. Stress signaling from the endoplasmic reticulum: A central player in the pathogenesis of amyotrophic lateral sclerosis. *IUBMB life* **63**, 754-763, doi:10.1002/iub.520 (2011).
269 Ma, Y., Brewer, J. W., Diehl, J. A. & Hendershot, L. M. Two distinct stress signaling pathways converge upon the CHOP promoter during the mammalian unfolded protein response. *Journal of molecular biology* **318**, 1351-1365 (2002).
270 Han, J. *et al.* ER-stress-induced transcriptional regulation increases protein synthesis leading to cell death. *Nature cell biology* **15**, 481-490, doi:10.1038/ncb2738 (2013).
271 Borghero, G. *et al.* A patient carrying a homozygous p.A382T TARDBP missense mutation shows a syndrome including ALS, extrapyramidal symptoms, and FTD. *Neurobiology of aging* **32**, 2327 e2321-2325, doi:10.1016/j.neurobiolaging.2011.06.009 (2011).
272 Mosca, L. *et al.* Wide phenotypic spectrum of the TARDBP gene: homozygosity of A382T mutation in a patient presenting with amyotrophic lateral sclerosis, Parkinson's disease, and frontotemporal lobar degeneration, and in neurologically healthy subject. *Neurobiology of aging* **33**, 1846 e1841-1844, doi:10.1016/j.neurobiolaging.2012.01.108 (2012).